A PROTEOMIC STUDY OF PROTEIN TYROSINE NITRATION

By

Sung Jung Hong
B.S., University of California at Los Angeles, 2003
M.S. University of Kansas, 2006

Submitted to the Department of Pharmaceutical Chemistry and the Faculty of the Graduate School of the University of Kansas in partial fulfillment of the requirements for the degree of Doctor of Philosophy

Dissertation Committee:

_____
Dr. Christian Schöneich (Chairman)

_____
Dr. Kenneth L. Audus

_____
Dr. Elias K. Michaelis

_____
Dr. John F. Stobaugh

_____
Dr. Jeffrey Krise

Dissertation Defended: July 25th of 2008

The Dissertation Committee for Sung Jung Hong certifies that this is the approved version of the following dissertation:

A PROTEOMIC STUDY OF PROTEIN TYROSINE NITRATION

_____

Dr. Christian Schöneich
Chairperson

Date Approved: July 25th of 2008

This Doctoral Dissertation is dedicated to my parents, Ok Seok Chon and Yong Duck Chon, my husband Tae Chung and our son Joseph

ACKNOWLEDGEMENTS:

First of all, I would like to thank my research advisor Dr. Christian Schöneich for his guidance and support throughout the length of my graduate career. Graduate school has taught me patience, perseverance, teamwork and independence.

I would like to thank the members of my committee: Dr. Kenneth Audus, Dr. Eli Michaelis, Dr. John Stobaugh and Dr. Jeffrey Krise for their time and for their constructive criticism.

I would like to give special thanks to Dr. John Stobaugh, Dr. Kenneth Audus and Dr. Jeffrey Krise for reading through my thesis dissertation and for their useful comments to improve it.

I would like to thank all past and present members of Dr. Schöneich's group for their friendship and camaraderie, for the insightful scientific conversations and for the great atmosphere where learning and teaching were constantly present. Thanks to Dr. Elena Dremina, Dr. Viktor Sharov, Dr. Xiaobao Li, Dr. Jarek Kanski, Dr. Hui Koon Kohr, Dr. Giridharan Gokulrangan, Dr. Vikram Sadineni, Dr. Olivier Mozziconacci, Dr. Geetha Hewawasam, Gary Gerstenecker, Asha Hewarathna and Maria Thorson for a great graduate experience.

I would like to thank the Mass Spectrometry Laboratory at the University of Kansas, in particular Dr. Todd Williams and Mr. Robert Drake for their help with the mass spectrometry analysis of full Calmodulin (CaM), and the Applied Proteomics Laboratory at the university of Kansas, in particular Dr. Nadzena Galeva for her help

with mass spectrometry analysis of CaM peptides after fluorogenic derivatization of this protein.

I would like to thank the Pharmaceutical Chemistry and the Higuchi Biosciences staff for their support, I am sure that I would have been very lost if it wasn't for them.

I would like to thank members of my class: Daniel Mudra, Pallabi Mitra, Sandipan Sinha, David Fischer, Ben Nelson, Gary Gerstenecker, Pradyot Nandi, Tim Kamerzell for their friendship, and I would like to especially thank Sumit Majumdar and Kelly Desino for going the extra mile in helping me prepare for the preliminary exams and for their support and friendship as well.

I would also like to thank Professor Heather Maynard at UCLA for welcoming me into her lab when I was an undergraduate student at UCLA. Her mentorship and excitement about science were very influential in my decision to pursue graduate school. I would like to thank members of Professor Maynard's group, Vimary Vasquez, Dr. Debora Bontempo and Dr. Jung Hwang for their friendship and mentorship.

I would like to thank my supervisors at Genentech Inc.: Dr. Junyan Ji and Dr. John Wang for the opportunity to spend a summer doing hands on pharmaceutical research, as well as learning about the biotech industry. I would like to thank members of Dr. Wang's group: Javier Rivera, Wilson Chen, Sabrina Lo, Dr. Tim Kamerzell, Dr. Aditya Wakankar, Rita Wong and Dr. Lipika Basumallick for their

help in becoming quickly acquainted with the lab and their help and friendship during my time at Genentech Inc.

I would like to thank the past and present members of the Korean Presbyterian Church of Lawrence for their prayers, spiritual support and friendship, in particular Pastor Paul Gim and his family, the young adult group and the family bible study groups lead by Mr. Jung Hee Lee and Mrs. Yong Sun Cho, and Mr. Yeong Mo Kim and Mrs. Jee Hyun Lee.

I would like to thank my parents Yong Duck Chon and Ok Seok Chon for opening different doors for me that eventually led me to pursue undergraduate and graduate school in the US. I would like to give special thanks to my mom for her support when our son Joseph joined our family.

I would like to thank my parents in-law Hea Mok Yu and Yoon Sook Yu for their constant support and understanding. Thank you for openly accepting me as a member of your family. I would like to thank John Ha and Esther Ha for being the best brother and sister in-law, words cannot describe how thankful I am for all of what you have done for us. I would also like to thank my husband's little brother Tim Chung for being supportive.

I would like to thank my husband Tae Chung for his patience, support and understanding, I know how stressful life was with both of us in school.

I would like to thank Joseph, our son, for introducing us to the joy of parenthood and for constantly fulfilling our lives with happiness as well as challenges. Thank you for being the light of our lives.

Finally, and most importantly, I would like to thank Jesus Christ my Lord and Savior for His guiding hand.

TABLE OF CONTENTS

TABLE OF FIGURES

2. In-vitro proteomic study of nitrated creatine kinase

3. In-vivo proteomic study of nitrated proteins in cardiac tissue as a function of aging

4. Fluorogenic derivatization of 3-Nitrotyrosine residues in Calmodulin with 4-aminobenzylbenzene sulfonic acid

6. Conclusion and Future Directions

Appendix 1: Boronate Affinity column characterization with model peptide FSAY(NO2)LER

1. Introduction

1.1 Genomics to Proteomics

Genomics, the study of the genomic composition of organisms through DNA mapping and DNA sequencing, has opened the door for the study of the gene products, the proteins that are encoded in the genes, and this derivative study has been defined as proteomics (1,2). As a better understanding of these fields developed through time, people involved in this field have learned that unlike genomics where DNA is chemically and physically more stable, work load is scalable and where experimental techniques are well established, proteomics studies present the researcher with a very challenging task because proteins are very dynamic and are constantly undergoing post-translational modifications induced environmentally or due to different cellular processes (1,3). Proteomics no longer focuses simply on the gene products, but at the same time, tries to understand what happens to the proteins after translation, protein function, protein-protein interactions and the post-translational changes that proteins undergo *in-vivo*, greatly diversifying the proteome by orders of magnitude (1,3). Indeed, it is very hard to keep up with the modifications that come after translation in order to serve specific functions, or are simply victims of their environment. For the most part, enzymatic post-translational modifications (PTMs) play an important role in cellular function, however, non-enzymatic PTMs are mostly results of the environment, which can be detrimental to the life of the protein because they may cause the loss of function (4). Most amino acids may undergo change, however, for the purposes of the work described in this thesis, we

will focus on the amino acid Tyr. Some enzymatic reactions that Tyr may undergo are phosphorylation, very important in signaling transduction, and halogenation, very important for the synthesis of hormones (5). Non-enzymatic PTMs are mainly due to oxidation (4) and an example of this would be protein Tyr nitration, which is the main focus of this dissertation.

1.2 Tyrosine Nitration

The post-translational modification of tyrosine to nitrotyrosine (3-NY) represents a marker, as discussed earlier, for protein oxidation, which in turn is a modification associated with various pathologies (6,7) and the process of biological aging (8-13). Protein nitration occurs as a result of oxidative stress, which leads to the oxidative metabolism of nitric oxide (NO), resulting in the formation of reactive nitrogen species (RNS) (10,14). Reactive oxygen species (ROS) are also generated as normal byproducts of oxidative metabolism (15), where estimates show that 2-5% of the oxygen flux through the mitochondrial electron transport chain suffers conversion into superoxide anion radical ($O_2^{\cdot-}$) (16). Superoxide reacts with nitrogen monoxide (NO) to form peroxynitrite ($ONOO^-$) (17), a powerful oxidant of aromatic and organosulfur compounds (18,19). In addition, $ONOO^-$ is able to nitrate Tyr via multiple reaction mechanisms, either via a direct reaction with Tyr (20,21), via catalysis by transition metals (14,19,21), or through the proton or CO_2-assisted formation of nitrogen dioxide ($^{\cdot}NO_2$) (20-23).

In biological systems, NO and superoxide coexist in a delicate balance, where even slight variations in the concentrations of these species dictate whether

oxidation or nitrosation pathways will be followed (24). The relative levels of superoxide have an effect on the levels of nitric oxide due to the diffusion–controlled reaction between NO and superoxide to form $ONOO^-$ (17,25). Superoxide dismutase (SOD) regulates the levels of superoxide and, therefore, has the potential to regulate redox-dependent signaling pathways through modulation of the effective levels of NO, superoxide, H_2O_2 and $ONOO^-$. The relative amounts of these species, in turn, control the levels of nitrosating species, such as N_2O_3, or oxidizing/nitrating species, such as $ONOO^-$ (26). Disruption of the delicate balance between NO and superoxide leads to a so-called "nitroso-redox imbalance", which may cause pathological conditions such as heart failure (27).

While protein nitrosation can be reversed chemically, protein nitration leads to a chemically stable protein modification. Hence, the accumulation of nitrated proteins in tissue may define the phenotype of biological aging or of any pathology. The knowledge of specific protein nitration sites represents the ultimate goal for a correlation between protein modification and protein structure and function. This can be illustrated by the targeted purification and analysis of specific nitrated proteins from tissue, such as SERCA. Here, biological aging leads to the selective nitration of the slow-twitch skeletal and cardiac muscle isoform SERCA2a nitrated at Tyr^{294} and Tyr^{295}, which can be linked to the loss of enzyme activity (28-31). Other proteins studied to similar functional detail include manganese superoxide dismutase (MnSOD) (32,33), prostacyclin synthase (34), and actin (35).

1.3 Role of Protein Tyr Oxidation in Redox Signaling

There is compelling evidence that the intracellular redox environment is directly related to the actions of protein kinases (responsible for phosphorylation) and phospatases (responsible for dephosphorylation), which play a major role in the signaling pathways that regulate cell cycle, cell survival, cell proliferation and cell adhesion (36). Within the past decade, compelling evidence has been accumulated for the role of protein thiol oxidation and protein Tyr nitration as regulators of protein Tyr phosphorylation (36), or the opposite, where protein Tyr phosphorylation/dephosphorylation may play a role in protein Tyr nitration (37). Protein Tyr phosphorylation only represents <<1% of the total phosphorylated proteome, however, it has been shown to play a major role in the cell signaling pathways (36). Therefore, maintenance of a well balanced redox environment is essential for the health of an organism. Levels of ROS and RNS are kept in check by protein and non-protein reducing agents such as superoxide dismutase (SOD), catalase and glutathione (GSH) peroxidase (36).

1.4 Mass Spectrometry in Proteomics Research

The most essential tool in proteomics is mass spectrometry, and therefore, most technological advancements have been done for this technique. However, mass spectrometry also has its limitations and using this technique alone is often not enough for identification and characterization of proteins and as a result, it is used in conjunction with other techniques such as immunoprecipitation, immunoblotting, 1D and 2D gel electrophoresis, chromatography, isotopic chemical tagging (4,38-41),

mainly as pre-fractionation techniques to reduce sample complexity. The use of different techniques may vary according to the goal of the proteomic study. The anti-body based techniques for example, are most essential for identification and confirmation of specific PTMs, i.e., protein Tyr nitration.

Mass spectrometry has been accomplished by the extensive protein database made available thanks to the efforts of the field of genomics. The instrumentation used for mass spectrometry analysis is comprised of an ion source, mass analyzer and a detector. The most common ion sources used for proteomics studies are matrix assisted laser desorption ionization (MALDI) and electrospray ionization (ESI) and the most common mass analyzers are ion traps, time of flight (TOF), quadrupole time of flight (QTOF), and Fourier transform ion cyclotron (FT-MS), which essentially differ in sensitivity, resolution and mass accuracy (40). Depending on the experiment, ion traps are usually good for routine analysis since they are the most economical, but have low mass accuracy. FT-MS is the most accurate mass analyzer however, it is also the most costly.

There are two approaches to proteomics with mass spectrometry, top-down proteomics and bottom-up proteomics. Both have evolved with time and are said to be complimentary techniques rather than one being a better approach than the other. In top-down proteomics, whole proteins (not subjected to enzymatic digestion) are subjected to mass spectrometry analysis (42,43). This approach provides orders of magnitude higher specificity at the expense of higher experimental requirements and has been successfully applied to proteins of 500 residues to 50 KDa molecular weight,

since larger fragments from larger proteins have higher backbone stability and fragmentation requires higher amounts of energy. This limit has been greatly extended by new methods of ionization such as prefolding dissociation, where variable thermal and collisional activation just after electrospray ionization are applied (42).

Bottom-up proteomics on the other hand, involves working with enzyme digested protein samples for mass spectrometry analysis. The proteomic information in this approach is built relying on database searches, which in turn rely on good protein coverage, which is usually orders of magnitude lower than the top-down approach, especially in complex protein mixtures (40,42,43). However, this approach is still the more popular and amenable approach due to its higher versatility and accessibility.

1.5 Conclusions and Perspectives on the Study of Protein Nitration

Proteomics, with the help of Genomics, is a relatively new field that is rapidly growing and proving to be essential for the understanding of biological processes such as aging, and also understanding disease. Proteins are the dynamic machinery that drive all processes in living organisms from conception to death. Identifying proteins and their function is a daunting task that proteomics work has undertaken, especially due to their existence in different modified states after translation. This is a field that is constantly growing and evolving, where new techniques are constantly being developed, especially for mass spectrometry and the study of PTMs and their

role. Protein Tyr nitration is a major PTM that has been linked to oxidative stress and more recently to cell signaling.

This thesis will present proteomic studies of protein Tyr nitration using traditional proteomics methods such as 1D and 2D gel electrophoresis, and antibody based techniques such as Western Blot analysis. Here, we will also present the application of a novel fluorescent tagging technique specific for hydroxytyrosine (DOPA) and nitrotyrosine after the reduction to aminotyrosine, developed by collaborations between our group and Dr. Stobaugh's group. This novel fluorescence tag will enhance sensitivity to the analyte and help overcome the problem of low protein abundance faced for mass spectrometry analysis. In addition, this new fluorescent tagging technique is both qualitative and quantitative, unlike most traditional proteomics techniques, which are mainly qualitative.

From a Scifinder search for Tyr nitration, we can observe that since protein Tyr nitration was first discovered in the 1970s, interest in this PTM has increased dramatically in the last decade and several proteins have been added to the nitrated proteome. Protein Tyr nitration with its link to oxidative stress, has been hypothesized to play a role in signal transduction if present at basal levels (9,36), however, accumulation of nitrated proteins has been linked to several disease states including inflammation (44), cancer (45,46), cardiovascular disease (47-49), atherosclerosis (50) and Alzheimer's disease (51-53). At the same time, the search for biomarkers of disease has been and continues to be a major concern both in the medical and the pharmaceutical fields (54).

All proteins in the nitrated proteome have a potential to be biomarkers of disease, however, only a few of them have been studied to functional detail and the effects of nitration have been characterized *in-vitro*. There remains a need for studying nitrated proteins to functional detail and more so, to understand whether nitration is the cause of the disease or the effect of disease. Such as in the case of Alzheimer's disease, which is characterized by senile plaques in the brain, formed by aggregates of proteolytic products of amyloid protein precursor due to protein misfolding (55) and the tau protein in neurons (56). To date, cause for these aggregates are not very well understood, however, it has been well reported as mentioned earlier, that oxidized proteins are more prone to aggregation and, or proteolytic degradation (14), therefore, the presence of oxidated proteins in this disease may offer some explanation to the cause of protein aggregation that causes disease progression.

There are a lot of pieces to several puzzles and the study and understanding of each individual piece is imperative to be able to put the puzzles together and get the "big picture". As important as global proteomics are to increase the number of pieces to the puzzle, individual focus by disease and protein will offer the most significant information towards the development of novel protein based therapeutics for the treatment of disease.

1.6 References

1. Tyers, M., and Mann, M. (2003) *Nature* **422**, 193-197

2. Belhocine, T. Z., Tait, J. F., Vanderheyden, J. L., Li, C., and Blankenberg, F. G. (2004) *J Proteome Res* **3**, 345-349

3. Julka, S., and Regnier, F. (2004) *J Proteome Res* **3**, 350-363

4. Gianazza, E., Crawford, J., and Miller, I. (2007) *Amino Acids* **33**, 51-56

5. Wold, F. (1981) *Annu Rev Biochem* **50**, 783-814

6. Turko, I. V., Li, L., Aulak, K. S., Stuehr, D. J., Chang, J. Y., and Murad, F. (2003) *J Biol Chem* **278**, 33972-33977

7. Turko, I. V., and Murad, F. (2002) *Pharmacol Rev* **54**, 619-634

8. Kanski, J., Hong, S. J., and Schöneich, C. (2005) *J Biol Chem* **280**, 24261-24266

9. Greenacre, S. A., and Ischiropoulos, H. (2001) *Free Radic Res* **34**, 541-581

10. Ischiropoulos, H. (2003) *Biochem Biophys Res Commun* **305**, 776-783

11. Hong, S. J., Gokulrangan, G., and Schoneich, C. (2007) *Exp Gerontol* **42**, 639-651

12. Kanski, J., Alterman, M. A., and Schoneich, C. (2003) *Free Radic Biol Med* **35**, 1229-1239

13. Kanski, J., Behring, A., Pelling, J., and Schöneich, C. (2005) *Am J Physiol Heart Circ Physiol* **288**, H371-381

14. Beckman, J. S. (1996) *Chem Res Toxicol* **9**, 836-844

15. Kozlov, A. V., Szalay, L., Umar, F., Kropik, K., Staniek, K., Niedermuller, H., Bahrami, S., and Nohl, H. (2005) *Biochim Biophys Acta* **1740**, 382-389

16. Traverse, J. H., Nesmelov, Y. E., Crampton, M., Lindstrom, P., Thomas, D. D., and Bache, R. J. (2006) *Am J Physiol Heart Circ Physiol* **290**, H2453-2458

17. Kissner, R., Nauser, T., Bugnon, P., Lye, P. G., and Koppenol, W. H. (1997) *Chem Res Toxicol* **10**, 1285-1292

18. Szábo, C. (2003) *Toxicol Lett* **140-141**, 105-112

19. Virag, L., Szábo, E., Gergely, P., and Szábo, C. (2003) *Toxicol Lett* **140-141**, 113-124

20. Lehnig, M. (1999) *Arch Biochem Biophys* **368**, 303-318

21. Beckman, J. S., Ischiropoulos, H., Zhu, L., van der Woerd, M., Smith, C., Chen, J., Harrison, J., Martin, J. C., and Tsai, M. (1992) *Arch Biochem Biophys* **298**, 438-445

22. Radi, R., Peluffo, G., Alvarez, M. N., Naviliat, M., and Cayota, A. (2001) *Free Radic Biol Med* **30**, 463-488

23. Prütz, W. A., Monig, H., Butler, J., and Land, E. J. (1985) *Arch Biochem Biophys* **243**, 125-134

24. Wink, D. A., Cook, J. A., Kim, S. Y., Vodovotz, Y., Pacelli, R., Krishna, M. C., Russo, A., Mitchell, J. B., Jourd'heuil, D., Miles, A. M., and Grisham, M. B. (1997) *J Biol Chem* **272**, 11147-11151

25. Nauser, T., and Koppenol, W. H. (2002) *J Phys Chem A* **106**, 4084-4086

26. Patel, R. P., Moellering, D., Murphy-Ullrich, J., Jo, H., Beckman, J. S., and Darley-Usmar, V. M. (2000) *Free Radic Biol Med* **28**, 1780-1794

27. Hare, J. M., and Stamler, J. S. (2005) *J Clin Invest* **115**, 509-517

28. Knyushko, T. V., Sharov, V. S., Williams, T. D., Schöneich, C., and Bigelow, D. J. (2005) *Biochemistry* **44**, 13071-13081

29. Schöneich, C., Viner, R. I., Ferrington, D. A., and Bigelow, D. J. (1999) *Mech Ageing Dev* **107**, 221-231

30. Viner, R. I., Ferrington, D. A., Williams, T. D., Bigelow, D. J., and Schöneich, C. (1999) *Biochem J* **340 (Pt 3)**, 657-669

31. Xu, S., Ying, J., Jiang, B., Guo, W., Adachi, T., Sharov, V., Lazar, H., Menzoian, J., Knyushko, T. V., Bigelow, D., Schöneich, C., and Cohen, R. A. (2006) *Am J Physiol Heart Circ Physiol* **290**, H2220-2227

32. Guo, W., Adachi, T., Matsui, R., Xu, S., Jiang, B., Zou, M. H., Kirber, M., Lieberthal, W., and Cohen, R. A. (2003) *Am J Physiol Heart Circ Physiol* **285**, H1396-1403

33. Quint, P., Reutzel, R., Mikulski, R., McKenna, R., and Silverman, D. N. (2006) *Free Radic Biol Med* **40**, 453-458

34. Zou, M. H., Leist, M., and Ullrich, V. (1999) *Am J Pathol* **154**, 1359-1365

35. Aslan, M., Ryan, T. M., Townes, T. M., Coward, L., Kirk, M. C., Barnes, S., Alexander, C. B., Rosenfeld, S. S., and Freeman, B. A. (2003) *J Biol Chem* **278**, 4194-4204

36. Monteiro, H. P., Arai, R. J., and Travassos, L. R. (2008) *Antioxid Redox Signal* **10**, 843-889

37. Shi, W. Q., Cai, H., Xu, D. D., Su, X. Y., Lei, P., Zhao, Y. F., and Li, Y. M. (2007) *Regul Pept* **144**, 1-5

38. Mann, M., and Jensen, O. N. (2003) *Nat Biotechnol* **21**, 255-261

39. Minden, J. (2007) *Biotechniques* **43**, 739, 741, 743 passim

40. Aebersold, R., and Mann, M. (2003) *Nature* **422**, 198-207

41. Leitner, A., and Lindner, W. (2004) *J Chromatogr B Analyt Technol Biomed Life Sci* **813**, 1-26

42. McLafferty, F. W., Breuker, K., Jin, M., Han, X., Infusini, G., Jiang, H., Kong, X., and Begley, T. P. (2007) *FEBS J* **274**, 6256-6268

43. Kelleher, N. L. (2004) *Anal Chem* **76**, 197A-203A

44. Aulak, K. S., Miyagi, M., Yan, L., West, K. A., Massillon, D., Crabb, J. W., and Stuehr, D. J. (2001) *Proc Natl Acad Sci U S A* **98**, 12056-12061

45. MacMillan-Crow, L. A., Greendorfer, J. S., Vickers, S. M., and Thompson, J. A. (2000) *Arch Biochem Biophys* **377**, 350-356

46. Ambs, S., Merriam, W. G., Bennett, W. P., Felley-Bosco, E., Ogunfusika, M. O., Oser, S. M., Klein, S., Shields, P. G., Billiar, T. R., and Harris, C. C. (1998) *Cancer Res* **58**, 334-341

47. Saraiva, R. M., and Hare, J. M. (2006) *Curr Opin Cardiol* **21**, 221-228

48. Davidson, S. M., and Duchen, M. R. (2006) *Cardiovasc Res* **71**, 10-21

49. Peluffo, G., and Radi, R. (2007) *Cardiovasc Res* **75**, 291-302

50. Leeuwenburgh, C., Hardy, M. M., Hazen, S. L., Wagner, P., Oh-ishi, S., Steinbrecher, U. P., and Heinecke, J. W. (1997) *J Biol Chem* **272**, 1433-1436

51. Davidsson, P., Westman-Brinkmalm, A., Nilsson, C. L., Lindbjer, M., Paulson, L., Andreasen, N., Sjogren, M., and Blennow, K. (2002) *Neuroreport* **13**, 611-615

52. Hensley, K., Maidt, M. L., Yu, Z., Sang, H., Markesbery, W. R., and Floyd, R. A. (1998) *J Neurosci* **18**, 8126-8132

53. Aksenov, M., Aksenova, M., Butterfield, D. A., and Markesbery, W. R. (2000) *J Neurochem* **74**, 2520-2527

54. Hanash, S. (2003) *Nature* **422**, 226-232

55. Hashimoto, M., Rockenstein, E., Crews, L., and Masliah, E. (2003) *Neuromolecular Med* **4**, 21-36

56. Hernandez, F., and Avila, J. (2007) *Cell Mol Life Sci* **64**, 2219-2233

2. *In-vitro* proteomic study of nitrated creatine kinase

2.1 List of abbreviations used inside the text

- ROS: Reactive oxygen species
- RNS: Reactive nitrogen species
- CK: Creatine Kinase
- HPLC-ESI-MS/MS: High performance liquid chromatography-electrospray ionization tandem mass spectrometry.
- 3-NY: 3-nitrotyrosine
- NO: nitrogen monoxide
- $ONOO^-$: peroxynitrite
- IAA: Iodoacetic acid
- ATP: Adenosine triphosphate
- ADP: Adenosine diphosphate
- NADH: β-nicotinamide adenosine dinucleotide
- PK/LDH: pyruvate kinase/lactic dehydrogenase
- ThioGlo-1™: 10-(2,5-Dihydro-2,5-dioxo-1H-pyrrol-1-yl)-9-methoxy-3-oxo-, Methyl Ester
- 1D SDS-PAGE/1DE: one dimensional sodium dodecyl sulfate polyacrylamide gel electrophoresis.
- BSA: bovine serum albumin
- DTT: dithiothreitol
- PVDF polyvinylidene difluoride
- RP nano LC MS: Reverse phase nano liquid chromatography mass spectrometry

2.2 Introduction

Creatine kinase (CK) is a 37 kDa protein expressed in high energy demanding tissues such as heart, skeletal muscle and brain. CK plays an important role in energy metabolism by effectively catalyzing the formation of ATP by the reversible transfer of the phosphoryl group on phosphocreatine to ADP (1,2). Equation 1 is a visual representation of this process, where the rate of CK reaction turnover exceeds the rate of ATP synthesis by an order of magnitude, allowing for cellular systems to keep up

with energy consumption by tissues such as skeletal muscle, especially during excersise or other high energy demand activities (2).

$$\text{Phorphocreatine} + \text{ADP} \leftarrow \text{CK} \rightarrow \text{Creatine} + \text{ATP} \quad \text{(Eq. 1)}$$

Some of the proposed cellular functions for CK range from regulation of oxidative phosphorylation, energy buffering, to regulation of chemical potential between sites of ATP production and consumption in the form of phosphocreatine (1-4). CK (brain isoform) has also been shown to be essential for ATP dependent signaling pathways directed to the cytoskeleton in the vascular system by interaction with protease-activated receptor-1 (PAR-1), responsible for mediating cellular responses to thrombin during blood coagulation, cell proliferation, changes in vascular permeability, tumor metastasis and injury to the nervous system (4).

The active site of CK contains a critical Cys residue, that, if unavailable, may significantly decrease enzymatic activity (2,5), thus making CK highly susceptible to protein oxidation by reactive oxygen species (ROS) such as superoxide (6,7) and reactive nitrogen species (RNS) such as peroxynitrite ($ONOO^-$) (2). Reduced CK activity due to posttranslational modifications has been reported in diseases such as Alzheimer's disease, Pick's disease and Lewy body dementia (3). The presence of nitrated CK isoforms has also been reported to accumulate as a function of aging (8,9), which led us to the present study.

In this study, we focused on the oxidative effects of peroxynitrite on CK. We treated CK with different levels of peroxynitrite and found that enzymatic activity decreases significantly with increasing levels of oxidant. In these *in-vitro* studies, we

found that the only oxidized Cys residue out of four cysteins was Cys^{283}, the critical Cys in CK's active site (2,5). This Cys residue is strategically positioned in the catalytic site of CK and is thought to directly participate in catalysis of energy metabolism. Therefore, any change in this Cys residue may trigger a change in the geometry and steric access of CK's active site, affecting its activity (10). Interestingly but not so surprisingly, Tyr^{82} was the main nitration site *in-vitro*, however, the main Tyr nitration sites found *in-vivo* were Tyr^{14} and Tyr^{20} (11). This experimental result illustrates that *in-vitro* studies do not always mimic processes that occur *in-vivo*.

2.3 Experimental

Materials

Creatine Kinase (CK), dithiotreitol (DTT), N-acetyl-Cys, Coomassie brilliant blue, iodoacetic acid (IAA), adenosine triphosphate (ATP), β-nicotinamide adenosine dinucleotide (NADH), phosphoenol pyruvate (PEP), pyruvate kinase/lactic dehydrogenase (PK/LDH), glutathione (reduced form) and creatine were purchased from Sigma-Aldrich Chemical Company (St.Louis, MO), and was nitrated with peroxynitrite ($ONOO^-$) synthesized in the laboratory according to Beckman et. al. (12). Tris/HCl, $MgCl_2$ sodium phosphate diabasic (Na_2HPO_4), guanidine-HCl and sequencing grade trypsin were purchased from Fisher Scientific (Pittsburg, PA). De-ionized distilled water was filtered by a Labconco purification system (Kansas City, MO). Pre-cast 4-20% SDS-PAGE gels and Tris-glycine SDS 2X sample buffer were purchased from Invitrogen (Carlsbad, CA) and the X-ray films were purchased from Kodak (Rochester, NY). The anti-3-nitrotyrosine (anti-3-NY) monoclonal antibody,

clone 1A6, was purchased from Upstate, Inc. (Charlottesville, VA), and the anti-mouse IgG Fc-peroxide-conjugated antibody was purchased from Pierce Biotechnology (Rockford, IL). ECL-Plus reagents were purchased from GE Healthcare (Piscataway, NJ). Powdered milk was purchased from Nestlé-Carnation (Glendale, CA). Polyvinylidine fluoride (PVDF) membranes were purchased from Millipore (Billerica, MA). 10-(2,5-Dihydro-2,5-dioxo-1H-pyrrol-1-yl)-9-methoxy-3-oxo-, Methyl Ester (ThioGlo-1™) was obtained from Covalent Associate Inc. (Woburn, MA).

In-vitro protein nitration

A 1 mg/ml solution of CK was prepared in 50 mM Tris/HCl-5mM $MgCl_2$ buffer at pH 8. The protein solution was distributed among 5 Eppendorf™ tubes, each aliquot containing 200 µl. The concentration of peroxynitrite in the stock solution was measured to be 88 mM by UVspectroscopy. Each aliquot was treated with different levels of peroxynitrite, 1mM, 0.5 mM, 0.2 mM, 0.1 mM and 0 mM in solution. The peroxynitrite was added to the inner wall of the tube right above the protein solution and vortexed for 5 seconds.

Gel electrophoresis

50 µl of each sample were diluted with 2X sample buffer for a total volume of 100 µl. These samples were distributed among 2 pre-cast SDS-PAGE gels, which were run simultaneously. The first gel was used for protein Coomassie blue staining (Figure 2.1) and the second gel was used for Western blot analysis.

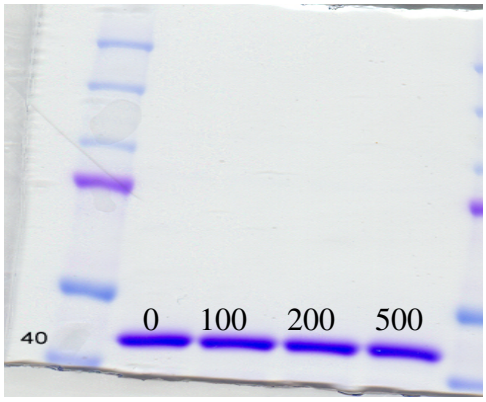

Figure 2.1 SDS-PAGE analysis for *in-vitro* nitrated creatine kinase (CK).

Total protein load by coomassie blue staining, ~12.5 µg of protein per lane. 0, 100, 200 and 500 represent the micromolar concentrations of $ONOO^-$ in each CK sample.

Western Blot

The second gel was taken from its cast and the proteins were transferred onto a PVDF membrane using a Hoeffer transfer apparatus (Hoeffer Scientific Instruments, San Francisco, CA). The transfer was done at 100 V for 2 hrs. The membrane was briefly washed in TBST buffer prepared by adjusting a solution of 150mM NaCl and 20mM Tris to a pH of 7.4, prior to the addition of 0.05% (v/v) Tween 20. The membrane was blocked overnight in a 5 % milk solution prepared also in TBST at 3^oC. The membrane was washed 3 times, 15 min each with TBST and then it was incubated with the primary ant-nitrotyrosine antibody for 1 hr in a ratio of 1:4000 also in TBST. The previous wash step with TBST for the membrane was repeated one more time. The membrane was then incubated with the secondary antibody at a ratio of 1:10000 in TBST for another hour. The wash step was repeated one more time and finally, the membrane was placed on a transparent film flat surface removing excess buffer. The ECL Plus reagent was applied according to manufacturer's directions and

was incubated for 5 min. The membrane was covered with another transparent film and was placed inside a developing cassette. In the dark room, an x-ray film exposed to the membrane by placing it directly on top of the membrane inside the cassette. The x-ray film was then developed according to film developing procedures. Figure 2.2 shows the Western blot for CK treated with different concentrations of $ONOO^-$.

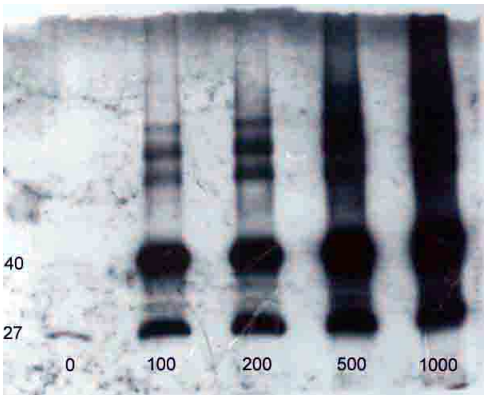

Figure 2.2 Western blot analysis of $ONOO^-$ treated CK with anti-3NY antibody

Visual display of the extent of Tyr nitration by the different levels of ONOO- applied to the samples.The numbers 0, 100, 200, 500 and 1000 represent the micromolar concentration of ONNO- in each sample.

Protein Activity Assay

The protocol for performing the activity assay for CK was obtained from Worthington Biochemical Corporation (WBC) at http://www.worthington-biochem.com/CRK/assay.html. Creatine kinase activity in this assay was determined by a coupled enzyme with pyruvate kinase (PK) and lactic dehydrogenase (LDH). Essentially, one activity unit in this assay is defined as the conversion of 1 μM of creatine to creatine phosphate in one minute at room temperature and at pH 8.9.

Cys Quantitation with ThioGlo-1™

ThioGlo-1™ (Figure 2.3) is a reagent that rapidly reacts with free thiols to yield fluorescent adducts. First, a 18.75 mM Na_2HPO_4 buffer solution was prepared. Then, 19.5 µl of each 1 mg/ml protein sample was taken and diluted with 630.5 µl of phosphate buffer for a total of 650 µl. To each of these samples, guanidine-HCl was added for denaturation at a final concentration of 6 M. A 50 mM ThioGlo™ solution was prepared in dimethylformamaide (DMF). 200 µl aliquots of each protein solution treated with different amounts of $ONOO^-$, were transferred to individual wells in a 96 well plate and 3 µl of ThioGlo-1™ were added to each well for a final concentration of 15 µM ThioGlo-1™ (this was step was done in 3 replicates). The standards were made with N-Acetyl-Cys. The blanks used were first 18.75 mM Na_2HPO_4, second 18.75 mM Na_2HPO_4 plus guanidine-HCl and third 18.75 mM Na_2HPO_4 plus guanidine-HCl plus ThioGlo-1™. The free Cys residues in the samples were determined from the milli fluorescence units extrapolated from the N-acetyl-Cys standard curve. (Figure 2.4)

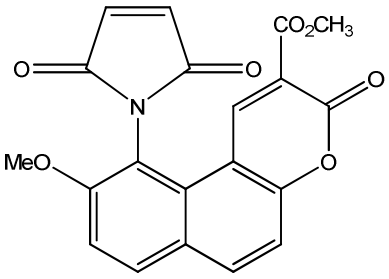

Figure 2.3 ThioGlo-1™ reagent

A)

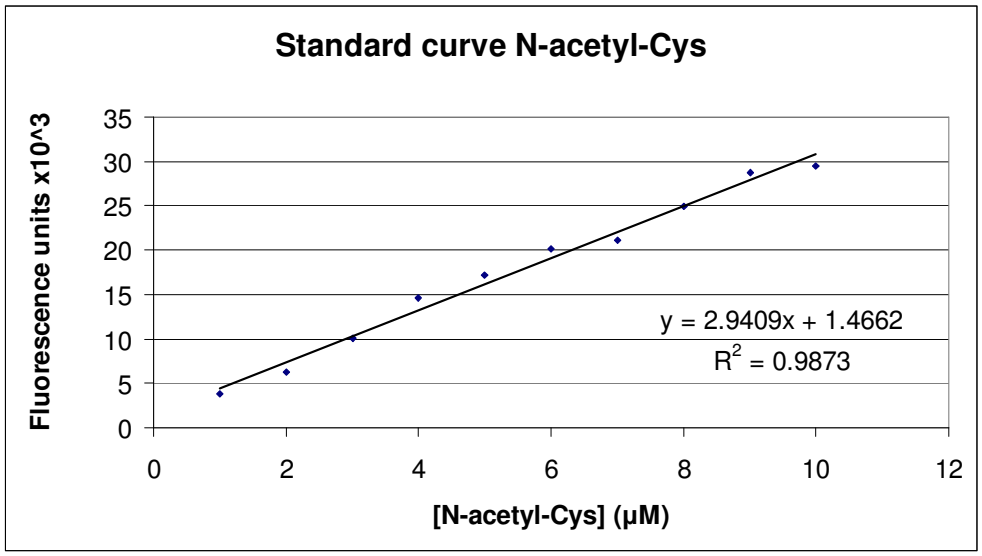

B)

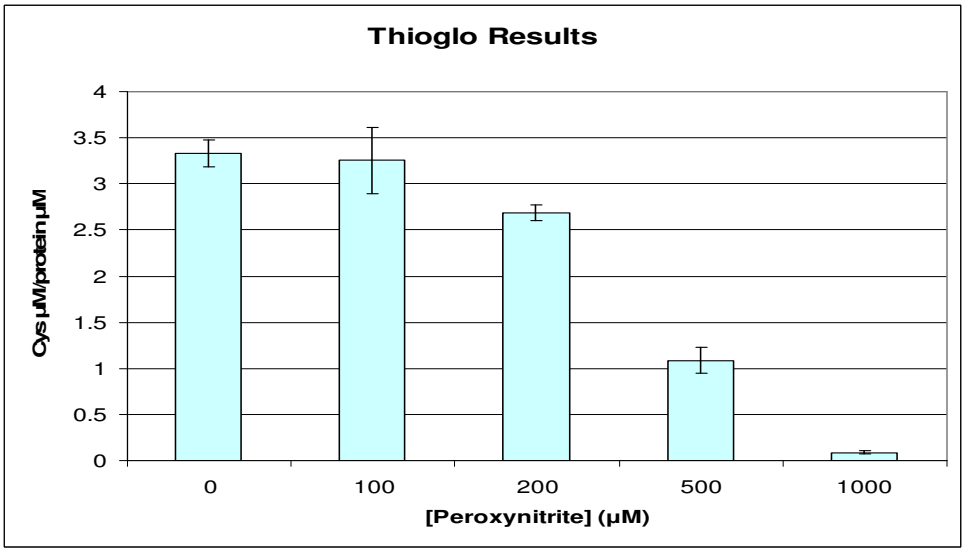

Figure 2.4 ThioGlo-1™ experiment results.

(A) Standard curve obtained from serial dilution of the standard N-acetyl-Cys taken from 10 µM to 1 µM. This standard curve was used to calculate micromoles of free Cys residues in our nitrated CK samples. Loss of free Cys residues due to increased oxidation by ONOO- was demonstrated by this experiment.

In-gel trypsin digestion

Protein bands from the Coomassie-stained gel were cut out and were subjected to an in-gel trypsin digest procedure. The gel bands were first crushed into smaller pieces and washed with 400 µl of a 200mM NH_4HCO_3/MeCN (50:50) solution by incubating them at 40^oC for 45 minutes. The previous wash step was repeated twice by switching the wash solution until all the blue color was washed off the gel pieces. Then, the final wash solution was removed and replaced with 200 µl of 200 mM NH_4HCO_3 buffer and 20 µl of 200 mM DTT for reduction of disulfide bonds. The samples were incubated at 55.9^oC for exactly 30 min at this step. Then, 20 µl of 500 mM IAA were added to each tube and incubated at room temperature for another 30 min for alkylation of free thiols. Following this step, all the solution was removed and 200 µl of wash solution were added to the tubes and were incubated for 1 hour. Then, the wash solution was removed and 200 µl of pure MeCN were added to dehydrate the gel pieces. Finally, 2 µg of trypsin were added to each sample in ~ 50 to 60 µl of 50 mM NH_4HCO_3 and incubated at 37^oC overnight. The digested protein samples were saved for mass spectrometry analysis.

Mass spectrometry analysis

Solution digests were analyzed by nanoHPLC-ESI-MS/MS on either a Thermoelectron LCQ Duo or a Thermoelectron Classic ion trap mass spectrometer, both equipped with a nanoelectrospray source (Thermoelectron, Waltham, MA). Separation of the tryptic peptides was achieved prior to MS/MS analysis on an in-house packed C18 Biobasic stationary phase (Thermoelectron, Waltham, MA)

nanoflow column (300 A, 10 cm x 75 μm, 15 μm tip size) (New Objective, Woburn, MA). The following chromatographic conditions were applied: mobile phase A: 0.1% formic acid in water, mobile phase B: 0.1% formic acid in acetonitrile. The flow rate was adjusted to 0.5 μl/min with the chromatographic flow delivered by either an Ultraplus 2 pump after 1:20 split (Microtech Inc, CA) or directly by an Xtreme simple nanoflow pump (Microtech Inc., CA). The gradient profile applied to the separation of peptides from in-gel digests included the following steps for mobile phase B: 0 to 5 minutes held at 10%, then linearly increased to 60% between 5 and 45 minutes; held at 60% until 50 minutes before being readjusted to the initial equilibration conditions for the next run (15 minutes). The following instrument conditions were used for the mass spectrometer: number of microscans = 3, length of microscans = 200 ms, capillary temperature = 160 $^{\circ}$C, spray voltage = 1.9 kV, capillary voltage = 35, tube lens offset = -14V. The tuning for both mass spectrometers was performed using a static nanospray setup with a 5 μM solution of angiotensin 1 (MW = 1296.5 Da) infused by a picotip emitter (New Objective) (13). The data acquisition was performed in a data-dependent manner such that an MS scan was followed by 3 or 4 MS/MS scans of the 3 or 4 most intense peaks with the normalized collision energy for MS/MS set at 35% and the isolation width of 2.0 m/z. A minimal signal threshold of 2 x 10^6 was set for acquiring the MS/MS data. Additionally, the dynamic exclusion option was enabled with the following parameters: repeat count = 3, repeat duration = 5 ms, exclusion list size = 25, exclusion mass width = 3.

Protein Identification

The MS/MS data were subjected to a protein database search using the Bioworks 3.1 software (Thermoelectron). The most recently updated non-redundant NCBI protein database was used for the searches when downloaded from ftp.ncbi.nlm.nih.gove/blast/db (13) with the following amino acid modifications included in the search options: oxidation of Met (+16 amu; amu = atomic mass units), alkylation of cysteine (+57 amu) and nitration of tyrosine (+45 amu). The protein was identified with a 77 % sequence coverage, where only Tyr 82 was found to be nitrated in these *in-vitro* studies.

2.4 Results

Previous *in-vivo* studies in cardiac muscle indicated that CK is one of the main targets for protein Tyr nitration in the heart (9). CK was also found to be nitrated in skeletal muscle at the same time these experiments were being conducted (11). The goal of this project was to study in better detail, a protein from the previous list of proteins found to be nitrated *in-vivo*. CK was of interest because of its importance in energy metabolism.

Commercially available CK was treated with various concentrations of $ONOO^-$. As expected, increasing concentrations of $ONOO^-$ resulted in increased protein oxidation levels. This was observed both by Western Blot analysis with a monoclonal anti-3-NY antibody, which showed Tyr nitration, and ThioGlo-1 analysis, which showed Cys oxidation. We also tested the activity of oxidized CK by $ONOO^-$ and found that results were in agreement with our hypothesis that increased levels of protein

oxidation result in increased loss of activity. There was a linear correlation between the oxidant concentration in the samples to loss of CK activity in the samples (Figure 2.5).

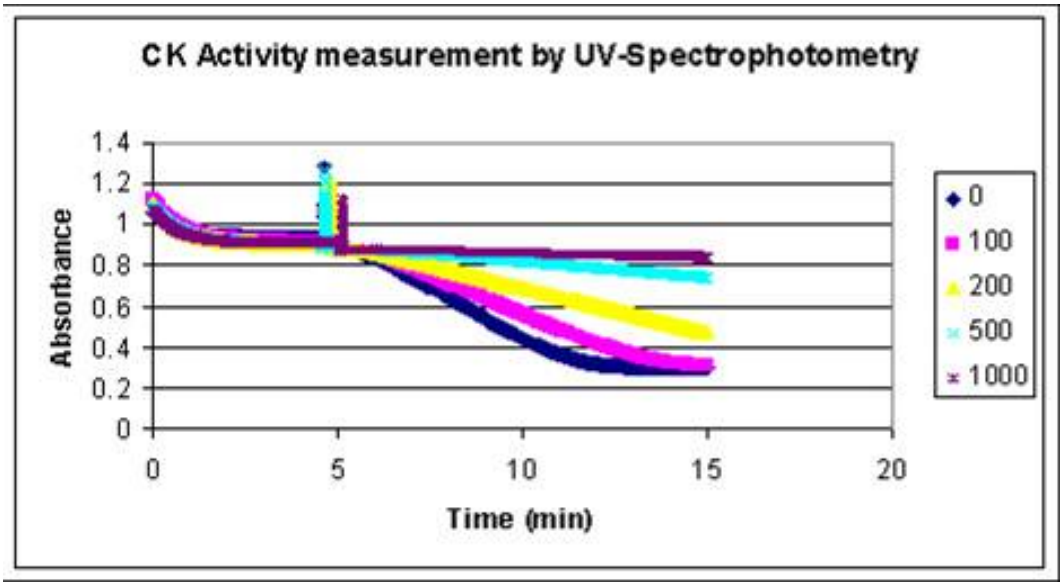

Figure 2.5 Measurement of CK activity

CK activity is defined as the conversion of 1 µM of creatine to creatine phosphate in 1 min at 25oC with the consumption of NADH. Here, we measured NADH consumption at 340 nm in a 20 minute frame. Here, there is a clear indication that activity (NADH consumption) decreases with increased levels of nitration.

Through mass spectrometry analysis, we identified CK with a sequence coverage of 77% (Figure 2.6), where nine Tyr out of ten residues were accounted. Only Tyr^{82} was found to be nitrated *in-vitro* as opposed to Tyr^{14} and Tyr^{20} found to be nitrated *in-vivo* studies in skeletal muscle proteins (11). Four Cys residues out of four Cys residues were accounted for, Cys^{74}, Cys^{146}, Cys^{254} and Cys^{283}. However, when we searched for Cys + 16 for sulfenic acid (Cys-SOH), Cys + 32 for sulfinic acid

(Cys-SO_2H) and Cys + 48 for sulfonic acid (Cys-SO_3H) in our mass spectrometry data, we only found Cys^{283} oxidized to sulfonic acid, although, loss of Cys residues was found to increase to near complete loss by ThioGlo-1™ with increasing levels of $ONOO^-$. This can be explained by the fact that mass spectrometry analysis was conducted under reducing conditions and therefore, cannot account for Cys oxidation due to disulfide bridge formation, or reduction of Cys sulfenic and Cys sulfinic acid to Cys under reducing conditions (14,15).

MPFGNTHNKF KLNYKPEEEY PDLSKHNNHM AKVLTLELYK KLRDKETPSG FTVDDVIQTG
VDNPGHPFIM TVGCVAGDEE SYEVFKELFD PIISDRHGGY KPTDKHKTDL NHENLKGGDD
LDPNYVLSSR VRTGRSIKGY TLPPHCSRGE RRAVEKLSVE ALNSLTGEFK GKYYPLKSMT
EKEQQQLIDD HFLFDKPVSP LLLASGMARD WPDARGIWHN DNKSFLVWVN EEDHLRVISM
EKGGNMKEVF RRFCVGLQKI EEIFKKAGHP FMWNQHLGYV LTCPSNLGTG LRGGVHVKLA
HLSKHPKFEE ILTRLRLQKR GTGGVDTAAV GSVFDVSNAD RLGSSEVEQV QLVVDGVKLM
VEMEKKLEKG QSIDDMIPAQ KL

Figure 2.6 Creatine Kinase protein amino acid sequence.

The sequences covered by mass spectrometry analysis are highlighted in red. The oxidized amino acids Tyr82 and Cys283 are highlighted in blue.

2.5 Discussion/Conclusions

In-vivo, skeletal muscle cytosolic CK was found to undergo nitration of both Tyr^{14} and Tyr^{20} but, Tyr residues at positions 39, 82, 125, 140, 173, 174, and 279 were not affected. In contrast, *in-vitro* exposure of CK to peroxynitrite was found to nitrate exclusively Tyr^{82}. This illustrates the continuous dilemma where *in-vitro* studies may not always be a reflection of what actually occurs *in-vivo*. These significant differences in nitration patterns between *in-vivo* and *in-vitro* samples were

not caused by any analytical discrimination against specific Tyr- and/or 3-NY-containing peptides because in both studies, we got good coverage of remaining unmodified Tyr residues. The distinct patterns of nitration may have been caused by one or a combination of the following factors. (i) Specific nitrated isoforms of CK may be degraded *in-vivo* through the proteasome, known for its ability to degrade proteins exposed to peroxynitrite (16). Specific nitrating agents may nitrate proteins predominantly at specific locations, while generating negligible amounts of 3-NY at other positions. The predominant nitrated species may be susceptible to proteasomal degradation, while the protein isoforms containing the non-specific nitration sites may be subject to accumulation with time and therefore detected by proteomic methods. (ii) I*n-vitro* reaction conditions were not physiological. The buffer used was 50 mM Tris/HCl-5 mM $MgCl_2$ at pH 8. These non-physiological conditions may cause some conformational changes in CK, making other regions more susceptible to oxidation, compared with *in vivo* conditions. (iii) There are other nitrating species *in-vivo,* in addition to peroxynitrite. Some evidence for protein nitration through $^{\cdot}NO_2$ has been provided (17), and to date it is not known to which extent peroxynitrite, peroxynitrite -CO_2 adduct, $^{\cdot}NO_2$, and/or potentially other hitherto unknown nitrating species, are responsible for protein nitration *in-vivo*. (iv) *In-vivo, CK* may exist in complexes with other proteins or small molecules such as phosphocreatine and ATP. These complexes may be largely responsible for the chemical selectivity for Tyr nitration. Such phenomena were demonstrated in previous experiments with calmodulin (CaM), where CaM complexation with calmodulin-binding peptides and

proteins, melittin and nitric oxide synthase 2, have changed its susceptibility to oxidation by peroxynitrite (18). In addition, Mihm *et al.*(19) have recognized a protective effect of phosphocreatine and ATP on CK toward oxidation by peroxynitrite.

To further illustrate how complexation can affect susceptibility to nitration, an earlier study focused on mitochondrial CK oxidation by peroxynitrite, showed evidence of Trp^{264} and Trp^{268} nitration but no Tyr nitration by MALDI-TOF mass spectrometry (20). These findings are different from our results with cytosolic CK, that displayed Tyr nitration both *in-vivo* and *in-vitro*. An important difference found between the cytosolic and mitochondrial isoforms of CK is their aggregation state. Cytosolic CK exists exclusively in dimers, whereas mitochondrial CK exists in octamers. The differential sensitivity of the individual isoforms toward the nitration of Tyr *vs.* Trp, and the differences in the cytosolic isoforms toward nitration *in-vivo* and *in-vitro*, highlight the importance of protein structure and environment on product formation during oxidative stress. One important aspect to note however, is that both CK isoforms (mitochondrial and cytosolic), suffer inactivation in part due to oxidation of a critical Cys residue, Cys^{278} (mitochondria) (20) and Cys^{283} (cytosol) (5).

2.6 References

1. Jacobus, W. E., and Diffley, D. M. (1986) J Biol Chem 261, 16579-16583

2. Konorev, E. A., Hogg, N., and Kalyanaraman, B. (1998) FEBS Lett 427, 171-174

3. Aksenov, M., Aksenova, M., Butterfield, D. A., and Markesbery, W. R. (2000) J Neurochem 74, 2520-2527

4. Mahajan, V. B., Pai, K. S., Lau, A., and Cunningham, D. D. (2000) Proc Natl Acad Sci U S A 97, 12062-12067

5. Sethuraman, M., McComb, M. E., Heibeck, T., Costello, C. E., and Cohen, R. A. (2004) Mol Cell Proteomics 3, 273-278

6. Miura, T., Muraoka, S., and Fujimoto, Y. (1999) Chem Biol Interact 123, 51-61

7. Miura, T., Muraoka, S., and Fujimoto, Y. (2001) Chem Biol Interact 134, 13-25

8. Kanski, J., Alterman, M. A., and Schöneich, C. (2003) Free Radic Biol Med 35, 1229-1239

9. Kanski, J., Behring, A., Pelling, J., and Schöneich, C. (2005) Am J Physiol Heart Circ Physiol 288, H371-381

10. Kenyon, G. L. (1996) Nature 381, 281-282

11. Kanski, J., Hong, S. J., and Schöneich, C. (2005) J Biol Chem 280, 24261-24266

12. Beckman, J. S., Beckman, T. W., Chen, J., Marshall, P. A., and Freeman, B. A. (1990) Proc Natl Acad Sci U S A 87, 1620-1624

13. Ducret, A., Van Oostveen, I., Eng, J. K., Yates, J. R., 3rd, and Aebersold, R. (1998) Protein Sci 7, 706-719

14. Carballal, S., Alvarez, B., Turell, L., Botti, H., Freeman, B. A., and Radi, R. (2007) Amino Acids 32, 543-551

15. Jeong, W., Park, S. J., Chang, T. S., Lee, D. Y., and Rhee, S. G. (2006) J Biol Chem 281, 14400-14407

16. Grune, T., Blasig, I. E., Sitte, N., Roloff, B., Haseloff, R., and Davies, K. J. (1998) J Biol Chem 273, 10857-10862

17. Prütz, W. A., Monig, H., Butler, J., and Land, E. J. (1985) Arch Biochem Biophys 243, 125-134

18. Hühmer, A. F., Nishida, C. R., Ortiz de Montellano, P. R., and Schöneich, C. (1997) Chem Res Toxicol 10, 618-626

19. Mihm, M. J., and Bauer, J. A. (2002) Biochimie 84, 1013-1019

20. Wendt, S., Schlattner, U., and Wallimann, T. (2003) J Biol Chem 278, 1125-1130

3. *In-vivo* proteomic study of nitrated proteins in cardiac tissue as a function of aging

3.1 List of abbreviations used inside the text

- ROS: Reactive oxygen species
- RNS: Reactive nitrogen species
- BN-F1: Fisher 344 Brown Norway F1 rats
- IEF: Isoelectric focusing
- HPLC-ESI-MS/MS: High performance liquid chromatography-electrospray ionization tandem mass spectrometry.
- 3-NY: 3-nitrotyrosine
- NO: nitrogen monoxide
- $ONOO^-$: peroxynitrite
- Mn-SOD: manganese superoxide dismutase
- GR: glutathione reductase
- SR: sarcoplasmic reticulum
- RyR: ryanodine receptor
- SERCA: sarco/endoplasmic reticulum Ca-ATPase
- 2DE: two-dimensional gel electrophoresis
- 1D SDS-PAGE/1DE: one dimensional sodium dodecyl sulfate polyacrylamide gel electrophoresis.
- N-RAP: nebulin-related anchoring protein
- BSA: bovine serum albumin
- DTT: dithiothreitol
- CHAPS: 3-[(3-Cholamidopropyl)dimethylammonio]-1-propanesulfonate
- PVDF polyvinylidene difluoride
- TBST: tris-buffered saline with tween
- RP nano LC MS: Reverse phase nano liquid chromatography mass spectrometry

3.1 Introduction

Protein nitration may affect protein structure, function, and turnover. An illustrative example is the mitochondrial manganese superoxide dismutase (Mn-SOD), which catalyzes the disproportionation of superoxide to O_2 and H_2O_2. Mn-SOD was found to undergo almost complete inhibition when nitrated at Tyr^{34} (1-3). The crystal structures of native Mn-SOD and nitrated Mn-SOD were found to be closely

superimposable; however, the nitration of Tyr^{34} disrupts the H-bonding network at the active site, which may be the reason for protein inactivation (1). A crystal structure was also obtained for nitrated glutathione reductase (GR) (4). Here, the nitration of two Tyr residues, Tyr^{106} and Tyr^{114}, was found to be responsible for protein inactivation. Comparison of the crystal structures of both native and nitrated GR shows that specifically the hydroxy group of 3-NY^{114} appears to be rotated by ~60^{o} due to the creation of a local negative charge that changes the electrostatics of the active site (4).

There is a significant age-dependent accumulation of 3-NY on proteins in cardiac (5) and skeletal muscle (6). Cardiac proteins are highly susceptible to nitration due to the periodic formation of NO and superoxide, mediating myocardial contractility (7-9). NO can regulate cardiac function through the S-nitrosation of effector molecules such as Ca^{2+} ion channels, in particular the plasmalemmal L-type calcium channel and the sarcoplasmic reticulum (SR) ryanodine receptor (RyR) (9,10). Through intermediary formation of peroxynitrite, NO also indirectly regulates the activity of another Ca^{2+}-transporting enzyme, the sarco/endoplasmic reticulum Ca-ATPase (SERCA) (11).

Earlier, we had communicated two-dimensional gel electrophoresis (2DE) experiments targeted at the identification of cardiac proteins susceptible to nitration, and a list of 48 putatively nitrated proteins was assembled (5). However, due to the known limitations of the 2DE method (limited sample load, discrimination against membrane proteins and proteins of very low and very high molecular weight and pI),

only one nitration site was actually located by MS/MS (for the electron transfer flavoprotein). In order to overcome the limitations of traditional 2DE, we have now applied a combination of solution isoelectric focusing, 1D SDS-PAGE and reversed-phase chromatography coupled to nanoelectrospray ionization-MS/MS analysis to identify cardiac proteins subject to age-dependent nitration. We will demonstrate here that biological aging results in the accumulation of 3-NY on distinct protein sequences, including a zinc-finger and nebulin-related anchoring protein (N-RAP). Of particular interest is also the accumulation of 3-NY on Tyr ^{491} of neurofibromin, observed for cardiac tissue from both young and old rats.

3.2 Experimental

Materials

The research protocol was approved by the University of Kansas Animal Care Facility; we used 17 Fisher 344/BN F1 rats (ten 34 months old and seven 5 months old) These rats were housed in a 12 hour light/dark cycle with food and water provided ad libitum. The animals were decapitated, the hearts were removed and frozen immediately at –80^{o}C and stored until needed.

For 1D gel electrophoresis experiments (1DE), Tris-glycine sample and running buffers and pre-cast 4-20% gels were obtained from Invitrogen (Carlsbad, CA). For Western blotting experiments, TBST buffer was prepared by adjusting a solution of 150mM NaCl and 20mM Tris, pH 7.4, prior to the addition of 0.05% (v/v) Tween 20. The anti-3-nitrotyrosine (anti-3-NY) monoclonal antibody, clone 1A6, was purchased from Upstate, Inc. (Charlottesville, VA), and the anti-mouse IgG Fc-

peroxide-conjugated antibody from Pierce Biotechnology (Rockford, IL). X-ray film was purchased from MIDSCI (St. Louis, MO). Powdered milk was purchased from Nestlé-Carnation (Glendale, CA). Polyvinylidine fluoride (PVDF) membranes were purchased from Millipore (Billerica, MA). ECL-Plus reagents were purchased from GE Healthcare (Piscataway, NJ). Sequencing grade trypsin was purchased from Fisher Scientific (Pittsburg, PA). Protein concentration was quantified with the reducing-agent compatible BCA Protein Assay Kit, purchased from Pierce Biotechnology (Rockford, IL). Complete EDTA-free protease inhibitor cocktail tablets were purchased from Roche Applied Science (Indianapolis, IN). Bovine serum albumin (BSA), sodium dodecyl sulfate (SDS), dithiothreitol (DTT) and iodoacetamide were obtained from Sigma Chemicals (St. Louis, MO), and the 3/10 ampholite solution for solution isoelectric focusing was provided by Bio-Rad, Inc. (Hercules, CA).

Sample Preparation

For each analysis proteins were pooled from either 2 or 3 hearts from 34 month or 5 month old rats, respectively. The hearts were cut into small pieces, and the tissue rinsed twice in tissue wash buffer (50mM Tris, 150mM NaCl, 10µg/ml protease inhibitor cocktail mixture) to remove as much hemoglobin as possible. Subsequently, the tissue was homogenized in 25 ml of lysis solution (6M urea, 2% CHAPS, 10mM Tris, 0.5mM PMSF, 10µg/ml protease inhibitor cocktail mixture, 20 mM DTT, pH 7.5) using an ultra-turrax T8 homogenizer (Fisher, Pittsburg, PA). Finally, the homogenate was centrifuged at 5,500 g at 4^{o}C for 30 minutes. The supernatant was

collected for analysis, taking care that the pellet was not disturbed during sampling of the supernatant.

1DE and Western Blot Analysis

Either total cardiac protein or proteins obtained in the individual fractions after solution isoelectric focusing were precipitated (see below). The precipitated proteins were redissolved in 100µl of 50mM NH_4HCO_3 buffer, pH 7.4, containing 0.02% SDS. Protein concentrations were measured with the BCA Protein Assay Kit according to the manufacturer's protocol. Protein samples were mixed with equal volumes of sample buffer, boiled for 5 minutes in the presence of 20mM DTT, and cooled for another 5 minutes prior to separation on precast 4-20% gels for 75 minutes at 5^{o}C, at a constant voltage of 200V.

For Western blot analysis, proteins were transferred from the gels onto 0.45µm polyvinylidene difluoride (PVDF) membranes at a constant voltage of 100V for 2hrs. The PVDF membranes were blocked with 5% (w/v) milk-TBST buffer for 1hr at room temperature. The membranes were incubated overnight at 3^{o}C with the primary anti-3-NY antibody (1:4000 dilution in 5% (w/v) milk-TBST buffer). Subsequently, the membranes were washed with 5%(w/v) milk-TBST buffer twice for 15 minutes prior to incubation with the anti-mouse IgG Fc-peroxide-conjugated secondary antibody (1:10,000 dilution in 5% (w/v) milk-TBST buffer) for 1hr at room temperature. The membranes were thoroughly washed with 2 short washes of 5% (w/v) milk-TBST buffer, followed by three 30 minute washes with TBST buffer alone. The immunoblots were visualized by chemiluminescence using the ECL kit

(GE Healthcare, Piscataway, NJ) according to the manufacturer's protocol. The images were captured on a Kodak X-ray film using a Kodak developer/fixer kit.

The densitometry analysis for both the SDS-PAGE and Western blot was achieved with the Image Quant software (Amersham Biosciences; Pittsburgh, PA).

Solution Phase Isoelectric Focusing (IEF)

To the supernatant of the homogenized and centrifuged cardiac tissue, 500µl of 3/10 carrier ampholite solution were added. The solution was slowly mixed for a few minutes and was loaded into a Bio-Rad Rotofor mini-focusing chamber (Figure 3.2) according to the manufacturer's protocol. Briefly, the anode membrane was conditioned in 0.1 M H_3PO_4 and the cathode membrane was conditioned in 0.1 M NaOH overnight. The apparatus was assembled according to the guidelines provided by the manufacturer. A total of 18 ml containing between 10-15mg/ml protein sample was applied to the Rotofor focusing chamber and fractionated at a constant power setting (12 W) at 4^{o}C. The voltage stabilized at 524 V after about 30-40 minutes and increased to 2400 V after 3 hours when protein fractionation was stopped. The samples were then collected into 20 test tubes, each representing a discrete pH region. These samples were processed further immediately.

Reduction, Alkylation and Protein Precipitation

50µl of each Rotofor fraction were adjusted to a volume of 100µl with 50mM NH_4HCO_3 buffer, pH 7.4. The fractions were treated with 2mM DTT for 30 min at 37^{o}C to reduce disulfide bonds, followed by alkylation with 5mM iodoacetamide for 30 min at room temperature. Subsequently, proteins were precipitated overnight at -

20°C by addition of 1 ml of pure ethanol to the reaction mixtures. The precipitated proteins were collected by centrifugation at 13,000g for 5 minutes. The supernatants were discarded and the solid protein pellets were saved for further processing.

Solution Digestion

Precipitated proteins were collected and re-dissolved in 100-200µl of 50mM NH_4HCO_3, pH7.4. To each sample, 2µg of trypsin were added and digestion was carried out overnight at 37°C. The digests were then analyzed by nanoHPLC-electrospray ionization (NSI)-tandem mass spectrometry (MS/MS).

Nanoelectrospray ionization-tandem mass spectrometry (NSI-MS/MS) analysis

Solution digests were analyzed by nanoHPLC-ESI-MS/MS on either a Thermoelectron LCQ Duo or a Thermoelectron Classic ion trap mass spectrometer, both equipped with a nanoelectrospray source (Thermoelectron). Separation of the tryptic peptides was achieved prior to MS/MS analysis on an in-house packed C18 Biobasic stationary phase (Thermoelectron, CA) nanoflow column (300 A, 10 cm x 75 µm, 15 µm tip size) (New Objective, Woburn, MA). The following chromatographic conditions were applied: mobile phase A: 0.1% formic acid in water, mobile phase B: 0.1% formic acid in acetonitrile. The flow rate was adjusted to 0.5 µl/min with the chromatographic flow delivered by either an Ultraplus 2 pump (after 1:20 split; Microtech Inc, CA) or directly by an Xtreme simple nanoflow pump (Microtech Inc., CA). The gradient profile applied to the separation of peptides from in-gel digests included the following steps for mobile phase B: 0 to 5 minutes held at 15%, then linearly increased to 70% between 5 and 35 minutes; held at 70% until 40

minutes before being readjusted to the initial equilibration conditions. For peptides recovered from solution digests, the increase in composition of B from 15 to 70% was instead accomplished over a much slower time period of 95 minutes such that the total run time was extended to 2 hours for each sample. The following instrument conditions were used for the mass spectrometer: number of microscans = 3, length of microscans = 200 ms, capillary temperature = 160 $^{\circ}$C, spray voltage = 41 V, tube lens offset = -10V. The tuning for both mass spectrometers was performed using a static nanospray setup with a 5 μM solution of angiotensin 1 (MW = 1296.5 Da) infused by a picotip emitter. The data acquisition was performed in a data-dependent manner such that an MS scan was followed by 3 or 4 MS/MS scans of the 3 or 4 most intense peaks with the normalized collision energy for MS/MS set at 35% and the isolation width of 2.0 m/z. A minimal signal threshold of 2 x 10^6 was set for acquiring the MS/MS data. Additionally, the dynamic exclusion option was enabled with the following parameters: repeat count = 3, repeat duration = 5 ms, exclusion list size = 25, exclusion mass width = 3.

Protein Identification

The MS/MS data were subjected to a protein database search using the Bioworks 3.1 software (Thermoelectron). The most recently updated non-redundant NCBI protein database was used for the searches when downloaded from ftp.ncbi.nlm.nih.gove/blast/db with the following amino acid modifications included in the search options: oxidation of Met (+16 amu; amu = atomic mass units), alkylation of cysteine (+57 amu) and nitration of tyrosine (+45 amu). Additionally,

the observed MS/MS data of proteins were manually examined for the presence of 3-NY-containing peptides.

Database Search and data interpretation

The following criteria were set for positive identification of nitrated peptides:

1) For singly, doubly, and triply charged peptides, we set Xcorr values (the cross-correlation value from the search for well matched peptides (12)) of $\geq$ 1.0, $\geq$ 2.0, 2.5, respectively.

2) The major peaks in the MS/MS spectra needed to be unambiguously assigned to peptide fragments of the nitrated protein.

3) Positive identification of nitrated proteins is contingent upon identification of at least one non-nitrated, native peptide from the respective protein besides the 3-NY containing peptide.

Once a list of proteins of interest was compiled, Protein Prospector v 4.0.6 MS-product (http://prospector.ucsf.edu/ucsfhtml4.0/msprod.htm) was used to analyze the data manually. During this procedure, we were able to find peaks corresponding to internal fragments, and neutral losses of H_2O, NH_3 and CO. The spectra with all major peaks labeled unambiguously identified the nitrated peptides found during the analysis.

3.3 Results

1D SDS-PAGE and Western blot analysis (Figure 3.1) confirmed our earlier data (5) that nitrated proteins are present in cardiac tissue, and that their abundance increases with age. Based on densitometry analysis, ca. 1.5 to 2 fold increase in

protein nitration, depending on the animal set, when 34 months old animals were compared to 5 months old animals. The data were normalized to account for some differences of protein load between the individual lanes.

(A) (B)

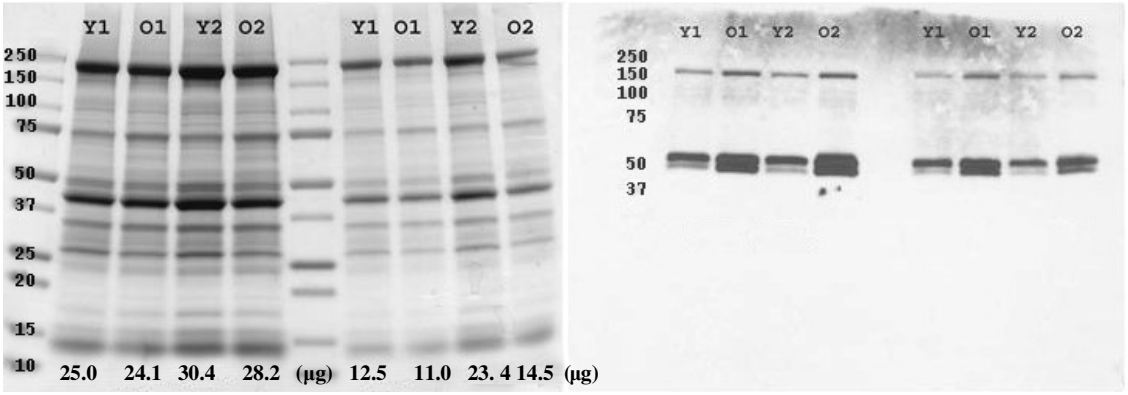

Figure 3.1 SDS-PAGE and Western blot analysis of whole heart homogenates from 4 different animals.

(A) total protein (by coomassie blue staining) and (B) the levels of 3-NY (using a anti-3-NY antibody). Four animals are represented in this figure, two 5 months old rat hearts (Y1, Y2) and two 34 months old rat hearts (O1 ,O2). The protein amounts in each lane were determined by densitometry analysis and normalized to conclude that there is a 1.5 to 2.0 fold increase in nitration with aging.

In the present work we applied solution IEF to pre-fractionate proteins prior to tryptic digestion and analysis of the resulting peptides with nano-HPLC-NSI-MS/MS (Figure 3.2). Solution IEF permits higher protein loads compared to gel IEF, the first step in a traditional 2DE, enhancing the likelihood for positive identification of

nitrated peptides. The initial protein amount applied to solution IEF was calculated based on the total amount of protein present in the homogenate.

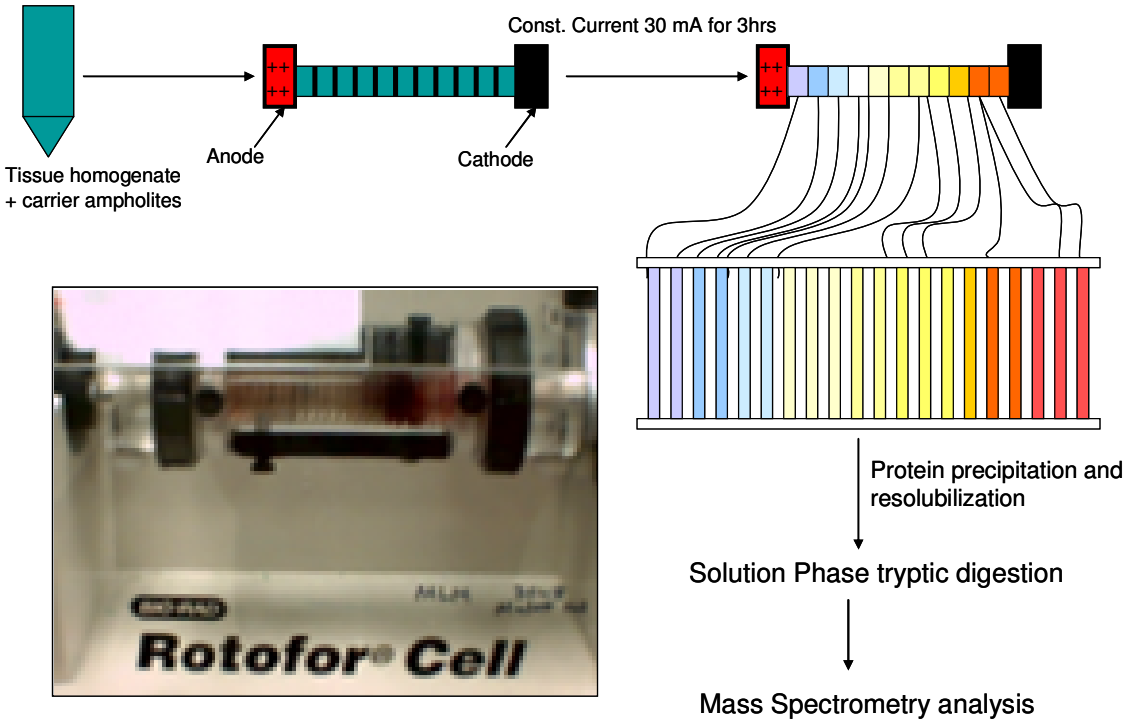

Figure 3.2 Solution phase isoelectric focusing scheme.

Protein resolution according to pI, in cardiac tissue homogenate of both young (5 months old) and old (34 months old) rats.

After IEF, aliquots from each of the collected fractions were used for pH measurements, and others were applied to 1DE analysis and recovered proteins were quantified by densitometry. Every fraction contained a different protein load, varying from ~1.4 mg/ml to ~56 mg/ml. The pH of the recovered fractions changed gradually from 3 to 10, where the pH changed by 0.5 or 1 unit every two or three fractions, as was expected based on the separation conditions used. The pIs of the identified

nitrated proteins did not necessarily match the pH of the rotofor fraction from which they were recovered. The latter may have various reasons such as additional post-translational modifications, or in vivo proteolysis yielding protein fragments rather than intact protein. Our 2 hour nanoHPLC separation prior to MS/MS analysis (Materials and Methods section) routinely yielded about 2500 identified peptides per fraction. Table 1 summarizes our MS/MS analysis of cardiac proteins from 5 and 34 months old rats. A total of 10 nitrated proteins were identified. Two of these, myosin heavy chain polypeptide 7 and neurofibromin were observed in cardiac homogenates from both ages. For each protein on the list, we were able to detect at least one 3-NY-containing peptide along with a number of non-nitrated peptides. Hence, identification of some native peptides in addition to the nitrated peptides confirmed the presence of the identified protein in the respective IEF fraction, improving the reliability of the protein identification.

We note that the molecular weights of the nitrated proteins identified by MS/MS analysis (Table 1), and those of the immunoresponsive bands in the Western blot analysis (Figure 1B) do not correlate. There are several possible reasons for this: (i) in vivo proteolysis of nitrated proteins (see also above); (ii) not all nitrated proteins detected by MS/MS will display immunoresponsive spots on the Western blot due to the fact that the anti-3-NY antibody can discriminate against selected nitrated proteins (13); (iii) not all immunoresponsive proteins on the Western blot will contain sufficient yields of 3-NY for the positive MS/MS identification of nitrated peptides. It is also important to note that the table of identified proteins by MS/MS in this paper is

very different from the list that was generated by traditional 2DE analysis in our previous study (5). The only protein that was found in common in both studies was Tropomyosin 1, α chain. This may again be due to the inherent differences in the methods that were applied to each study.

MS/MS spectra are shown for all of the proteins identified in the samples from 34 months old rat cardiac tissue. These include the nitrated peptide Glu[5968]-Arg[5978] (Figure 3.3) from nebulin-related anchoring protein (N-RAP) isoform C (GenInfo accession number 109468170), nitrated at Tyr[5969], the nitrated peptide

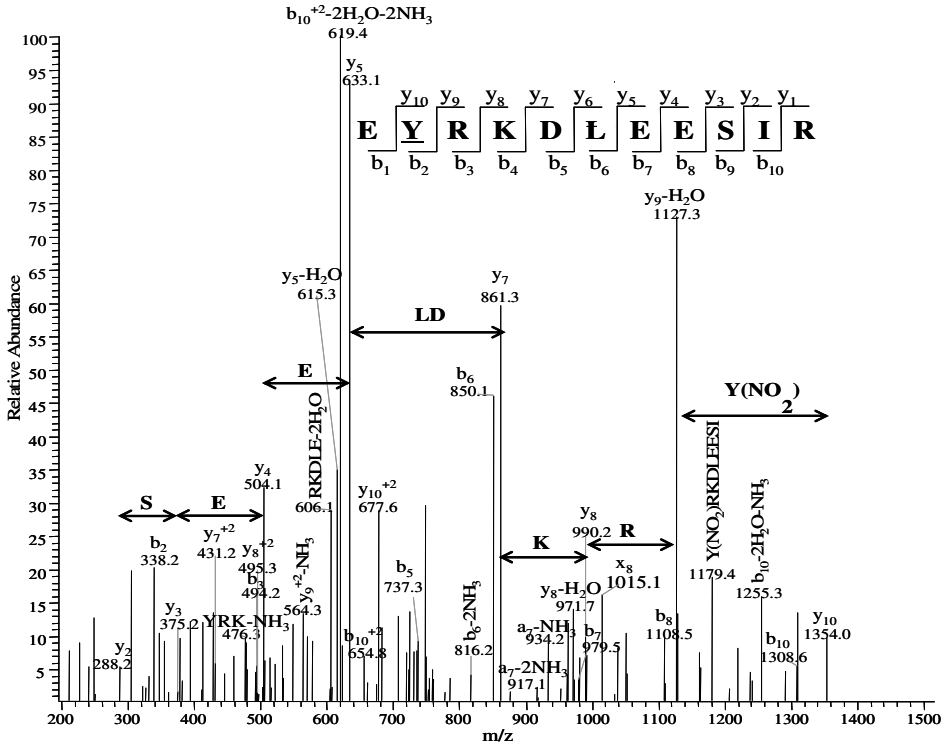

Figure 3.3 Representative MS/MS spectrum of nebulin-related anchoring protein (N-RAP)

Displayed is the MS/MS of the nitrated peptide sequence Glu5968-Arg5978 detected for nebulin-related anchoring protein (N-RAP), in cardiac tissue of 34 months old Fisher 344 BN-F1 rats. Here we have highlighted the y-ions covered in the series, y2-y10.

Sample	*Protein*	*GI no.* [a]	*Molecular mass (KDa)*	*% Coverage*	*No. of identified peptides*	*Nitrated peptide*	*Sequence*	*Cellular location and function*
5 months old rat cardiac tissue	Myosin heavy chain polypeptide 7	8393807	222.9	5.27	9	WLPV<u>Y</u>NAQVVAA<u>Y</u>R	130-143	Cytoskeleton, muscle contraction
	Neurofibromatosis 1	6981264	316.9	1.84	3	SYK<u>Y</u>LLLSMVK	488-498	Cytoskeleton, tumor suppressor protein
	NADH dehydrogenase (Ubiquinone) Fe-S	9506913	12.8	29.31	4	TGTCA<u>Y</u>CGLQFK	101-112	Mitochondria, NADH reduction and oxydation
34 months old rat cardiac tissue	Myosin-5C	109483639	202.2	3.24	3	FAESKLI<u>Y</u>T<u>Y</u>SGILVAMNPYK	91-111	Cytoplasmic, organelle transport
	Myosin heavy chain polypeptide 6	8393804	223.4	5.68	7	ERYAAWMI<u>Y</u>T<u>Y</u>SGLFCVTVNPYK	106-128	Cytoskeleton, converts chemical energy into mechanical energy through the hydrolysis of ATP
	Tropomyosin 1, α isoform e	78000196	32.7	44.72	16	<u>Y</u>EEEIK	221-226	Cytoskeleton, muscle contractionthrough the tropomyosin-troponin-Ca^{2+}system.
	Neurofibromatosis 1 (Neurofibromin)	6981264	316.9	1.17	6	SYK<u>Y</u>LLLSMVK	488-498	Cytoskeleton, tumor suppressor protein
	Cadherin EGF-LAG seven pass G-type receptor 2	22095545	220.0	1.88	2	EPCEN<u>Y</u>MRCVSVLR	460-473	Cell membrane, cell adhesion mediator
	Dynein, cytoplasmic, heavy chain 1	31377489	531.9	0.34	3	QLTA<u>Y</u>MK	665-671	Cytoplasm, cytoplasmic motor transport protein that propels membrane organelles towards (-) ends of polarized microtubules through ATP hydrolysis
	Nebulin-related anchoring protein isoform C (N-RAP)	109468170	771.7	0.57	9	E<u>Y</u>RKDLEESIR	5968-5978	Cytoskeleton, thin filament length and assembly regulation
	Cys2/His2 Zn finger protein (rKr1)	21426789	73.8	6.00	5	LLIKEGQ<u>Y</u>K	282-290	Nucleus, transcriptional regulator
	Myosin heavy chain polypeptide 7	8393807	222.9	16.33	17	WLPV<u>Y</u>NAQVVAA<u>Y</u>R	130-143	Cytoskeleton, muscle contraction

[a] Gen Info accession number.

Table 3.1 List of nitrated proteins identified by solution IEF and NSI-LC-MS/MS in cardiac tissue studies

The study was done on cardiac tissue of 5 months old and 34 months old Fisher 344 BN-F1 rats. The specific nitrated sequences for each protein are shown here.

Glu[106]-Lys[128] (Figure 3.4) from myosin heavy chain polypeptide 6 (GenInfo accession number 8393804), nitrated at both Tyr[114] and Tyr[116], the nitrated peptide

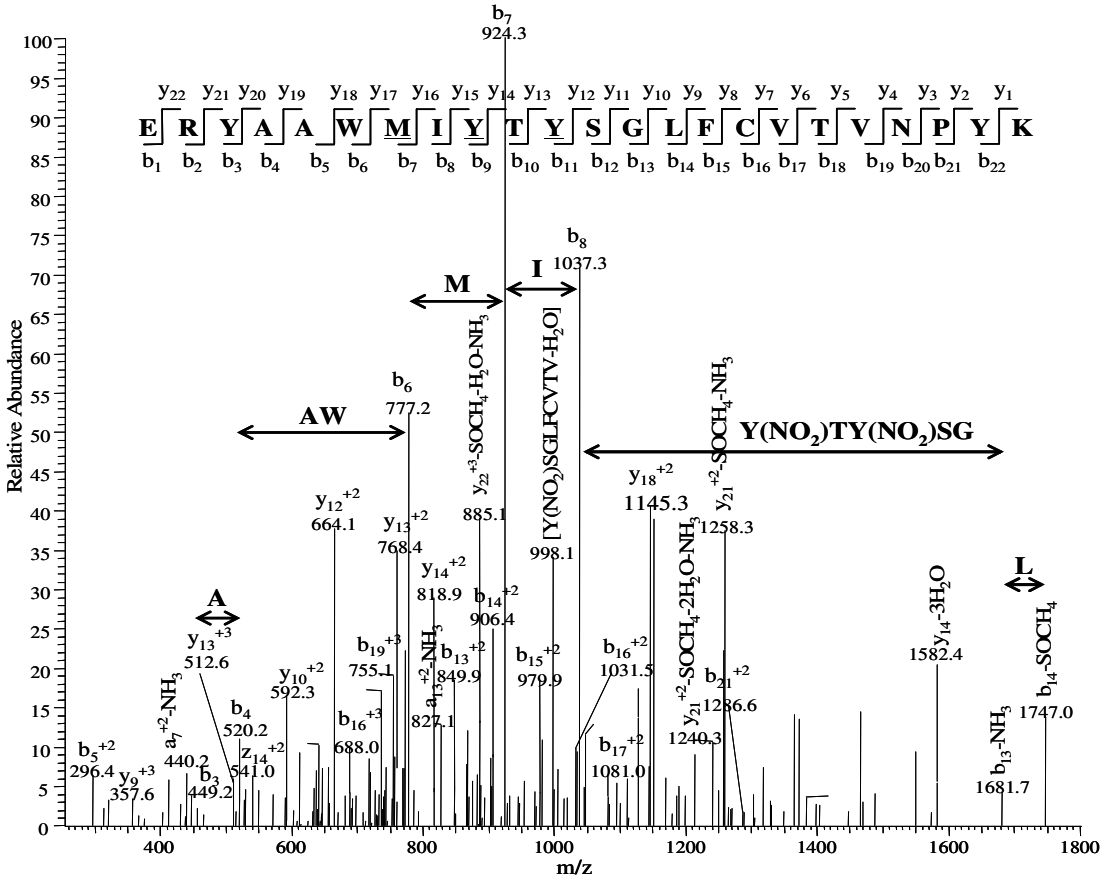

Figure 3.4 Representative MS/MS spectrum of myosin heavy chain polypeptide 6.

Displayed here is the MS/MS spectrum of the nitrated peptide sequence Glu106-Lys128 detected for myosin heavy chain polypeptide 6, in cardiac tissue of 34 months old Fisher 344 BN-F1 rats. Here we have highlighted the b-ions covered in the series, b3-b14.

Tyr[221]-Lys[226] (Figure 3.5) from tropomyosin 1, α isoform e (GenInfo accession number 78000196), nitrated at Tyr[221], the nitrated peptide Ser[488]-Lys[498] (Figure 3.6) from neurofibromatosis 1 (neurofibromin) (GenInfo accession number 6981264),

nitrated at Tyr[491], the nitrated peptide Phe[91]-Lys[111] (Figure 3.7) from Myosin-5C (GenInfo accession number 109483639), nitrated at both Tyr[98] and Tyr[100], the nitrated

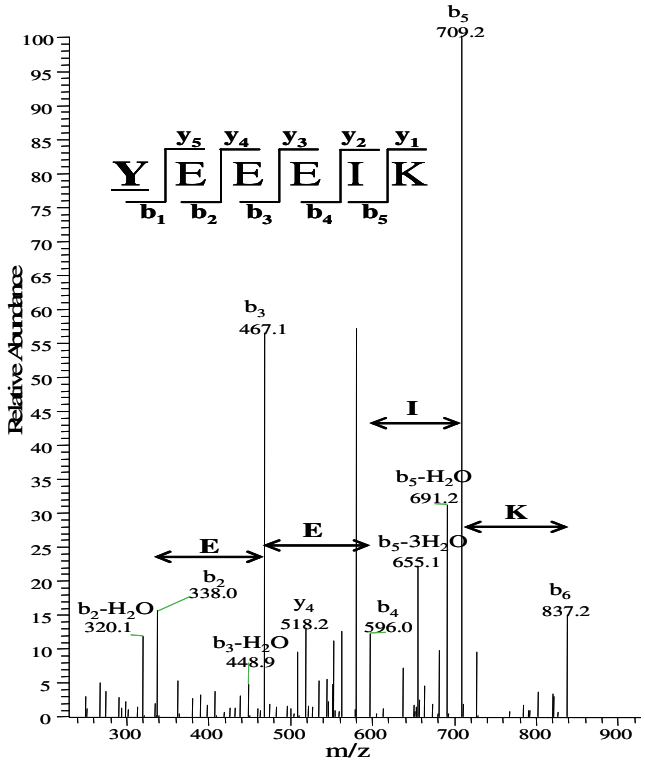

Figure 3.5 Representative MS/MS spectrum of tropomyosin.

Diplayed here is the MS/MS spectrum for the nitrated peptide sequence Tyr221-Lys226 detected for tropomyosin, in cardiac tissue of 34 months old Fisher 344 BN-F1 rats. Here we have highlighted the b-ions covered in the series, b2-b6.

peptide Glu[460]-Arg[473] (Figure 3.8) from Cadherin EGF-LAG seven pass G-type receptor 2 (GenInfo accession number 22095545), nitrated at Tyr[465], the nitrated peptide Gln[655]-Lys[671] (Figure 3.9) from Dynein heavy chain1 (GenInfo accession number 31377489), nitrated at Tyr[659], the nitrated peptide Leu[282]-Lys[290] (Figure 3.10) from Cys2/His2 Zn finger protein (GenInfo accession number 21426789), nitrated at

Tyr[289], and finally, the nitrated peptide Trp[130]-Arg[143] (Figure 3.11) from Myosin heavy chain polypeptide 7 (GenInfo accession number 8393807), nitrated at both Tyr[134] and Tyr[142].

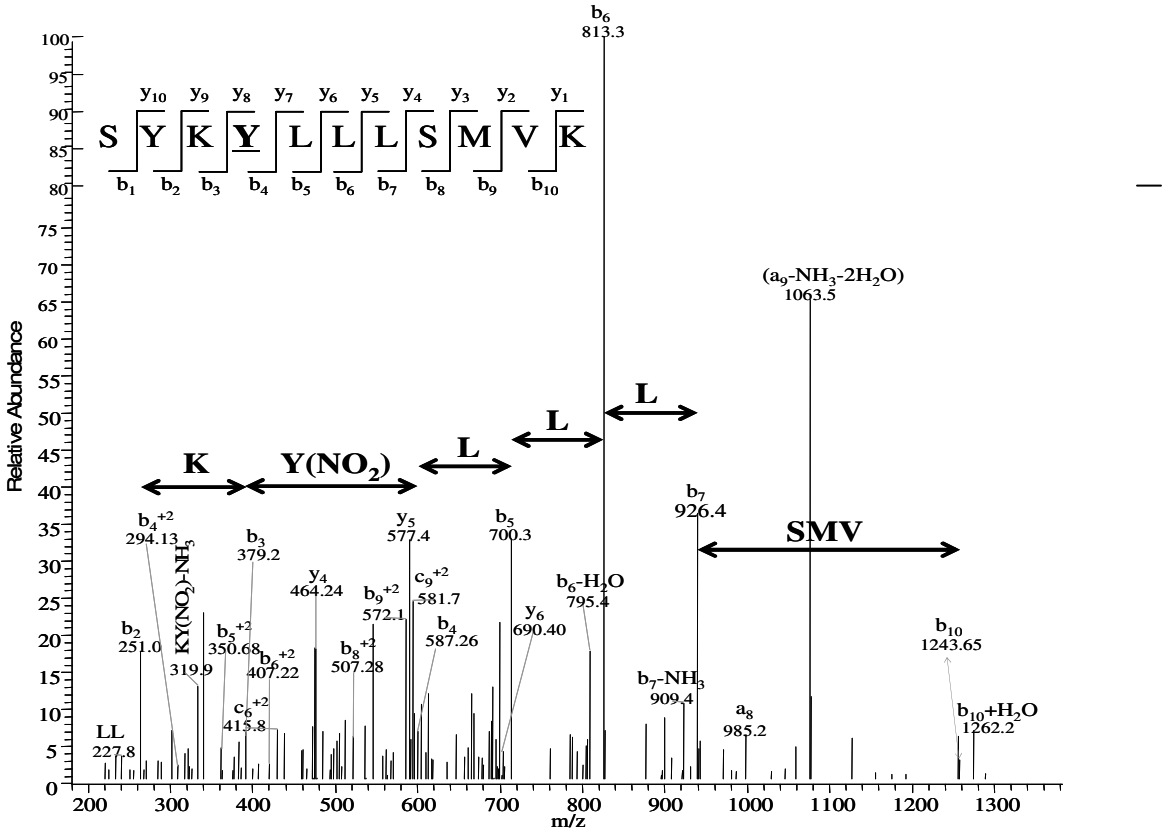

Figure 3.6 Representative MS/MS spectrum of neurofibromin.

Displayed here is the MS/MS spectrum for the nitrated peptide sequence Ser488-Lys498 detected for neurofibromin, in cardiac tissue of 34 months old Fisher 344 BN-F1 rats. Here we have highlighted the b-ions covered in the series, b2-b10.

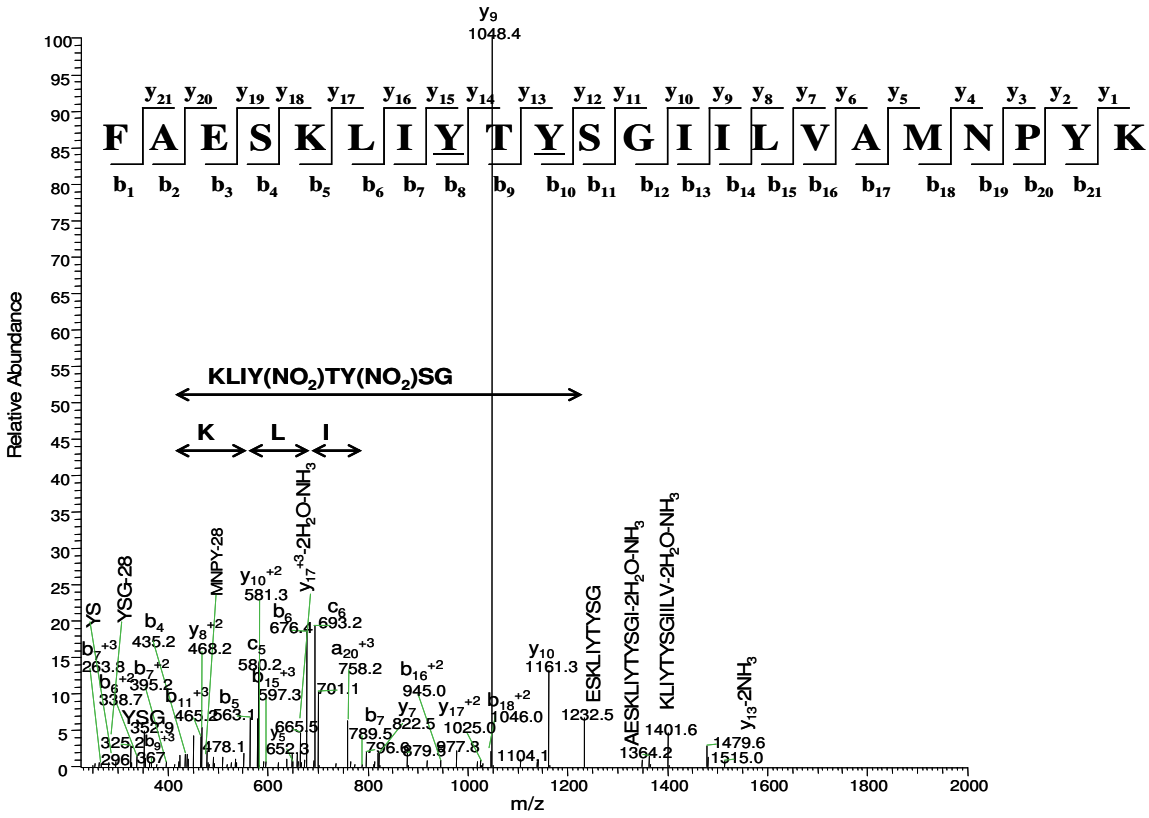

Figure 3.7 Representative MS/MS spectrum of Myocin-5C.

Displayed here is the MS/MS spectrum for the nitrated peptide sequence Phe91-Lys111 detected for Myocin-5C, in cardiac tissue of 34 months old Fisher 344 BN-F1 rats. Here we have highlighted the b-ions covered in the series, b5-b7 and the internal fragment b5-b12 containing both nitrated Tyr98 and Tyr100.

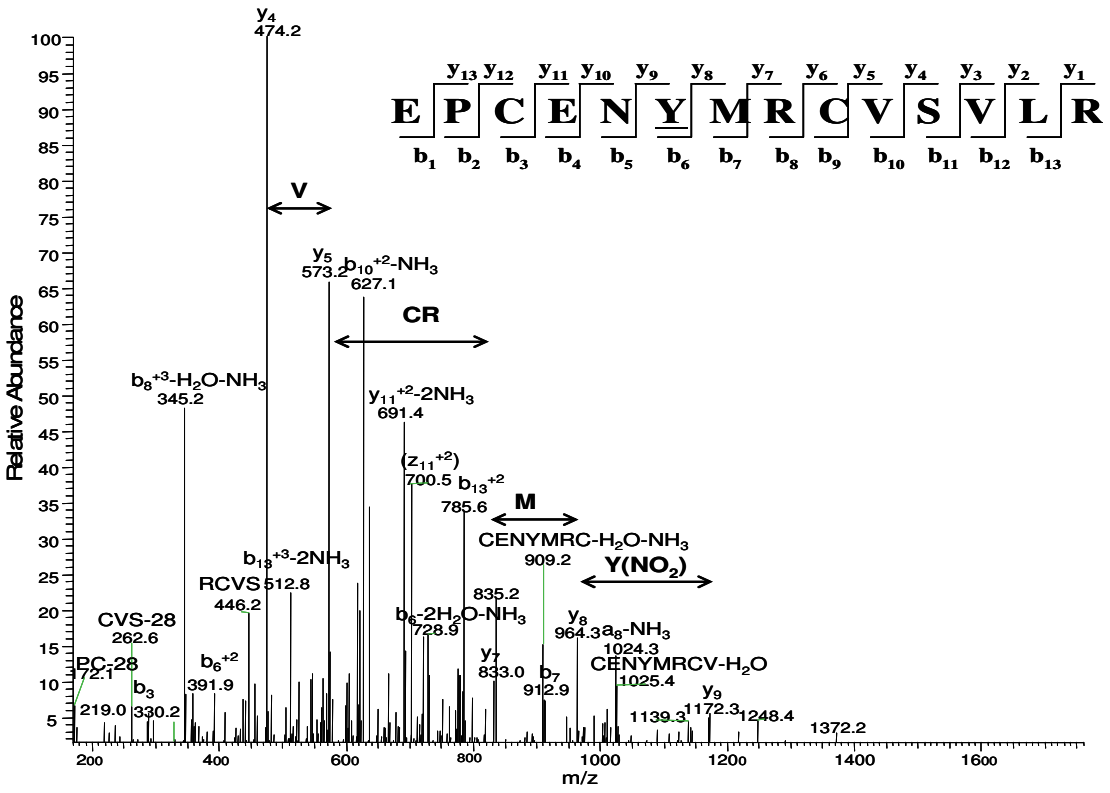

Figure 3.8 Representative MS/MS spectrum of cadherin EGF-LAG seven pass G type receptor 2. Displayed here is the MS/MS spectrum for the nitrated peptide sequence Glu460-Arg473 detected for cadherin EGF-LAG seven pass G-type receptor 2, in cardiac tissue of 34 months old Fisher 344 BN-F1 rats. Here we have highlighted the y-ions covered in the series, y5-y9.

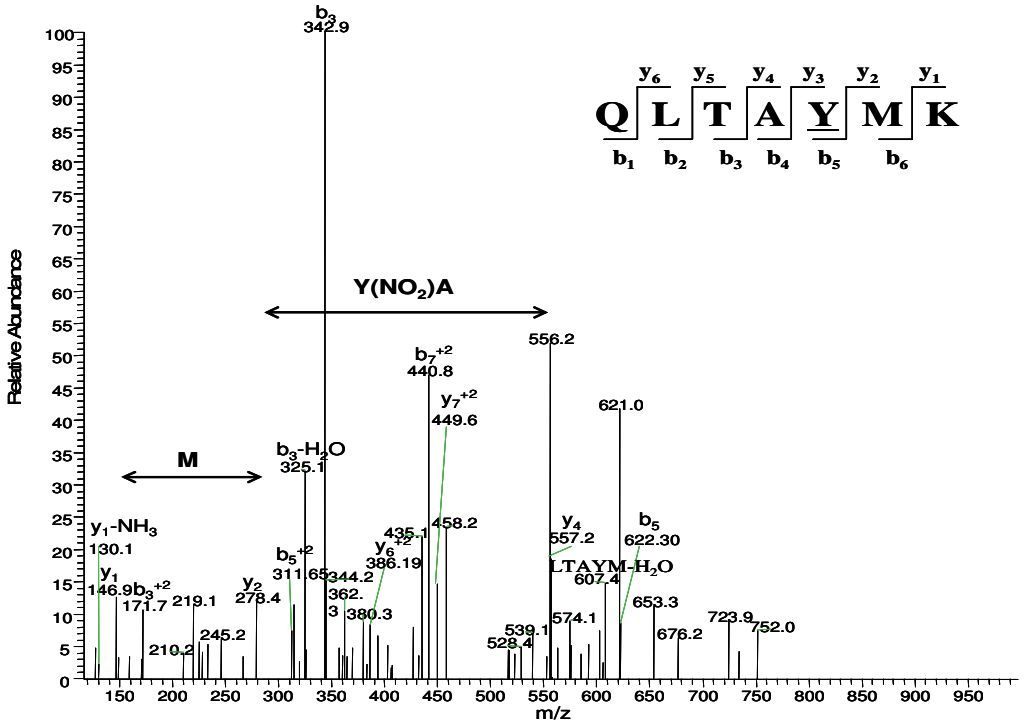

Figure 3.9 Representative MS/MS spectrum of dynein.

Displayed here is the MS/MS spectrum for the nitrated peptide sequence Gln665-Lys671 detected for dynein, in cardiac tissue of 34 months old Fisher 344 BN-F1 rats. Here we have highlighted the y-ions covered in the series, y2-y4.

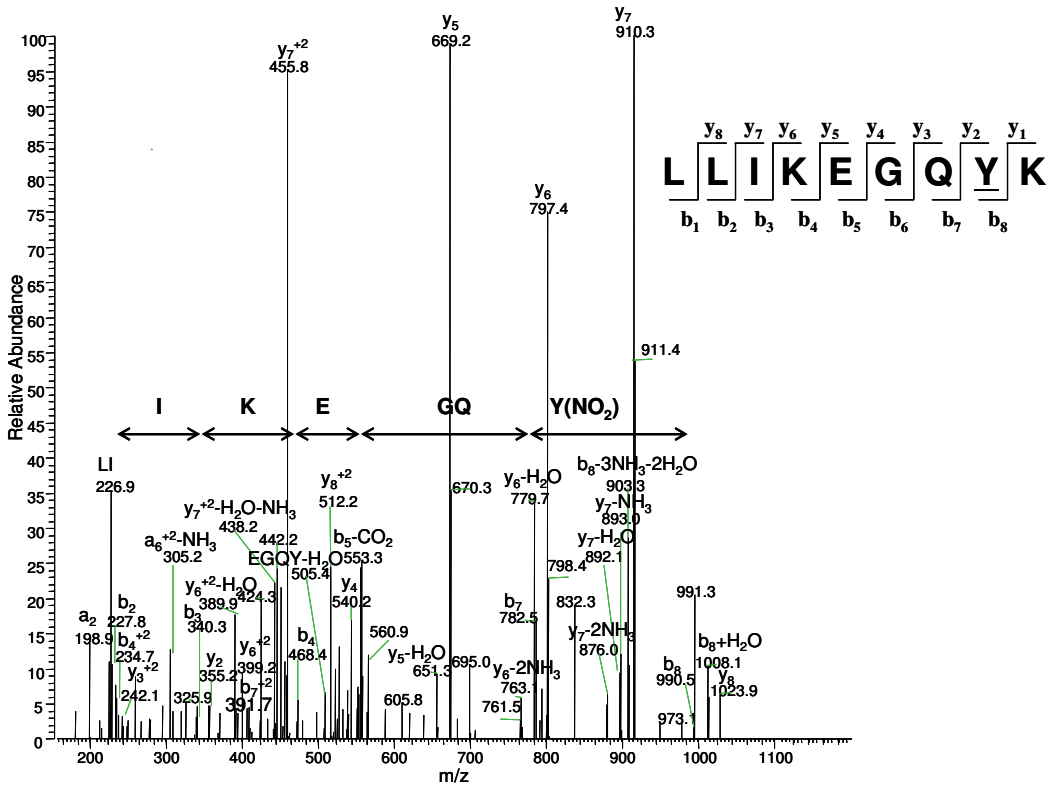

Figure 3.10 Representative MS/MS spectrum of Cys2/His2 Zn finger protein (rKr1).

Displayed here is the MS/MS spectrum for the nitrated peptide sequence Leu282-Lys290 detected for Cys2/His2 Zn finger protein (rKr1), in cardiac tissue of 34 months old Fisher 344 BN-F1 rats. Here we have highlighted the b-ions covered in the series, b3-b8.

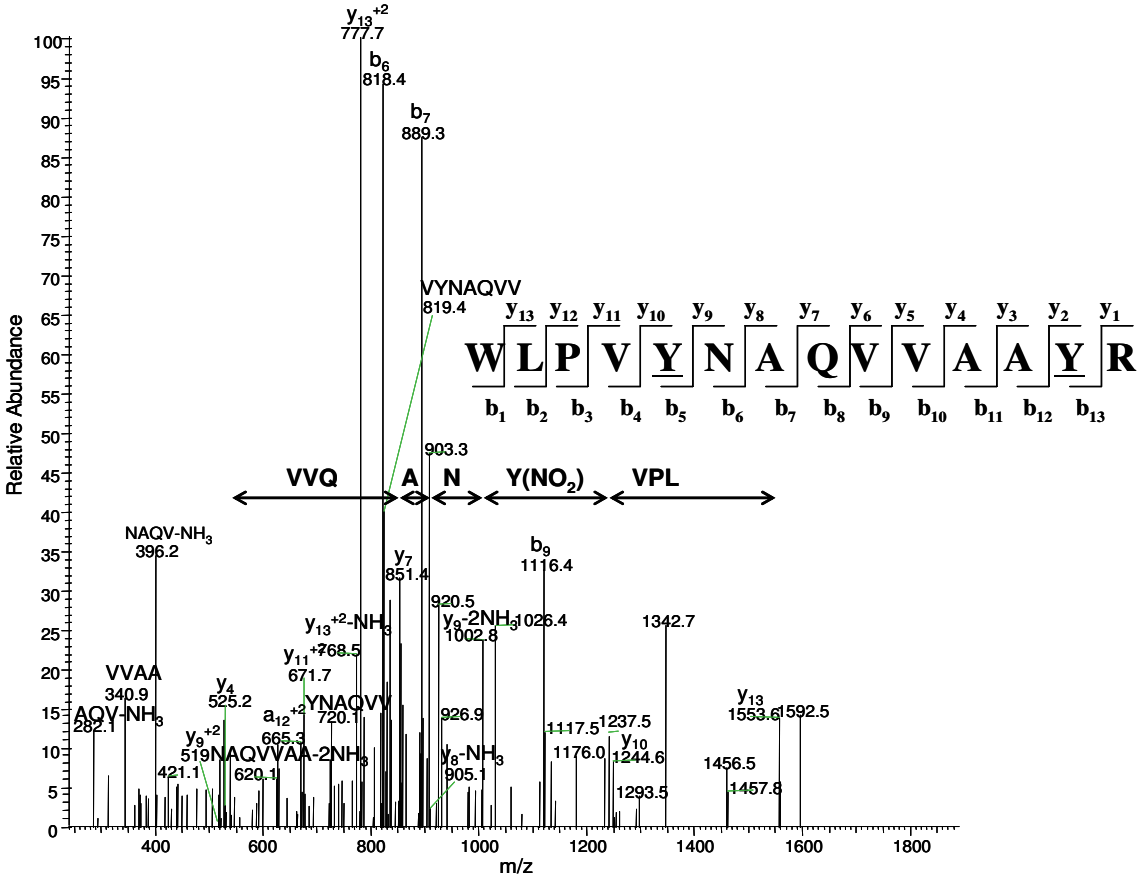

Figure 3.11 Representative MS/MS spectrum of myosin heavy chain polypeptide 7.

Displayed here is the MS/MS spectrum for the nitrated peptide sequence Thr130-Arg143 detected for myosin heavy chain polypeptide 7, in cardiac tissue of 34 months old Fisher 344 BN-F1 rats. Here we have highlighted the y-ions covered in the series, y5-y13.

It is interesting to note that several of the nitrated proteins detected after solution IEF are located in the cytoskeleton, whereas our previous 2DE experiments (5), localized many nitrated cardiac proteins to the mitochondria. This difference between the nature of identified proteins via two independent methods reflects, again a phenomenon commonly observed during proteomic experiments, where different techniques lead to the identification of different subsets of proteins (13).

Significantly fewer (a total of three) nitrated proteins were detected in the analysis of cardiac tissue from young (5 months old) rats (Table 1). Here, only NADH dehydrogenase was not detected in the heart of old (34 month) rats, whereas both myosin heavy chain polypeptide 7 and neurofibromin were also detected in the aging heart. Figure 3.12 displays a representative MS/MS spectrum for the nitrated peptide Thr^{101}-Lys^{112} from NADH dehydrogenase (GenInfo accession number 9506913), nitrated at Tyr^{106}.

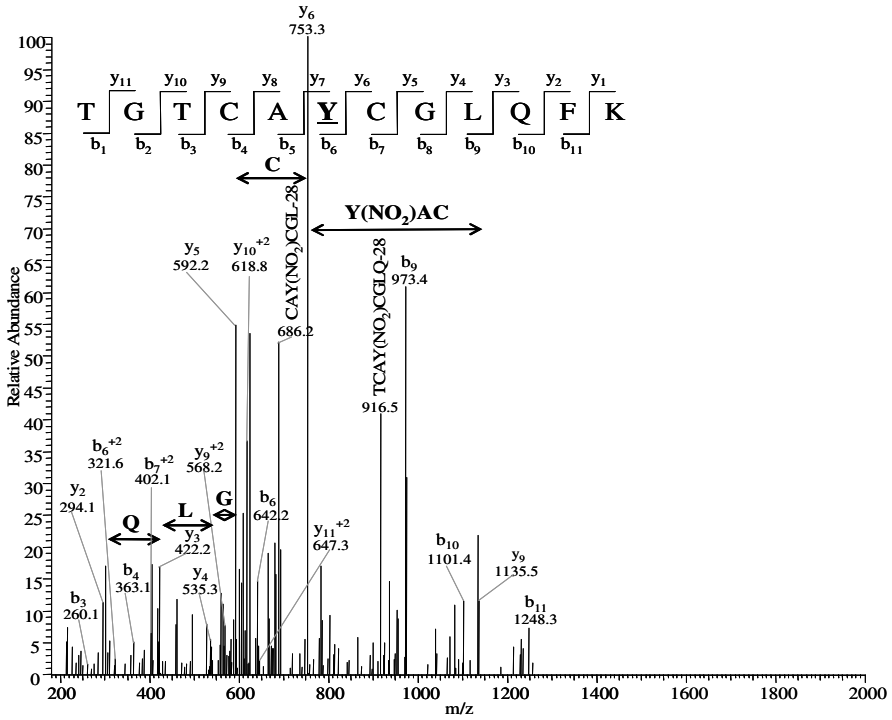

Figure 3.12 Representative MS/MS spectrum of NADH dehydrogenase (ubiquinone) Fe-S.

Displayed here is the MS/MS spectrum for the nitrated peptide sequence Thr101-Lys112 detected for NADH dehydrogenase (ubiquinone) Fe-S, in cardiac tissue of 5 months old Fisher 344 BN-F1 rats. Here we have highlighted the y-ions covered in the series, y2-y9.

3.4 Discussion/Conclusion

NO plays an important role in signal transduction to regulate proper cardiac muscle function (14,15). NO specifically integrates cell system responses by controlling oxygen supply and demand, especially during an ischemic attack (15). NO regulates proper hemoglobin function and cardiac smooth muscle contractility to coordinate the respiratory cycle in order to ensure proper oxygen delivery to target tissues (15-17). Therefore, cardiac muscles are periodically exposed to fluxes of endogenous NO (synthesized by local NOS) (15), and superoxide (18). This creates

an environment amenable for the formation of peroxynitrite ($ONOO^-$), a major nitrating species (19), through the diffusion controlled reaction of NO and superoxide (20). Therefore, the formation of nitrated proteins in cardiac muscle is not unexpected. Importantly, aging leads to an accumulation of nitrated proteins, which may affect cardiac function (5). This accumulation may be, in part, an indication of an age-dependent slower proteasomal degradation of nitrated proteins (21), higher concentrations of nitrating species (5), and/or slower repair by the putative protein "denitrase" (22,23) (or a combination of all three parameters). We note that peroxynitrite is not the only reagent which can nitrate proteins in vivo, but that other nitrating species, such as nitrogen dioxide ($^{\cdot}NO_2$), may be involved as well.

Tyrosine nitration can affect protein structure and function. The magnitude of such effect will primarily depend on the location of 3-NY within the protein and its quantity. Densitometry measurements quantify a ca. 1.5-2.0 fold overall age-dependent increase in protein nitration. The location of 3-NY within the detected proteins has been addressed in this study through the MS/MS analysis of individual nitrated peptides. Quantitation of 3-NY within each of the individual target proteins by our mass spectrometric method was not possible. Such quantitation and experimental proof of potential functional and structural consequences of nitration will be part of future studies focusing on the targeted purification of the proteins identified in the present study. In the following we will provide a discussion of the potential effects of tyrosine nitration within these peptide sequences.

Some of the more interesting nitrated proteins detected in this work are located in the cytoskeleton, namely myosin, N-RAP (isoform C), tropomyosin, and neurofibromin. For myosin, we detected nitration at Tyr^{114} and Tyr^{116} for polypeptide 6, and nitration at Tyr^{134} and Tyr^{142} for polypeptide 7. It has been observed that an age-dependent slower muscle movement is due to functional and structural changes of myosin, in particular the heavy chain (24). This is important to note, especially in view of the slow turnover rate, and decreased rate of synthesis and degradation of this protein (24). The myosin heavy chain converts chemical energy, present in the form of ATP, into mechanical energy (25). Therefore, structural changes that can affect the normal function of these proteins may explain the age dependent loss of muscle force and contractile speed (24). Figure 3.13 displays a cartoon locating the 3-NY residue within these protein sequences of myosin polypeptides.

To date, relatively little information is available about the functional roles of N-RAP (isoform C). It has been proposed that N-RAP anchors the terminal actin filaments in the myofibril to the membrane as well as transmits the tension from the

Figure 3.13 Cartoon displaying the relative location for the nitrated peptides of myosin heavy chain that were found in the present study.

In this cartoon, we display the whole myosin complex, composed of two heavy chains, and two light chains. The two heavy chains are shown in gray, and the light chains that wrap around the neck of the two myosin light chains are shown in black. The 3-NY modification is located in the head region of the myosin heavy chain.

myofibrils to the extracellular matrix. N-RAP is specifically expressed in skeletal and cardiac muscles (26,27). The N-RAP super repeats have been shown to bind actin very tightly analogous to nebulin. This suggests that N-RAP binding to actin filaments is a highly cooperative process, which leads to the transmission of the tension created during myofibril contraction and relaxation. N-RAP displays a sequence homology to the C-terminal half of nebulin, as well as the LIM domain (a Cys rich domain, that can bind to two Zn ions) at the N-terminus, responsible for mediating protein-protein interactions (27). Figure 3.14 shows a cartoon indicating that the nitration of N-RAP targets specifically the C-terminal domain involved in actin binding.

Figure 3.14 Cartoon displaying the relative location for the nitrated peptide of nebulin-related anchoring protein (N-RAP) found in the present study.

N-RAP is composed of three distinct regions. The LIM-domain, nebulin like simple repeats domain and the actin binding domain. The 3-NY modification is located at the actin-binding domain of N-RAP.

Tropomyosin regulates the interactions between actin and actin-binding proteins (28). Tropomyosin 1 represents the predominant isoform present in the cardiac muscle and fast skeletal muscle fibers. Mutations of the TPM1 gene (which encodes for Tropomyosin 1), result in different types of myopathies causing abnormal

muscle function (28,29). Figure 3.15 shows a cartoon locating the 3-NY residue within the protein sequence of Tropomyosin.

Figure 3.15 Cartoon displaying the reported shape of this protein and the relative location for the nitrated peptide of tropomyosin found in the present study.

The 3-NY modification in this protein is located towards the C-terminus of its amino acid sequence.

Neurofibromin, encoded by the gene NF1, represents a tumor suppressor protein which acts as a negative regulator of Ras. Mutations to NF1 or the absence of the NF1 gene can cause congenital heart disease associated with neurofibromatosis type 1, e.g. benign neurofibromas, leukemias and multiple cardiac abnormalities (30). These disorders likely depend on an unregulated Ras signaling pathway, which may stimulate cell growth or inhibit apoptosis. The 3-NY^{491} residue in this protein is located very close to a mutation site, Tyr^{489}, commonly found in genetic studies of patients suffering neurofibromatosis type 1 (31). Nitration of Tyr^{491} may have a similar negative effect on the protein as mutation to Tyr^{489} within the same protein domain. Figure 3.16 displays a cartoon locating the 3-NY residue within the protein sequence of neurofibromin.

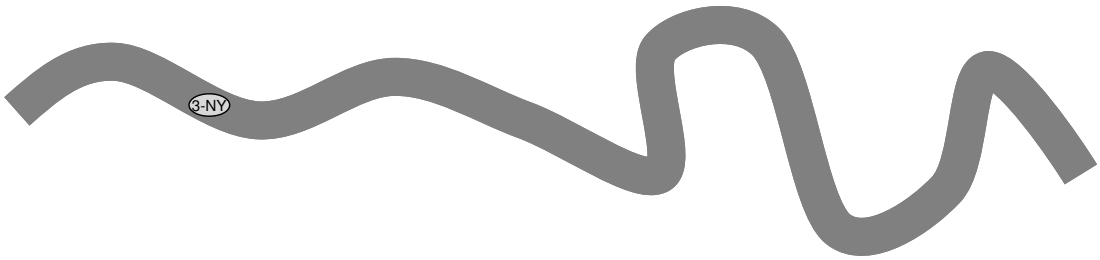

Figure 3.16 Cartoon displaying the relative location for the nitrated peptide of neurofibromin found in the present study.

This protein is being shown in its denatured form. The 3-NY modification in this protein is located towards the N-terminus of its amino acid sequence.

Some of the other nitrated proteins identified in this work (Table 3.1) play important roles in cellular function, such as for example, organelle transport by myosin 5C, cell membrane adhesion regulation by cadherin EGF-LAG seven pass G-type receptor 2, and transcriptional regulation in the nucleus by the Cys/His Zn-finger protein. The modifications to these proteins together with the cytoskeletal proteins already discussed, may offer some rationale for cardiac dysfunction, though it can be expected that additional nitrated proteins may be detected in the heart as more sensitive proteomic methods become available.

Some oxidized and nitrated proteins are susceptible to accelerated turnover (32,33), while others tend to accumulate (34,35). Our earlier (5) results suggest a rather selective accumulation of a few nitrated cardiac proteins. In addition to selective turnover, other parameters such as cellular location, protein structure, and protein-protein interactions, will define the susceptibility to nitration (34). The target proteins that we have identified in this work serve as evidence for age dependent

protein nitration *in-vivo*. Future studies must now focus on a targeted isolation of identified proteins to quantitate age-dependent nitration, the possible accumulation of additional modifications, and to correlate these modifications with protein function. In collaboration with Dr. Stobaugh and members of his group, we have taken a step forward to achieve this goal. A fluorogenic derivatization method specific for 3-NY and hydroxytyrosine has been developed and it has been shown to work well for small molecules and peptides (36). In the next chapters of this thesis, we will discuss how this new derivatization method has been successfully applied to the protein Calmodulin (CaM).

3.5 References

1. Quint, P., Reutzel, R., Mikulski, R., McKenna, R., and Silverman, D. N. (2006) *Free Radic Biol Med* **40**, 453-458
2. Xu, S., Ying, J., Jiang, B., Guo, W., Adachi, T., Sharov, V., Lazar, H., Menzoian, J., Knyushko, T. V., Bigelow, D., Schöneich, C., and Cohen, R. A. (2006) *Am J Physiol Heart Circ Physiol* **290**, H2220-2227
3. MacMillan-Crow, L. A., and Thompson, J. A. (1999) *Arch Biochem Biophys* **366**, 82-88
4. Savvides, S. N., Scheiwein, M., Bohme, C. C., Arteel, G. E., Karplus, P. A., Becker, K., and Schirmer, R. H. (2002) *J Biol Chem* **277**, 2779-2784
5. Kanski, J., Behring, A., Pelling, J., and Schöneich, C. (2005) *Am J Physiol Heart Circ Physiol* **288**, H371-381

6. Kanski, J., Hong, S. J., and Schöneich, C. (2005) *J Biol Chem* **280**, 24261-24266

7. Adeghate, E. (2004) *Mol Cell Biochem* **261**, 187-191

8. Hare, J. M., and Stamler, J. S. (2005) *J Clin Invest* **115**, 509-517

9. Saraiva, R. M., and Hare, J. M. (2006) *Curr Opin Cardiol* **21**, 221-228

10. Hare, J. M. (2004) *N Engl J Med* **351**, 2112-2114

11. Adachi, T., Weisbrod, R. M., Pimentel, D. R., Ying, J., Sharov, V. S., Schöneich, C., and Cohen, R. A. (2004) *Nat Med* **10**, 1200-1207

12. MacCoss, M. J., Wu, C. C., and Yates, J. R., 3rd. (2002) *Anal Chem* **74**, 5593-5599

13. Arab, S., Gramolini, A. O., Ping, P., Kislinger, T., Stanley, B., van Eyk, J., Ouzounian, M., MacLennan, D. H., Emili, A., and Liu, P. P. (2006) *J Am Coll Cardiol* **48**, 1733-1741

14. Balligand, J. L., Kelly, R. A., Marsden, P. A., Smith, T. W., and Michel, T. (1993) *Proc Natl Acad Sci U S A* **90**, 347-351

15. Gong, L., Pitari, G. M., Schulz, S., and Waldman, S. A. (2004) *Curr Opin Hematol* **11**, 7-14

16. Davidson, S. M., and Duchen, M. R. (2006) *Cardiovasc Res* **71**, 10-21

17. Wolin, M. S., Hintze, T. H., Shen, W., Mohazzab, H. K., and Xie, Y. W. (1997) *Biochem Soc Trans* **25**, 934-939

18. Reid, M. B., Khawli, F. A., and Moody, M. R. (1993) *J Appl Physiol* **75**, 1081-1087

19. Beckman, J. S. (1996) *Chem Res Toxicol* **9**, 836-844

20. Nauser, T., and Koppenol, W. H. (2002) *J Phys Chem A* **106**, 4084-4086

21. Conconi, M., and Friguet, B. (1997) *Mol Biol Rep* **24**, 45-50

22. Irie, Y., Saeki, M., Kamisaki, Y., Martin, E., and Murad, F. (2003) *Proc Natl Acad Sci U S A* **100**, 5634-5639

23. Kamisaki, Y., Wada, K., Bian, K., Balabanli, B., Davis, K., Martin, E., Behbod, F., Lee, Y. C., and Murad, F. (1998) *Proc Natl Acad Sci U S A* **95**, 11584-11589

24. Höök, P., Sriramoju, V., and Larsson, L. (2001) *Am J Physiol Cell Physiol* **280**, C782-788

25. Lompre, A. M., Nadal-Ginard, B., and Mahdavi, V. (1984) *J Biol Chem* **259**, 6437-6446

26. Luo, G., Zhang, J. Q., Nguyen, T. P., Herrera, A. H., Paterson, B., and Horowits, R. (1997) *Cell Motil Cytoskeleton* **38**, 75-90

27. Luo, G., Herrera, A. H., and Horowits, R. (1999) *Biochemistry* **38**, 6135-6143

28. Clarkson, E., Costa, C. F., and Machesky, L. M. (2004) *J Pathol* **204**, 407-417

29. Ilkovski, B., Nowak, K. J., Domazetovska, A., Maxwell, A. L., Clement, S., Davies, K. E., Laing, N. G., North, K. N., and Cooper, S. T. (2004) *Hum Mol Genet* **13**, 1727-1743

30. Yutzey, K. E., Colbert, M., and Robbins, J. (2005) *Physiology (Bethesda)* **20**, 390-397

31. Messiaen, L. M., Callens, T., Mortier, G., Beysen, D., Vandenbroucke, I., Van Roy, N., Speleman, F., and Paepe, A. D. (2000) *Hum Mutat* **15**, 541-555

32. Grune, T., Reinheckel, T., and Davies, K. J. (1997) *Faseb J* **11**, 526-534

33. Souza, J. M., Choi, I., Chen, Q., Weisse, M., Daikhin, E., Yudkoff, M., Obin, M., Ara, J., Horwitz, J., and Ischiropoulos, H. (2000) *Arch Biochem Biophys* **380**, 360-366

34. Greenacre, S. A., and Ischiropoulos, H. (2001) *Free Radic Res* **34**, 541-581

35. Harman, D. (1956) *J Gerontol* **11**, 298-300

36. Pennington, J. P., Schöneich C., Stobaugh J. (2007) *Chromatographia* **66**, 649-659

4. Fluorogenic derivatization of 3-Nitrotyrosine residues in Calmodulin with 4-aminobenzylbenzene sulfonic acid

4.1 List of abbreviations used inside the text

- ROS: Reactive oxygen species
- RNS: Reactive nitrogen species
- CaM: Human Calmodulin, UniProtKB/Swiss-Prot entry P62158, MW 16706.4 Da
- $NaBH_4$: Sodium Borohydride
- Ni/Pt: Nickel/ Platinum Catalyst
- $K_3Fe(CN)_6$: Potassium Ferricyanide
- ABS: 4-aminobenzylbenzene sulfonic acid
- 3-NY: Nitrotyrosine
- 3-AY: Aminotyrosine
- K: Lysine
- TNM: Tetranitromethane
- ICAT: Isotope-Coded Affinity Tag
- PMA: Phenymethylamine
- PBO: 2-phenylbenzoxazole

4.2 Introduction

Protein nitration leads to a chemically stable protein modification and the accumulation of nitrated proteins in tissue may define the phenotype for biological aging or any pathology. Most of the nitrated proteome in literature has qualitative data and quantitative measurement remains a challenge since a lot of nitrated proteins *in-vivo* have low abundance and usually fall below the detection limits of currently available quantitative methods (1).

Some of the most commonly applied methods for 3-NY proteomics are antibody based methods, such as Western blot analysis (2-5), enzyme-linked immunosorbent assay (ELISA) (6-8), and immunoprecipitation (4,9). All these have relied on monoclonal anti-3-NY antibodies, which are known to recognize only a

subset of nitrated epitopes (10) which, may explain low reactivity in some samples. Anti-body techniques are mostly qualitative and sometimes, may be used semi-quantitatively because they don't provide information on total protein content, only on the levels of 3-NY. Therefore, these antibody based techniques are usually used in conjunction with 1D and 2D gel electrophoresis. 1D gel electrophoresis separates proteins in the sample by molecular mass, therefore used as a size exclusion technique to simplify complex samples. Also, 1D gel electrophoresis offers some quantitation by protein staining although, this is dependent on the dynamic range of the protein stain used, usually Coomassie blue or Silver staining for higher sensitivity. 2D gel electrophoresis separates proteins according to their pI in the first dimension and size in the second dimension, offering a protein map also amenable for some quantitation by protein staining in the same way as 1D gel electrophoresis. The only drawbacks of these in-gel techniques are that total protein loads are limited and for 2D gels, it has been shown that they are biased against highly hydrophobic, low abundance and high molecular weight and extreme pI proteins (11).

Lack of absolute quantitative techniques for the study of protein Tyr nitration have driven the inspiration for the set of experiments described in this and the following chapters. In collaboration with Dr. Stobaugh and his group, our lab has developed a novel derivatization technique specific for nitrotyrosine (3-NY) after amino reduction to aminotyrosine (3-AY) and hydroxytyrosine (DOPA), that is amenable for quantitation by both fluorescence spectroscopy and mass spectrometry analysis of derivatized 3-NY in the samples with isotope coded tags, an approach

similar to the isotope coded affinity tag (ICAT) derivatization technique (12). Since the focus of this thesis is on 3-NY, we will focus on the derivatization of 3-NY.

It has been previously reported that a selective fluorogenic derivatization of ortho-substituted phenol derivatives such as hydroxytyrosine (DOPA) and 3-NY after nitroreduction to 3-AY with benzylamine yields a 2-phenylbenzoxazole (PBO) product (Figure 4.1) (12). After further investigation and experimentation with biological macromolecules, i.e., peptides such as Angiotensin I and proteins such as Phosphorylase b, the need for a more water soluble tag became apparent and a slightly modified version of PMA with a sulfonic acid moiety was synthesized in our lab by Dr. Xiabao Li. The new tag was called 4-(aminomethyl)benzene sulfonic acid (ABS) (Figure 4.2).

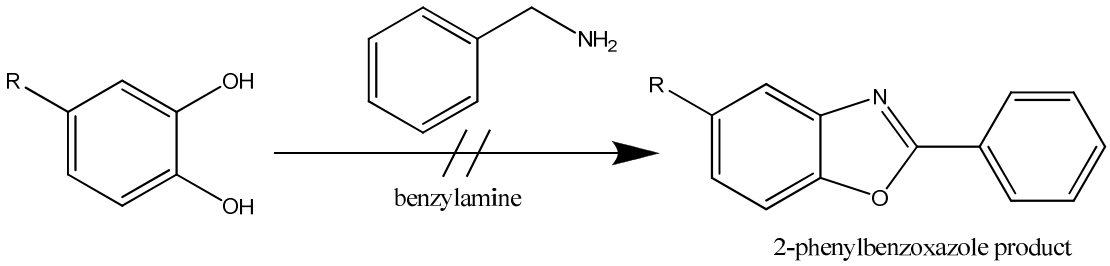

Figure 4.1 Catechol reaction with benzylamine to yield the 2-phenylbenzoxazole product (1).

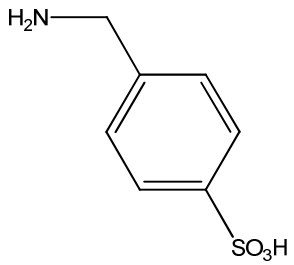

Figure 4.2 Synthesized (aminomethyl)benzene sulfonic acid (ABS).

This is a more water soluble version of benzylamine to be used as the derivatization agent in reactions with biological molecules.

The derivatization reaction of 3-NY with ABS after nitroreduction to 3-AY were conducted in phosphate buffer with high molar excess of the tagging reagent to analyte and differing iron concentrations in the form of potassium ferricyanide ($K_3Fe(CN)_6$). Fluorescence after derivatization was evident however, the fluorescent products were not well characterized by mass spectrometry. Therefore, a peptide model system was developed by synthesizing a partial sequence of muscle phosphorylase b (PhB) with a nitrated Tyr residue, $^{545}FSAY(NO_2)LER^{555}$ (13). Experimentation with this PhB peptide and ABS yielded two different PBO derivatives that were formed depending on the reaction conditions, more specifically, they were found to be dependent on the iron concentration used for the derivatization reaction (13). Figure 4.3 shows the structure of the two derivatization products from the reaction of 3-NY with ABS.

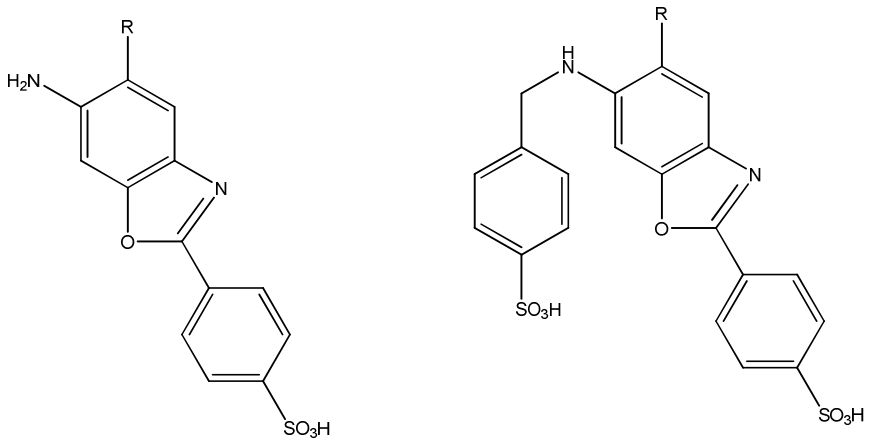

Figure 4.3 Structure of the two derivatization products identified with model peptide studies.
(A) is the product with one ABS tag attached and (B) is the product with two ABS tags attached to the nitrated Tyr residue.

Since well characterized products were not observed when working with full protein PhB, a relatively large protein (194kDa) found to be nitrated both *in-vitro* and *in-vivo* on multiple Tyr residues (14), in this study, we wanted to investigate if we could characterize ABS labeling on a full protein using a simpler model protein. For this purpose, we chose Calmodulin (CaM) as our model protein to apply the ABS tagging method. CaM is a relatively small protein (16706.4 Da) and it only contains 2 Tyr residues at positions 99 and 138. This is a ubiquitous Ca^{2+} binding protein that is very important for cellular regulation as presented by Cheung et. al. in Figure 4.4 (15). The calcium ion $Ca^{2+}$is very important for regulation of biological processes such as muscle contraction, cellular motility, endocytosis and exocytosis (15). This protein lacks Cys residues and hydroxyproline, which contributes to its high flexibility to

assume a tertiary structure able to interact with its many Ca^{2+} dependent receptor proteins. Inactivation of this protein by oxidation thus, would disrupt the Ca^{2+} homeostasis resulting in cellular imbalance and potentially cell death (15).

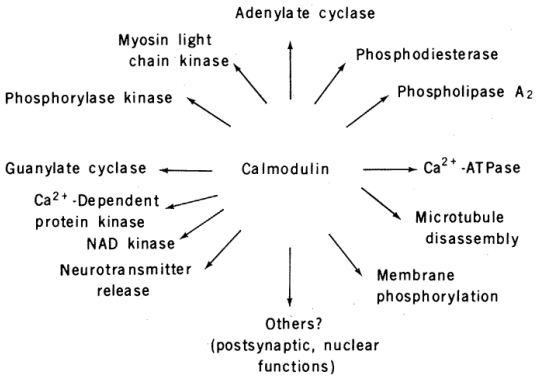

Fig. 4. Calmodulin-regulated enzymes or cellular processes. The roles of calmodulin on some of the enzymes or cellular processes listed above have not been established beyond doubt. The evidence indicating the effect of calmodulin on phopholipase A_2, guanylate cyclase, Ca^{2+}-dependent protein kinase, microtubule disassembly, and neurotransmitter release appears preliminary. The postulated roles of calmodulin in postsynaptic, nuclear, and other functions are speculative.

Figure 4.4 This figure was extracted from Cheung's 1980 article , to illustrate the magnitude of CaM important presence in cellular regulation (15).

CaM has been shown to be highly susceptible to nitration by tetranitromethane (TNM), peroxynitrite ($ONOO^-$), and hydrogen peroxide (H_2O_2) *in-vitro* (16-19). TNM in the presence of Ca^{2+} has been shown to effectively nitrate both Tyr residues in this protein (19,20), providing a simple model to study the derivatization reaction with ABS on a system where secondary and tertiary structures are present. Through this study, we found the presence of the two products previously observed with model peptide FSAY(NO_2)LER, the addition of 1 ABS molecule (Tyr+196) and the addition of 2 ABS molecules (Tyr+366) (2,3) as presented in Figure 4.3, with good MS/MS evidence. In addition, we found a third product involving an intra-molecular cross-link of Lys (K) with the derivatized Tyr residue

(Tyr +179). This lead us to a deeper understanding of this ABS tagging method and conclude that any primary amine in close proximity to the Tyr residue of interest could serve to activate the first step of the reaction involving the C5 of the aromatic 6-membered ring in aminotyrosine (3-AY), as shown in the reaction Scheme in Figure 4.5.

4.3 Experimental

Materials

For CaM overexpression, BL21(DE3) cells were purchased from Novagen (La Joya, CA). 3-(N-morpholino)propanesulfonic acid (MOPS), M9 media components, tetranitromethane (TNM), ethylene diamine tetraacetic acid (EDTA), potassium ferricyanide ($K_3Fe(CN)_6$), sodium borohydride ($NaBH_4$), hydrazine hydrate, cetyl methylammonium bromide (CTAB), chloroplatinic acid and nickel sulfate were purchased from Sigma-Aldrich (St. Louis, MO). Pre-cast 4-20% SDS-PAGE gels and 10DG Desalting columns were purchased from Bio-Rad (Hercules, CA), protein assay Bradford Reagents were purchased from PIERCE (Rockford, IL). Amicon Ultra-15 centrifugal filter units with Ultracel-3 membranes were purchased from Millipore (Billerica, MA). 4-aminobenzylbenzene sulfonic acid (ABS) was synthesized in house by Dr. Xiabao Li. De-ionized distilled water was filtered by a Labconco purification system (Kansas City, MO). Tris-Glycine SDS 2X sample buffer was purchased from Invitrogen (Carlsbad, CA). Tris-HCl, potassium hydroxide (KOH) and sodium phosphate (Na_2HPO_4) and sequencing grade trypsin were purchased from Fisher Scientific (Pittsburg, PA).

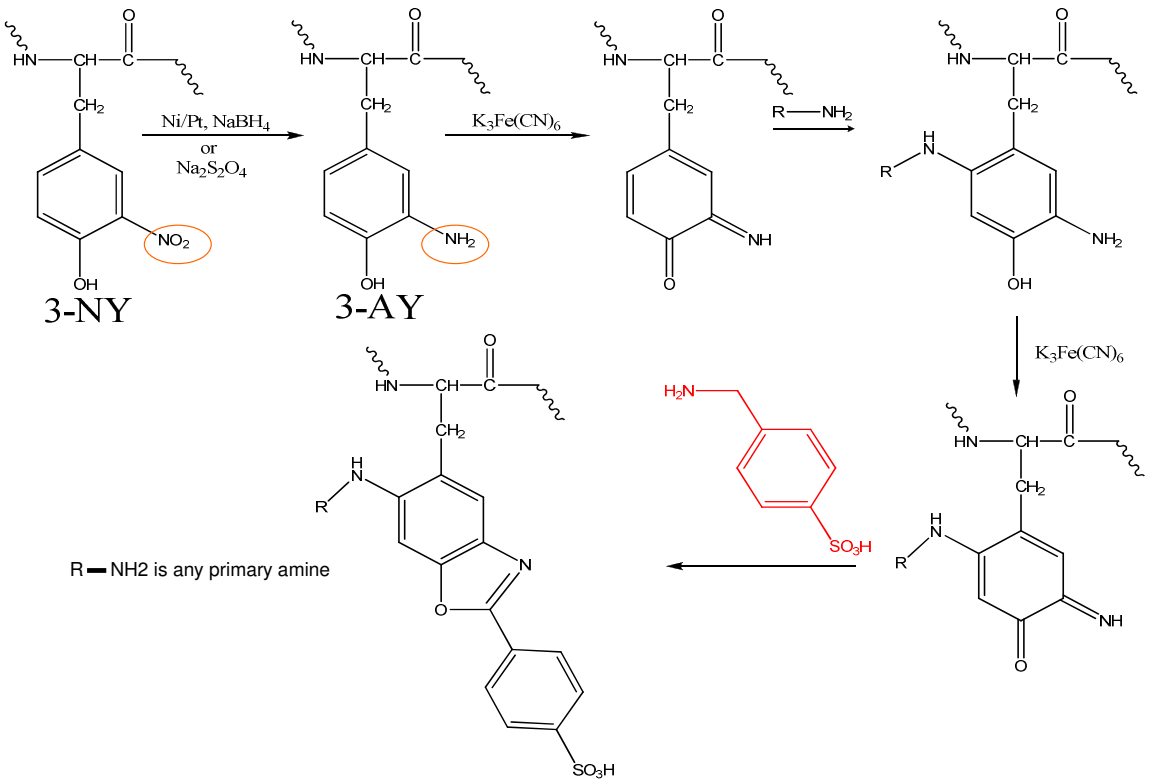

Figure 4.5 Reaction scheme for 3-NY derivatization with ABS fluorescent tag.

Reaction involves first reduction of nitro group in 3-NY to an amino group to 3-AY. This step is followed by oxidation by K3Fe(CN)6 and Michael addition of species containing primary amine at C5 on the aromatic ring of Tyr. Then, a second oxidation step takes place and finally, one ABS tag molecule is added to the Tyr of interest.

CaM expression

CaM overexpression was achieved by transformation of the recombinant plasmid containing the gene encoding CaM (generously provided by Eric Gorman and Dr. Yunsong Li from the Department of Pharmaceutical Chemistry at the University of Kansas) into BL21(DE3) cells (Novagen, La Joya, CA). Transfection was done according to the manufacturer's protocol and overexpression was done at

37^{o}C in M9 minimal media , essentially following the protocol previously described by Li et. al (21).

CaM purification

CaM was purified both from transfected (i)BL21(DE3)-T1^{R} competent E. coli cells purchased from Sigma (St. Louis, MO) , generously provided by Eric Gorman, University of Kansas, and (ii) Novagen BL21(DE3) cells which we transfected in our laboratory. The cells were washed and re-suspended in MOPS buffer prior to lysing them using a French press. The lysed cells were centrifuged and the supernatant was collected and loaded onto an ÄKTA FPLC system (Amersham Biosciences, Piscataway, NJ) with a pre-equilibrated (50 mM Tris-HCl, pH 7.5, 1mM $CaCl_2$) XK26 (26 mm i.d. x 10 cm) column (GE Healthcare Bio-Sciences Corp., Piscataway, NJ) packed with Phenyl–Sepharose. After a few washes with equilibration buffer, CaM was eluted with 10 mM Tris-HCl, pH 7.5 and 10 mM EDTA. The peak containing CaM was collected into ~twelve 1 ml fractions and concentrated using an Amicon Ultra-15 centrifugal filter unit with an Ultracel-3 membrane (21,22). At the final centrifugation step, the protein was buffer exchanged into 50 mM Tris, pH 8, and stored at -80 ^{o}C until used.

CaM Nitration

A stock solution of TNM was washed by 3 water extractions. Then, an 840 mM stock solution of TNM in Ethanol was prepared and stored at 3 ^{o}C. After determining protein concentration of the CaM stock solution using the Bradford Reagent method, 300 µl of stock protein solution were added to 2700 µl of nitration

buffer composed of 50 mM Tris, pH8 and 5mM $CaCl_2$. We added Ca^{2+} to our nitration buffer because previous studies have shown that in the absence of Ca^{2+} Tyr^{138} is more susceptible to nitration by TNM than Tyr^{99}. However, in the presence of Ca^{2+}, both nitration of Tyr^{99} and Tyr^{128} can be achieved (19,20). For the nitration reaction, we calculated a 50X molar excess of TNM to tyrosine. The reaction mixture was stirred vigorously for 1hr at 25°C. The nitrated protein was then cleaned up using a 10DG desalting column by gravity filtration. Eight 1 ml fractions were collected from the desalting column and each one was tested for the presence of nitrated CaM by scanning the absorbance from 200 to 600 nm using a Cary 50 UV spectrophotometer. Only the fractions giving an absorbance at 280 and ~430 nm were pooled and saved. After pooling the fractions, an absorbance scan was performed again to determine the 3-NY content, by diluting 50 µl of sample in 0.1% NaOH and taking into account the dilution factor and using the extinction coefficient for 3-NY □=4400 $M^{-1}cm^{-1}$ (Conc. of 3-NY=(Abs at 430nm/4400)x(dilution factor)) (23). Once our 3-NY content was established, we measured our total protein concentration in the nitrated sample and determined that we had ~0.67 mol 3-NY per mol of CaM.

Synthesis of Ni/Pt Catalyst

The protocol for synthesis of the Ni/Pt catalyst used for 3-NY reduction to 3-AY prior to fluorogenic labeling with ABS was obtained from Jacque Killmer's PhD Thesis. A 5 ml solution of 14 mM nickel sulfate (Sigma, St Louis MO), 580 µM chloroplatinic acid, and 100 mM cetyl methylammonium bromide (CTAB) was purged with nitrogen gas for 5 min. The solution was sealed and stirred magnetically

for 30 minutes at room temperature. Then, 30 µl of hydrazine hydrate (Sigma, St Louis MO), and 200 µl of 50% KOH, in water were added to the reaction mixture and continued to stir at room temperature until the solution turned black. The reaction mixture was transferred to 15 ml centrifuge tubes. Step one of particle recovery was to centrifuge the reaction mixture at 5000g for 2 to 5 minutes. Step two was to remove the supernatant and washing the particles 10 times with water repeating steps one and two. After the final wash, the particles were dried in a centrivap (model no. 7810000, Labconco, Kansas City, MO) and stored for future use.

CaM 3-NY reduction to 3-AY

A water suspension was made that contained 500 µg/ml of Ni/Pt particles. For the 3-NY reduction step, the concentration of $NaBH_4$ was adjusted to be 200 mM in the reaction mixture and 5 µl of Ni/Pt catalyst solution were added per 300 µl of reaction volume. The reaction mixture was vortexed and incubated at 37 ^{o}C for 1hr. Then, the reaction was quenched by the addition of hydrochloric acid (HCl), to have a final concentration of 200mM HCl in the reaction. The protein was precipitated from the reaction mixture by the addition of excess EtOH and incubating the solution at -20 ^{o}C overnight. The precipitated proteins were collected by centrifugation at 13000g in a microcentrifuge.

Tagging Reaction

Protein concentration in the 3-AY containing CaM sample was measured by the Bradford reagent method and adjusted to 10 µM. This protein solution was aliquoted into 400 µl volumes for the ABS tagging reactions. For the control samples,

we also had 10 µM 3-NY containing CaM sample and a 10 µM native CaM sample, also at 400 µl. To check protein concentration in each sample after adjustment we run an SDS-PAGE gel of the 3-NY, 3-AY, and native CaM samples, Figure 4.6.

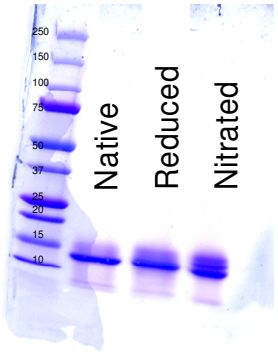

Figure 4.6 SDS-PAGE gel of native, nitro-reduced and in-vitro nitrated CaM stained with coomassie blue.

We can see that our protein normalization for protein concentration is good. All the samples, controls and reactions have the same protein concentrations.

In the first set of experiments, we tested the effects of iron concentration in the reaction since it was previously shown with a model peptide FSAYLER (13) that iron concentration had an important role in the fluorescence and formation of the right fluorescent products after derivatization, having either one tag molecule reacting with 3-AY or two tag molecules reacting with 3-AY (Figure 4.3). The source of iron in our reactions was from $K_3Fe(CN)_6$. All reactions were done in 100 mM phosphate at pH 9.

The second set of experiments was to determine the limit of detection of 3-NY for our derivatization. For this purpose, the 10 µM 3-AY CaM sample was serially diluted into 10 µM native CaM sample to achieve different 3-AY concentrations in our samples without affecting the total protein concentration.

Fluorescence Characterization

Fluorescence characterization of each tagged sample was done using a fluorescence spectrophotometer (RF 5000U Shimadzu, Japan). Both excitation and emission wavelengths were determined using a 400 µl fluorescence quartz cuvette. Samples were diluted 50 times in 100 mM Phosphate, pH 9 in order to obtain readings within the instrument's data window. Excitation for ABS labeled compounds was found to be 360 nm and the emission was found to be 480 nm, Figure 4.7.

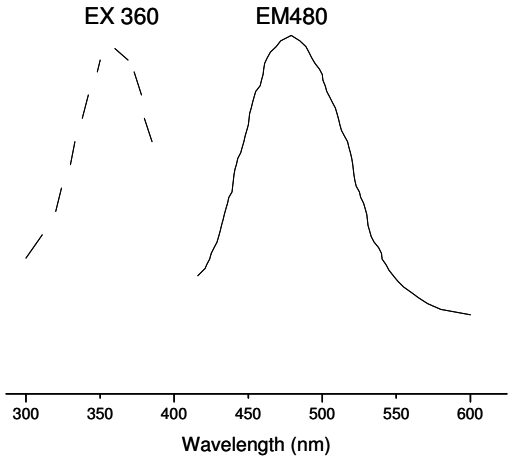

Figure 4.7 Exitation and emission wavelengths of ABS tagged CaM.

Gel electrophoresis

Derivatized proteins, using different iron concentrations, were submitted to SDS-PAGE on 4-20 % Tris-HCl pre-cast gels. 25 µl of each sample were diluted with 2X sample buffer for a total volume of 50 µl. The gel was run at 200 V for 35 minutes.

The gels were removed from their casing and placed under a hand held UV lamp, Figure 4.8 (Model UVL-56 115 V, 60 Hz, 0.16 A, UVP, Inc., San Gabriel, CA 91778). The fluorescent bands were cut out and followed by in-gel trypsin digestion (24). The trypsin digests were then submitted for MS/MS analysis.

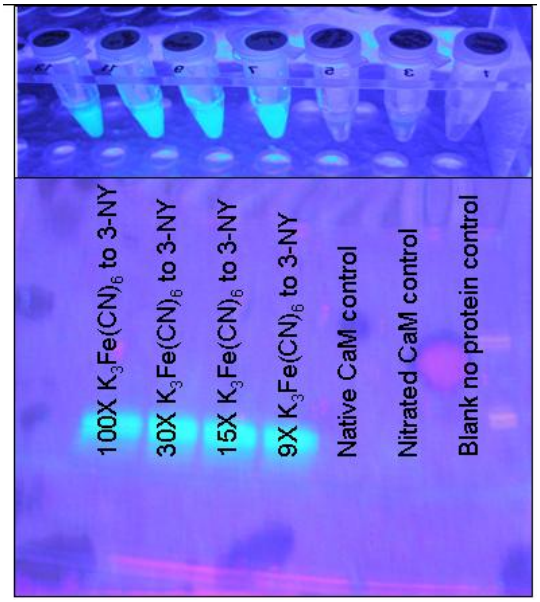

Figure 4.8 SDS-PAGE of ABS tagged CaM.

Here, reactions were done in the presence of different iron concentrations (K3Fe(CN)6). Here, we can observe that the controls do not have any fluorescence.

In-gel trypsin digestion

The excised gel bands were first crushed into smaller pieces and 200 µl of pure MeCN were added to dehydrate the gel pieces. Then, 2 µg of trypsin were added to each sample in ~ 50 to 60 µl of 50 mM NH_4HCO_3 and incubated at 37^{o}C overnight. The digested protein samples were saved for mass spectrometry analysis with the FT-

ICR mass spectrometer available in the Multidisciplinary Research Building (MRB) here at the University of Kansas.

Mass Spectrometry Analysis

Full protein MS analysis was performed on a Q-TOF-LCMS instrument by Dr. Todd Williams and Mr. Bob Drake at the University of Kansas Mass Spectrometry Lab. The MS data analysis was done using Mass-Lynx 3.5 software (Micromass, UK). The multiply charged spectrum obtained from the mass spectrometer was transformed to a full protein, uncharged spectrum using this software. This full protein spectrum was used for analysis of full protein derivatization data.

Peptide MS/MS were performed on an LTQ-FT hybrid linear quadrupole ion trap Fourier transform ion cyclotron resonance (FT-ICR) mass spectrometer (ThermoFinnigan, Bremen, Germany) via capillary liquid chromatography by Dr. Nadezhda Galeva at the University of Kansas. Prior to MS and MS/MS analysis, peptides were separated by reversed phase chromatography. The raw acquisition data was processed by BioWorks 2.2 software (Thermo Scientific, Waltham, MA) followed by peptide/protein identification using Sequest (Thermo Finnigan) and Mascot (Matrix Science, Boston, MA) and X!Tandem (The Global Proteome Machine Organization) database-searching programs. The MS/MS spectra were then validated by Scaffold 1.7 (Proteome Software Inc., Portland Oregon), a software that operates on a statistical method by setting confidence thresholds to the data obtained.

4.4 Results

The fluorescent tagging method was very efficient. Samples were observed to fluoresce just 30 seconds after adding the tagging reagent to the sample. In the iron dependence experiment, we found that there was an optimal concentration of iron needed in order to have maximum fluorescence. If iron concentration falls below or exceeds this optimal concentration, fluorescence yields were observed to decrease. Five different iron concentrations were tested and the optimal conditions for maximum fluorescence was observed to be 120 X molar excess to 3-NY present in the sample as observed in Figure 4.9. However, from studies done previously on the model peptide FSAY(NO2)LER, the best ratio of iron to 3-NY was a 30X molar excess of iron, to arrive at the desired products as identified by RP-HPLC and mass spectrometry (3).

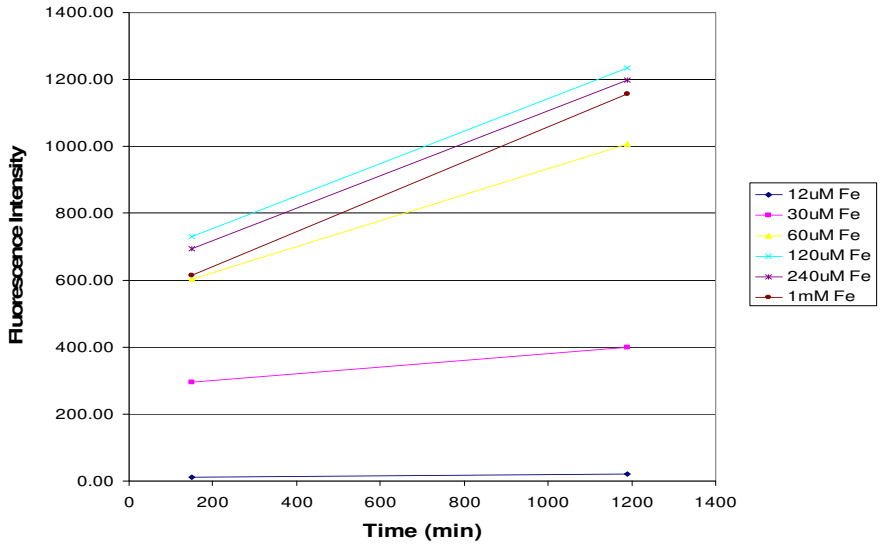

Figure 4.9 CaM samples tagged with 200 mM ABS and different K3Fe(CN)6 concentrations.

As observed with studies done with the model peptide FSAY(NO2)LER (3), there was an optimal concentration of iron for maximum fluorescence, in this case, 120X to 3-NY.

We also tested the tagging reaction's limit of detection by diluting the 3-NY content in the samples and keeping the total protein concentration constant, and the iron ratio of 30X molar excess. The concentrations of 3-NY tested were 0.3 µM , 1.3 µM , 2.3 µM , and 3.3 µM . We observed a linear response in fluorescence to the 3-NY content in the samples (Figure 4.10). However, for full protein detection of tagged protein derivatives by mass spectrometry, 3.3 µM 3-NY in the samples was needed.

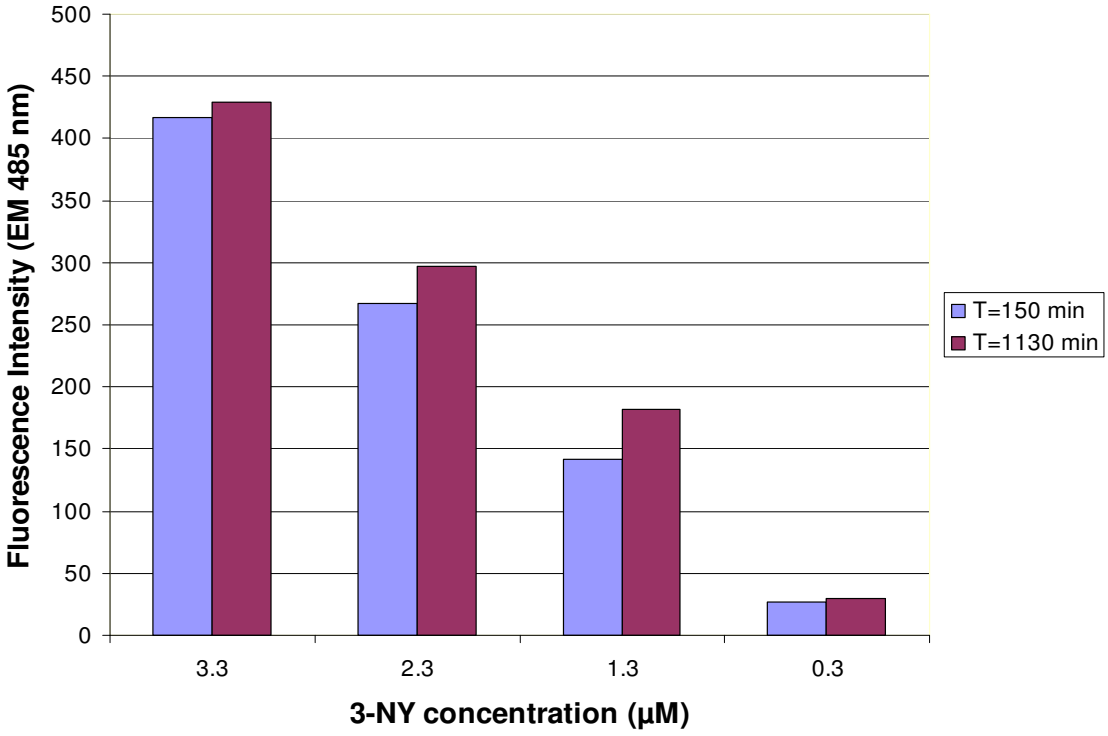

Figure 4.10 Fluorescence emission was linearly dependent on the amount of analyte present in the sample.

At 3 nM analyte concentration, the fluorescence in the sample was still detectable by fluorescence spectroscopy, however, the desired products were only detected in the sample with 3.3 µM 3-NY by full protein mass spectrometry analysis with Q-TOF LC MS.

From previous studies with the model peptide FSAY(NO_2)LER (4), two major dervatized Tyr residue products were expected as observed in the tagging scheme presented in Figure 4.5. Structures of the expected products are shown in Figure 4.3, one product containing 2 tagging molecules with a mass addition of 366 amu (atomic mass units), confirmed by MS/MS as shown in Figure 4.11 and the other containing 1 tagging molecule plus an NH_2 group with a mass addition of 196 amu also confirmed by MS/MS (Figure 4.12).

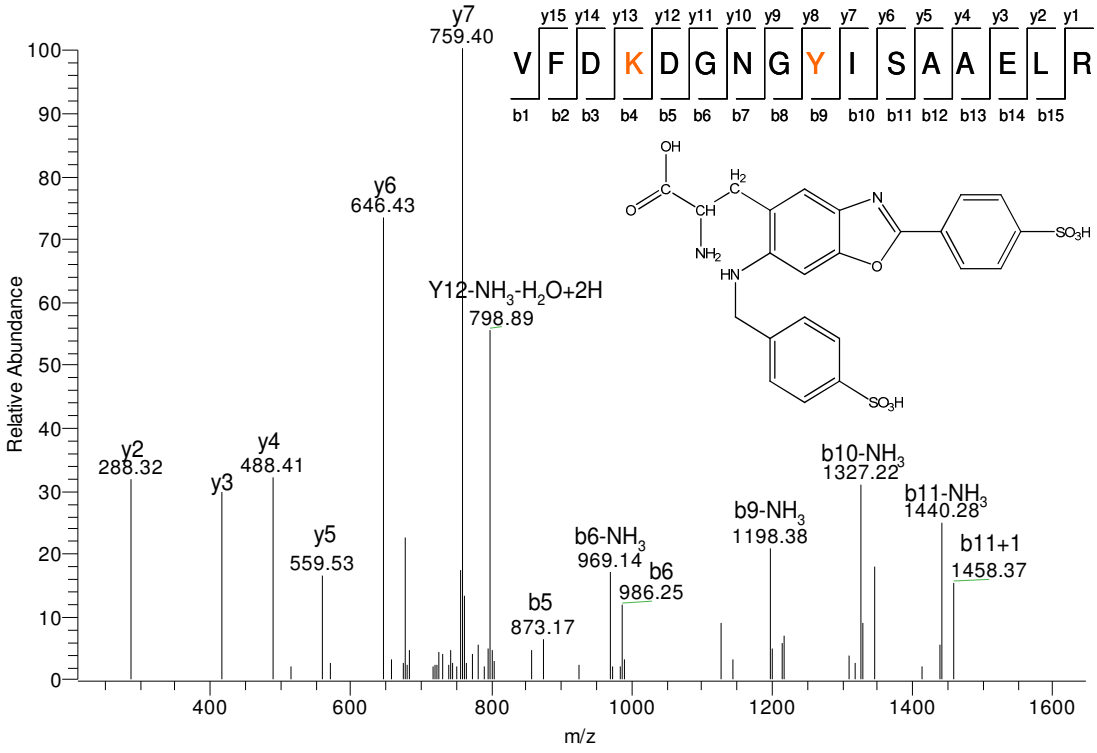

Figure 4.11 MS/MS of the CaM peptide VFDKDGNGYISAAELR with 2 ABS tag molecules (Tyr+366).

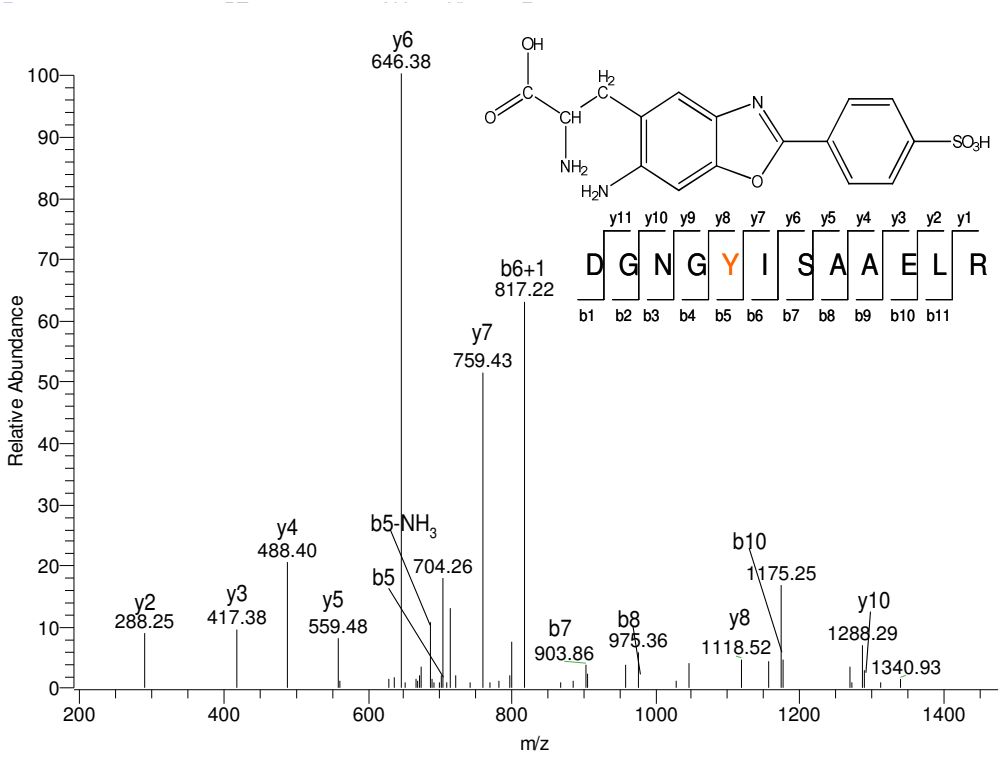

Figure 4.12 MS/MS of the CaM peptide DGNGYISAAELR with 1 ABS tag molecule and an NH_2 group (Tyr+196).

Through this study with CaM, we have identified a third product from the tagging reaction which, in this case turned out to be the major product under the reaction conditions used. This product involves an intra-molecular crosslink between the derivatized Tyr residue and a neighboring Lys residue, separated by 4 amino acid residues, taking the place of the second tagging reagent, or the NH_2 group, as observed in Figure 4.13. Each step prior to derivatization and the samples after derivatization were submitted to full protein MS analysis by Q-TOF MS. Figure 4.14

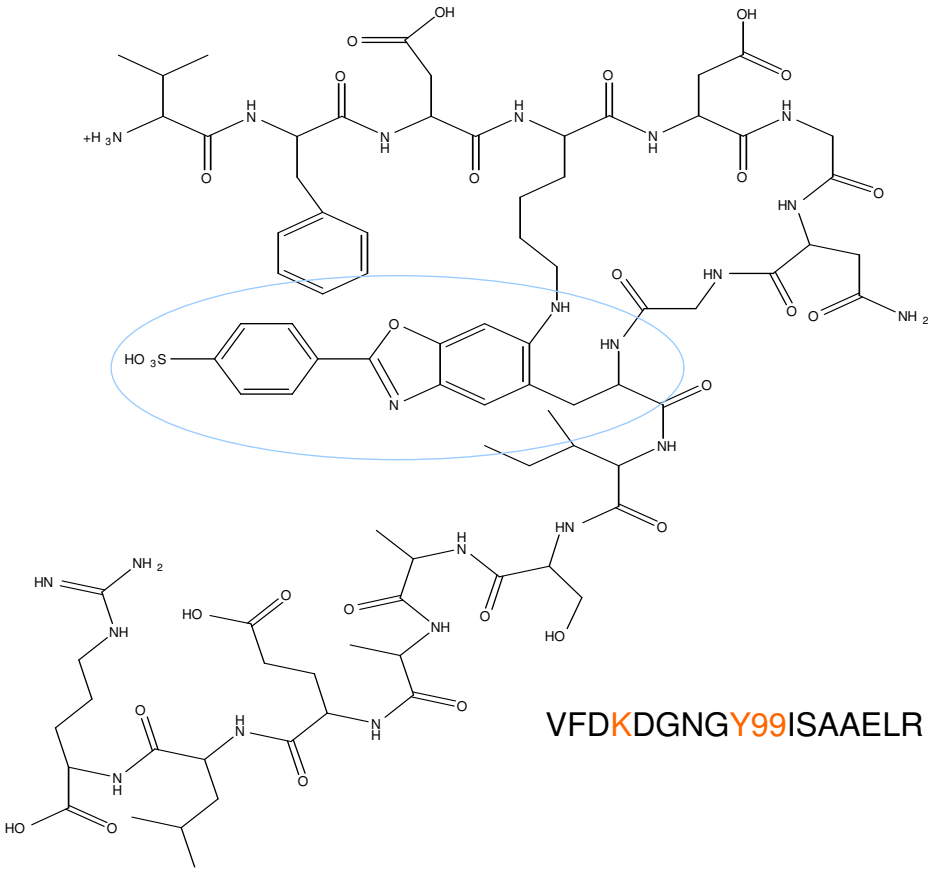

Figure 4.13 CaM peptide VFDKDGNGYISAAELR where Lys 94 was found to cross-link with Tyr 99 during fluorescence derivatization with ABS.

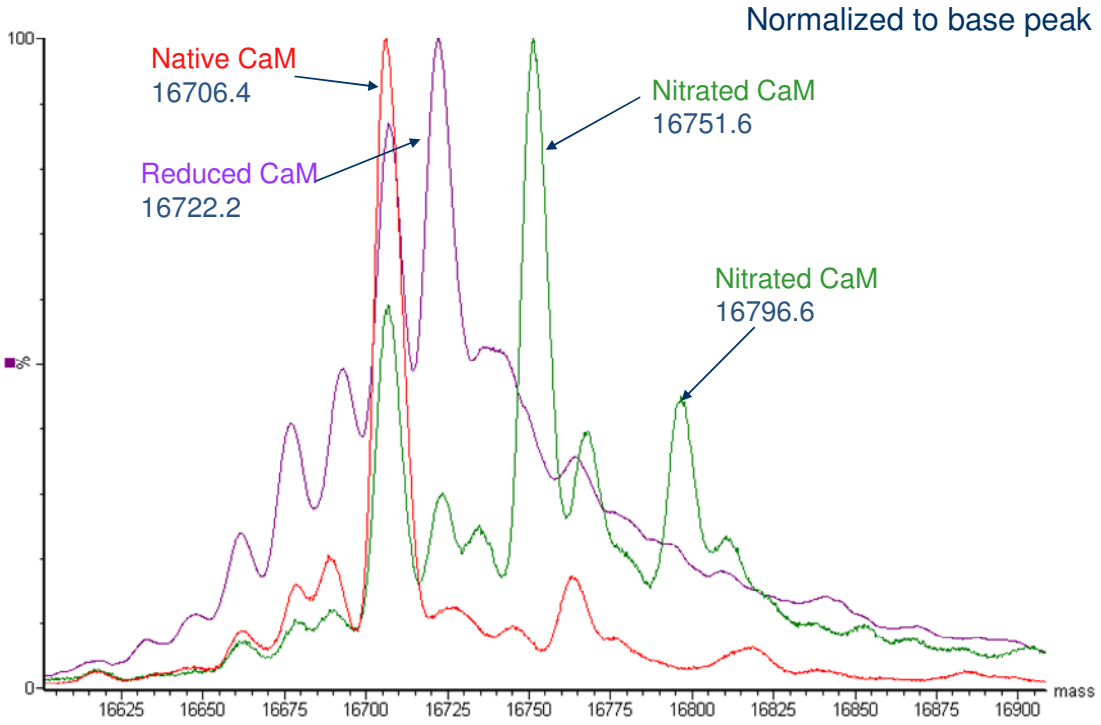

Figure 4.14 Q-TOF MS of native, nitrated and nitro-reduced CaM prior to derivatization with ABS.

There are 2 Tyr residues present in CaM and each nitration to the Tyr residues is calculated by the addition of 45 amu to the molecular weight of native CaM which is 16706.4. Reduction of the nitro-group in 3-NY to 3-AY was calculated by the addition of 16 amu to the molecular weight of native CaM.

shows transformed Q-TOF spectra by MassLynx 3.5 for the steps prior to derivatization from native to nitrated to nitro-reduced. A representative transformed spectra for the tagged sample is shown in Figure 4.15, where the third product was observed to be the major one under the reaction conditions with 2 mM ABS that we used. The formation of this product was also confirmed by FT-LC MS as shown in

Figure 4.16, where we show the doubly charged MS and Figure 4.17, where we show the MS/MS identifying the sequence of the derivatized peptide.

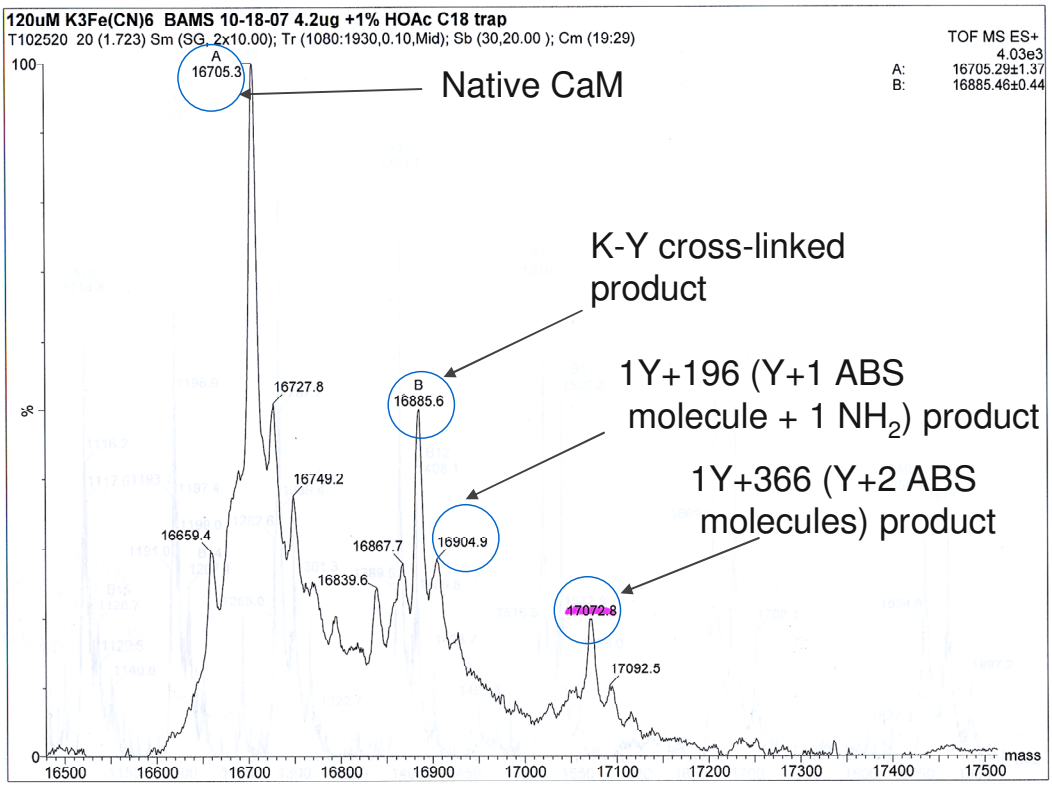

Figure 4.15 Representative transformed full protein MS for the sample tagged with 120 molar excess of K3Fe(CN)6 and 2 mM ABS.

We can clearly observe the formation of all three products expected from the fluorescent derivatization reaction. (Y+179 for cross-linked, Y+196 for 1ABS molecule+NH2, and Y+366for 2 ABS molecules).

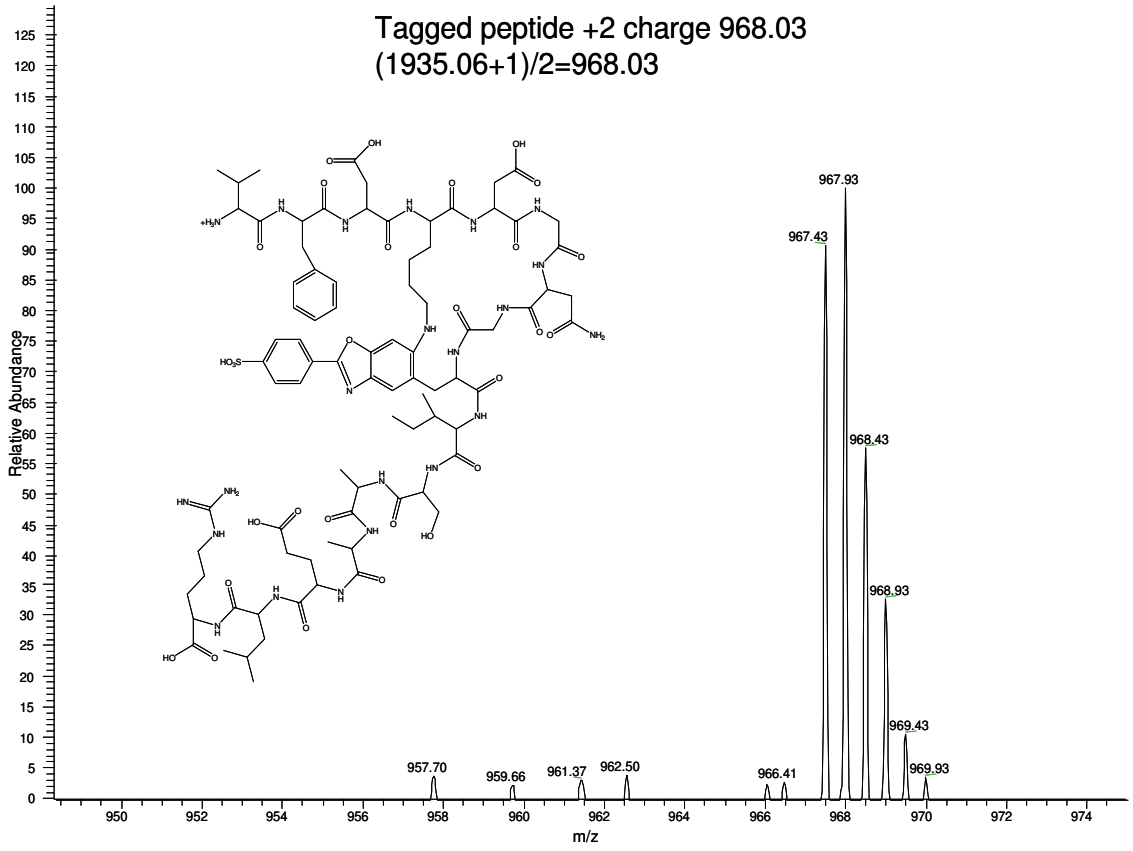

Figure 4.16 MS 1 of doubly charged CaM cross-linked peptide VFDKDGNGYISAAELR.

The actual peak mass for the most abundant peak shown in this spectrum is 967.93, which is 0.1 units away from the calculated mass of 968.03. The other peaks on either side represent the isotopic distribution of this peak.

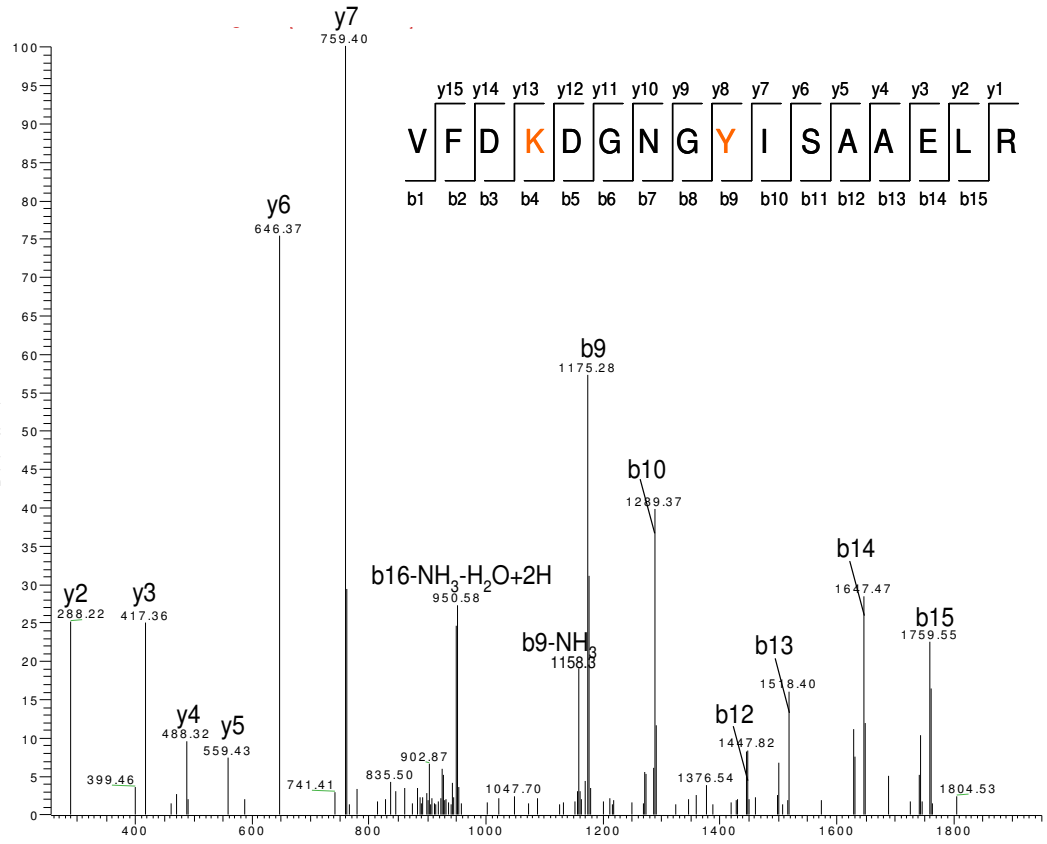

Figure 4.17 MS/MS of the CaM peptide VFDKDGNGYISAAELR with intra-molecular cross-link between K94 and Y99 (Tyr+179) after derivatization with ABS.

4.5 Discussion/Conclusion

The data presented in this chapter show that we have successfully applied the ABS fluorogenic derivatization of 3-NY to a full protein. We have also shown that this derivatization method can be relatively quantitative by fluorescence spectroscopy when we tested it with different concentrations of 3-NY in the samples. Formation of the desired products (Tyr+196 and Tyr+366) previously shown by studies on model peptides and small molecules (2,3) was confirmed by both Q-TOF full protein MS and by FT-MS of digested derivatized protein. In addition to the two products expected from the reaction, we found that primary amines in proximity to the Tyr of interest can participate in the derivatization reaction. In this case, we found that Lys 94 participated in the tagging reaction of Tyr 99 in CaM, resulting in an intra-molecular cross-link (Tyr+179). In a more complex system such as whole tissue homogenates, the number of products that could form from this derivatization reaction will increase significantly since the source of primary amines in more complex samples will be orders of magnitude higher than in the current study where we only had one protein present in our sample. Therefore, derivatization of full proteins is a more fruitful approach in the identification of nitrated proteins by mass spectrometry through this method due to the great sample simplification compared to working with protein digests. As a result, a key step prior to derivatization would be good protein denaturation to increase the accessibility to the residues of interest.

4.6 References

1. Pennington, J. P., Schöneich C., Stobaugh J. (2007) *Chromatographia* **66**, 649-659
2. Hong, S. J., Gokulrangan, G., and Schoneich, C. (2007) *Exp Gerontol* **42**, 639-651
3. Kanski, J., Alterman, M. A., and Schöneich, C. (2003) *Free Radic Biol Med* **35**, 1229-1239
4. Kanski, J., Behring, A., Pelling, J., and Schöneich, C. (2005) *Am J Physiol Heart Circ Physiol* **288**, H371-381
5. Kanski, J., Hong, S. J., and Schöneich, C. (2005) *J Biol Chem* **280**, 24261-24266
6. Banerjee, A. G., Gopalakrishnan, V. K., and Vishwanatha, J. K. (2007) *Mol Cell Biochem* **305**, 113-121
7. Rawlingson, A., Shendi, K., Greenacre, S. A., England, T. G., Jenner, A. M., Poston, R. N., Halliwell, B., and Brain, S. D. (2003) *Am J Pathol* **162**, 1373-1380
8. Sun, Y.-C., Chang, P.-Y., Tsao, K.-C., Wu, T.-L., Sun, C.-F., Wu, L. L., and Wu, J. T. (2007) *Clinica Chimica Acta* **378**, 175-180
9. Ou, J., Wang, J., Xu, H., Ou, Z., Sorci-Thomas, M. G., Jones, D. W., Signorino, P., Densmore, J. C., Kaul, S., Oldham, K. T., and Pritchard, K. A., Jr. (2005) *Circ Res* **97**, 1190-1197

10. Ghosh, S., Janocha, A. J., Aronica, M. A., Swaidani, S., Comhair, S. A., Xu, W., Zheng, L., Kaveti, S., Kinter, M., Hazen, S. L., and Erzurum, S. C. (2006) *J Immunol* **176**, 5587-5597

11. Kolkman, A., Dirksen, E. H., Slijper, M., and Heck, A. J. (2005) *Mol Cell Proteomics* **4**, 255-266

12. Sharov, V. S., Dremina, E.S., Pennington, J., Killmer, J., Asmus, C., Thorson, M., Hong, S.J., Li, X., Stobaugh, J.F., and Schöneich, C. (2007) *Methods in Enzymology* **(in press)**

13. Sharov, V. S., Dremina, E. S., Li, X., Gokulrangan, G., Stobaugh, J. F., Dobrowsky, R. T., Schöneich, C. . (2008) **(in preparation)**

14. Sharov, V. S., Galeva, N. A., Kanski, J., Williams, T. D., and Schoneich, C. (2006) *Exp Gerontol* **41**, 407-416

15. Cheung, W. Y. (1980) *Science* **207**, 19-27

16. Steiner, R. F., and Marshall, L. (1985) *Biopolymers* **24**, 547-563

17. Sharov, V. S., Ferrington, D. A., Squier, T. C., and Schöneich, C. (1999) *FEBS Lett* **455**, 247-250

18. Galeva, N. A., Esch, S. W., Williams, T. D., Markille, L. M., and Squier, T. C. (2005) *J Am Soc Mass Spectrom* **16**, 1470-1480

19. Richman, P. G., and Klee, C. B. (1978) *Biochemistry* **17**, 928-935

20. Richman, P. G. (1978) *Biochemistry* **17**, 3001-3005

21. Li, Y., Williams, T. D., Schowen, R. L., and Topp, E. M. (2007) *Anal Biochem* **366**, 18-28

22. Li, Y., Williams, T. D., and Topp, E. M. (2007) *Pharm Res*

23. Gow, A. J., McClelland, M., Garner, S. E., Malcolm, S., and Ischiropoulos, H. (1998) *Methods Mol Biol* **100**, 291-299

24. Kanski, J., Alterman, M. A., and Schoneich, C. (2003) *Free Radic Biol Med* **35**, 1229-1239

5. Fluorogenic derivatization of 3-Nitrotyrosine residues in Calmodulin with (3R,4S)-1-(4-(aminomethyl)phenylsulfonyl)pyrrolidine-3,4-diol

5.1 List of abbreviations used inside the text

- APPD: (3R,4S)-1-(4-(aminomethyl)phenylsulfonyl)pyrrolidine-3,4-diol
- ROS: Reactive oxygen species
- PMA: Phenylmethylamine
- RNS: Reactive nitrogen species
- CaM: Human Calmodulin, UniProtKB/Swiss-Prot entry P62158, MW 16706.4 Da
- MeCN: Acetonitrile
- $K_3Fe(CN)_6$: Potassium Ferricyanide
- ABS: 4-aminobenzylbenzene sulfonic acid
- 3-NY: Nitrotyrosine
- 3-AY: Aminotyrosine
- K: Lysine
- TNM: Tetranitromethane
- ICAT: Isotope-Coded Affinity Tag
- $Na_2S_2O_4$: Sodium dithionite
- NH_4HCO_3: Ammonium Bicarbonate
- K_2HPO_4: Potassium Phosphate

5.2 Introduction

In the previous chapter, we have described the fluorogenic derivatization of calmodulin (CaM) with a relatively water soluble form of phenylmethiylamine (PMA), 4-aminobenzylbenzene sulfonic acid (ABS). We demonstrated that the derivatization method works well with our model protein, CaM. To push this derivatization method forward and to add new capabilities to the 3-NY specific fluorescence derivatization method, a new version of the tag was synthesized by Dr. Xiabao Li. This new fluorescent tag is also a derivative of PMA that has the same water soluble characteristics as ABS and in addition, it possesses an affinity moiety for boronate affinity, (3R,4S)-1-(4-(aminomethyl)phenylsulfonyl)pyrrolidine-3,4-diol

(APPD), shown in Figure 5.1. The boronate affinity packing material was also synthesized and the columns were packed in our laboratory by Dr. Xiabao Li (1).

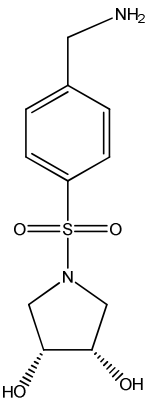

Figure 5.1 Chemical Structure of (3R,4S)-1-(4-(aminomethyl)phenylsulfonyl)pyrrolidine-3,4-diol (APPD).

The boronate affinity character of APPD gives the fluorescence derivatization technique discussed in Chapter 4, a whole new dimension for derivatized protein enrichment and purification. This property will be especially significant when working with *in-vivo* complex samples such as cell lysates and whole tissue homogenates. Being able to single out only derivatized proteins from all other proteins present in the samples, will greatly increase sensitivity for mass spectrometry analysis. Also, Tyr nitration is a low abundance post-translational modification *in-vivo* because nitrated proteins tend to be subjects to proteasomal degradation, or repair by a putative denitrase enzyme has been proposed to reverse protein nitration, although this path for repair has not been elucidated yet (2). Protein-3-NY *in-vivo* has been reported to be 10-100 pmol/mg, corresponding to only 1 to 5 nitrated Tyr

residues in a pool of 10000 (3). Therefore, enrichment through affinity chromatography would allow for processing of larger sample volumes to collect and analyze only the nitrated and derivatized proteins, diminishing ion suppression by higher abundance proteins.

The boronate affinity chromatographic separation of APPD derivatized molecules from non-derivatized molecules is based on the pH dependent formation of a pentacyclic complex of boronic acid in the stationary phase with *cis*-diol on APPD (4). However, unlike traditional boronate affinity columns, that require pH values of 9 or higher for the binding phase and pH of ~4.5 to 5 for eluting, our synthetic column works closer to physiological pH for binding (pH 7.5) and pH 2.5 for eluting. Originally designed for the purification and enrichment of catechols, which are unstable at high pH values (5), working at physiological pH is also good for working with biological samples to avoid protein degradation pathways such as deamidation that tend to accelerate at high pH (6).

Another nice characteristic of APPD is that the derivatization experiments can be performed in the same way as the experiments for ABS, achieving a selective fluorogenic derivatization of nitrotyrosine (3-NY) residues after reduction to aminotyrosine (3-AY) and is also amenable for isotopic labeling to obtain isotope coded tags for quantitation (7,8).

In the same manner as ABS, esperiments with APPD were performed on calmodulin (CaM), a relatively small 16.7 kDa protein that contains only two Tyr residues at positions 99 and 128. As was observed with ABS, experimentation with

APPD also yielded two to three different derivatization products depending on the reaction conditions (9); (i) Tyr + 1 APPD (Tyr + 281.1), (ii) Tyr +2 APPD (Tyr +536.2) and (iii) Tyr cross-linked with Lys + 1 APPD (Tyr + 264.1). In this study, we wanted to test and characterize the affinity properties of APPD as well as the boronate affinity column. The tagging reactions were straight forward. However, in these set of experiments, instead of testing the effects of iron concentration in the reaction, we tested the effects of the concentration of derivatization reagent in the reaction. Interestingly, increasing tagging reagent by ten fold in the reaction from 2 mM to 20 mM, significantly increased the fluorescence in the sample and by boronate affinity and full protein mass spectrometry, we were able to characterize the products of the tagging reaction. Increasing APPD concentration, increased formation of Tyr derivatized with 2 APPD molecules. Also by mass spectrometry, we confirmed that the derivatized product with the 2 APPD molecules has the highest affinity to the boronate affinity column, and that the intra-molecular cross-linked product has no affinity to the Boronate affinity column, probably because its conformation does not allow the cis-diol moiety to interact with the column.

5.3 Experimental

Materials

For CaM overexpression, BL21(DE3) cells were purchased from Novagen (La Joya, CA). 3-(N-morpholino)propanesulfonic acid (MOPS), M9 media components, tetranitromethane (TNM), ethylene diamine tetraacetic acid (EDTA), potassium ferricyanide ($K_3Fe(CN)_6$), and sodium dithionite ($Na_2S_2O_4$) were purchased from

Sigma-Aldrich (St. Louis, MO). 10DG Desalting columns were purchased from Bio-Rad (Hercules, CA). Protein assay Bradford Reagents were purchased from PIERCE (Rockford, IL). Amicon Ultra-15 centrifugal filter units with Ultracel-3 membranes were purchased from Millipore (Billerica, MA). (3R,4S)-1-(4-(aminomethyl)phenylsulfonyl)pyrrolidine-3,4-diol (APPD) was synthesized in house by Dr. Xiabao Li. De-ionized distilled water was filtered by a Labconco purification system (Kansas City, MO). Tris-HCl, potassium phosphate (K_2HPO_4), HPLC grade Acetonitrile (MeCN), sequencing grade trypsin, and phosphoric acid were purchased from Fisher Scientific (Pittsburg, PA).

CaM expression

CaM overexpression was achieved by transformation of the recombinant plasmid containing the gene encoding CaM (generously provided by Eric Gorman and Dr. Yunsong Li from the Department of Pharmaceutical Chemistry at the University of Kansas) into BL21(DE3) cells (Novagen, La Joya, CA). Transfection was done according to the manufacturer's protocol and overexpression was done at 37^{o}C in M9 minimal media , essentially following the protocol previously described by Li et. al (10).

CaM purification

CaM was purified both from transfected (i)BL21(DE3)-T1^{R} competent E. coli cells purchased from Sigma (St. Louis, MO) , generously provided by Eric Gorman, University of Kansas, and (ii) Novagen BL21(DE3) cells which we transfected in our laboratory. The cells were washed and re-suspended in MOPS buffer prior to lysing

them using a French press. The lysed cells were centrifuged and the supernatant was collected and loaded onto an ÄKTA FPLC system (Amersham Biosciences, Piscataway, NJ) with a pre-equilibrated (50 mM Tris-HCl, pH 7.5, 1mM $CaCl_2$) XK26 (26 mm i.d. x 10 cm) column (GE Healthcare Bio-Sciences Corp., Piscataway, NJ) packed with Phenyl–Sepharose. After a few washes with equilibration buffer, CaM was eluted with 10 mM Tris-HCl, pH 7.5 and 10 mM EDTA. The peak containing CaM was collected into ~twelve 1 ml fractions and concentrated using an Amicon Ultra-15 centrifugal filter unit with an Ultracel-3 membrane (10,11). At the final centrifugation step, the protein was buffer exchanged into 50 mM Tris, pH 8, and stored at -80 ^{o}C until used.

CaM Nitration

A stock solution of TNM was washed by 3 water extractions. Then, an 840 mM stock solution of TNM in ethanol was prepared and stored at 3 ^{o}C. After determining protein concentration of the CaM stock solution using the Bradford Reagent method, 300 µl of stock protein solution were added to 2700 µl of nitration buffer composed of 50 mM Tris, pH 8 and 5 mM $CaCl_2$ (12). For the nitration reaction, we calculated 50X molar excess of TNM to tyrosine. The reaction mixture was mixed by rotation for 3 hrs at room temperature. The nitrated protein was then cleaned up using a 10DG Desalting column by gravity filtration and at the same time, the buffer was exchanged to 50 mM NH_4HCO_3. Eight 1 ml fractions were collected from the desalting column and each one was tested for the presence of nitrated CaM by scanning absorbance from 200 to 500 nm using a Cary 50 UV spectrophotometer.

Only the fractions giving an absorbance at 280 and ~430 nm were pooled and saved. After pooling the fractions, an absorbance scan was performed again to determine the 3-NY content, by diluting 50 µl of sample in 0.1% NaOH taking into account the dilution factor and using the extinction coefficient for 3-NY □=4400 $M^{-1}cm^{-1}$ (Conc. of 3-NY=(Abs at 430nm/4400)x(dilution factor)) (13). Once our 3-NY content was established, we measured our total protein concentration in the nitrated sample and determined that we had ~2.6 mol 3-NY per mol of CaM.

CaM 3-NY reduction to 3-AY

The first 4 fractions from the 10DG column contained the nitrated protein sample in 50 mM NH_4HCO_3 and were pooled. 200 µl of this sample were saved for measuring 3-NY content and the rest were submitted to 3-NY reduction with sodium dithionite. A disappearance of the characteristic yellow color from 3-NY was observed when the concentration of sodium dithionite was at 300 µM in the reaction. 3 ml of this sample were cleaned using a new 10DG column and 50 mM NH_4HCO_3 as the equilibration buffer. Again, protein was observed to be present in only the first 4 fractions. These fractions were pooled and a 1.5 ml of this sample was aliquoted for solution phase trypsin digestion. 800 µl of this sample was saved for measuring protein concentration and the rest was precipitated in excess 100% EtOH at -70^oC overnight. The precipitated proteins were resolubilized in 100 mM K_2HPO_4 buffer. Protein concentration at all steps was measured by the Bradford reagent method.

Tagging Reaction

CaM Peptides

The trypsin digested CaM samples were aliquoted into 3 Eppendorf™ tubes, each containing 500 µl. Two were used for tagging and the third was used as one of the controls.

The samples were set up as follows:

- C1: 250 µM $K_3Fe(CN)_6$ + 2 mM APPD + 500 µl 50 mM NH_4HCO_3
- C2: 250 µM $K_3Fe(CN)_6$ + 12.7 µM CaM digest (500 µl)
- C3: 250 µM $K_3Fe(CN)_6$ + 20 mM APPD + 500 µl 50 mM NH_4HCO_3
- C4: 250 µM $K_3Fe(CN)_6$ + 2 mM APPD + 12.7 µM CaM digest (500 µl)
- C5: 250 µM $K_3Fe(CN)_6$ + 20 mM APPD + 12.7 µM CaM digest (500 µl)

After adding all tagging components to the tubes, they were rapidly centrifuged and incubated at room temperature for 3 hrs before measuring the fluorescence spectra for the samples.

Whole protein labeling

After nitroreduction, CaM was precipitated in EtOH and resolubilized in 1 ml of 100mM K_2HPO_4. The samples were diluted to give a final concentration of 8 µM CaM in the reaction. These samples were labeled simultaneously with the CaM digest samples.

The samples were set up as follows:

- C2: 160 µM $K_3Fe(CN)_6$ + 8 µM CaM (500 µl)
- C4: 160 µM $K_3Fe(CN)_6$ + 8 µM CaM (500 µl) + 2 mM APPD

- C5: 160 µM $K_3Fe(CN)_6$ + 8 µM CaM (500 µl) + 20 mM APPD

Controls C1 and C3 for the peptide reaction set were shared with this whole protein reaction set. Fluorescence spectra for these samples were also taken after 3 hrs of reaction time at room temperature.

Iron concentrations for these set of reactions were kept at a 10X molar excess to 3-NY in the samples since this was the optimal iron concentration found in the labeling study of the model peptide FSAY(NO_2)LER.

Fluorescence Characterization

Fluorescence characterization of each tagged sample was done using a fluorescence spectrophotometer (RF 5000U Shimadzu, Japan). Both excitation and emission wavelengths were determined using a 400 µl fluorescence quartz cuvette. Samples were diluted 10 times in 100 mM phosphate, pH 9 in order to obtain readings within the instrument's data window. Excitation (EX) for APPD labeled products was found to be 350-360 nm and the emission (EM) was found to be 500-515 nm depending on the nature of the analyte. For peptides, the EM was observed to have a slight red shift compared to whole protein samples.

Gel electrophoresis

Derivatized proteins with different iron concentrations were submitted to SDS-PAGE on 4-20 % Tris-HCl pre-cast gels. 25 µl of each sample were diluted with 2X sample buffer for a total volume of 50 µl. The gel was run at 200 V for 35 minutes. The gels were removed from their casing and placed under a hand held UV lamp, (Model UVL-56 115 V, 60 Hz, 0.16 A, UVP, Inc., San Gabriel, CA 91778).

The fluorescent bands were cut out and followed by in-gel trypsin digestion (14). The trypsin digests were then submitted for MS/MS analysis.

In-gel trypsin digestion

The excised gel bands were first crushed into smaller pieces and 200 µl of pure MeCN were added to dehydrate the gel pieces. Then, 2 µg of trypsin were added to each sample in ~ 50 to 60 µl of 50 mM NH_4HCO_3 and incubated at 37^{o}C overnight. The digested protein samples were saved for mass spectrometry analysis with the FT-ICR mass spectrometer available in the Multidisciplinary Research Building (MRB) here at the University of Kansas.

Boronate Affinity

The boronate affinity material was synthesized in our laboratory by chemical modification of Nucleosil, 5 µm, 500 Å pore size silica gel obtained from Macherey-Nigel as described in (1) by Dr. Xiabao Li. The silica gel was modified with 4-(3 butenylsulfonyl) phenylboronic acid, synthesized as shown in the reaction Schemes 1 and 2 of Li, et. al. (1). In order to functionalize the silica with the synthetic boronic acid, the boronic acid was mixed and sonicated with aezotropically dried silica slurry for 1 hr, heated to 120^{o}C and refluxed for 24 hrs in a moisture free environment. The final boronate affinity functionalized silica was extensively washed with chloroform, deionized water and methanol prior to drying it at 120^{o}C. A slurry of the boronate affinity functionalized silica was made in acetone and the boronate affinity column was packed into a stainless steel column (4.6 i.d x 50 mm) under a pressure of 8000 psi, using an air driven fluid pump (Haskel) (1). The synthetic boronate affinity

column was connected to a Varian (Star 9050) HPLC instrument capable of running a 3 solvent system, after optimization with the model peptide FSAY(NO_2)LER. The pump was coupled with a Varian UV detector (Star 9012), set at 214 nm and a Shimadzu fluorescence detector (RF-10AXL) set at EX 350 nm and EM 510 nm. The injection loop capacity was 100 µl.

Mobile Phases

A: 10 mM K_2HPO_4 in 10% MeCN, pH 7.4

B: 10 mM K_2HPO_4 in 50% MeCN, pH 7.4

C: 0.02% TFA in 50% MeCN, pH 2.5

Gradient

The first chromatographic step was done in 100% A for 10 min. Then, the gradient was changed from 100% A to 100% B in one min and kept in 100% B for another 10 min to wash all unspecific binding since the column was found to have affinity and reverse phase characteristics. Finally, for the affinity elution step, the mobile phase was changed from 100% B to 100% C in one min and kept at a 100% C for 13 min. After every run, the column was equilibrated back to 100% A at least for 10 min.

Mass Spectrometry Analysis

Full protein MS analysis was performed on a Q-TOF-LCMS instrument by Dr. Todd Williams and Mr. Bob Drake at the University of Kansas Mass Spectrometry Lab. The samples were desalted just prior to mass spec analysis with a reversed phase C4 column. The MS data analysis was done using Mass-Lynx 3.5 software

(Micromass, UK). The multiply charged spectrum obtained from the mass spectrometer was transformed to a full protein, uncharged spectrum using this software. This full protein spectrum was used for analysis of full protein derivatization data.

Peptide MS/MS were performed on an LTQ-FT hybrid linear quadrupole ion trap Fourier transform ion cyclotron resonance (FT-ICR) mass spectrometer (ThermoFinnigan, Bremen, Germany) via capillary liquid chromatography by Dr. Nadezhda Galeva at the University of Kansas. Prior to MS and MS/MS analysis, peptides were separated by reversed phase chromatography. The raw acquisition data was processed by BioWorks 2.2 software (Thermo Scientific, Waltham, MA) followed by peptide/protein identification using Sequest (Thermo Finnigan) and Mascot (Matrix Science, Boston, MA) and X!Tandem (The Global Proteome Machine Organization) database-searching programs. The MS/MS spectra were then validated by Scaffold 1.7 (Proteome Software Inc., Portland Oregon), a software that operates on a statistical method by setting confidence thresholds to the data obtained.

5.4 Results/Discussion

We followed the same tagging method as for ABS, discussed in Chapter 4. We found that APPD basically behaves in the same way as ABS, however, the emission wavelength is slightly red shifted in comparison to ABS and appears at 510 nm (Figure 5.2). For these sets of experiments with APPD, CaM nitration and nitro-reduction prior to derivatization was also monitored by full protein Q-TOF analysis.

Figure 5.3 shows the full MS for nitrated CaM and Figure 5.4 shows the full protein MS for nitro-reduced CaM with sodium dithionite.

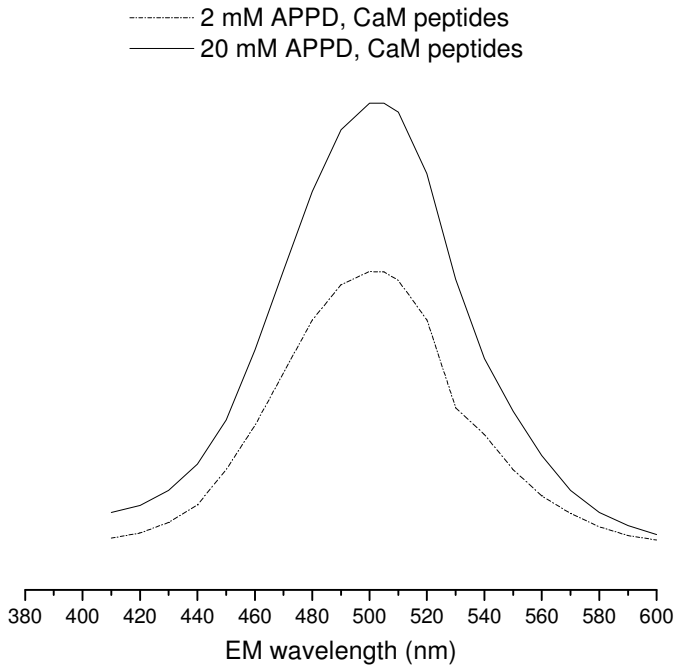

Figure 5.2 Emission spectra for derivatized CaM.

Two different concentrations of tagging reagent in the reaction were tested, 2 mM APPD (-----) and 20 mM APPD (____). Derivatization with 2 mM APPD yielded at least 2 different products with different fluorescent properties.

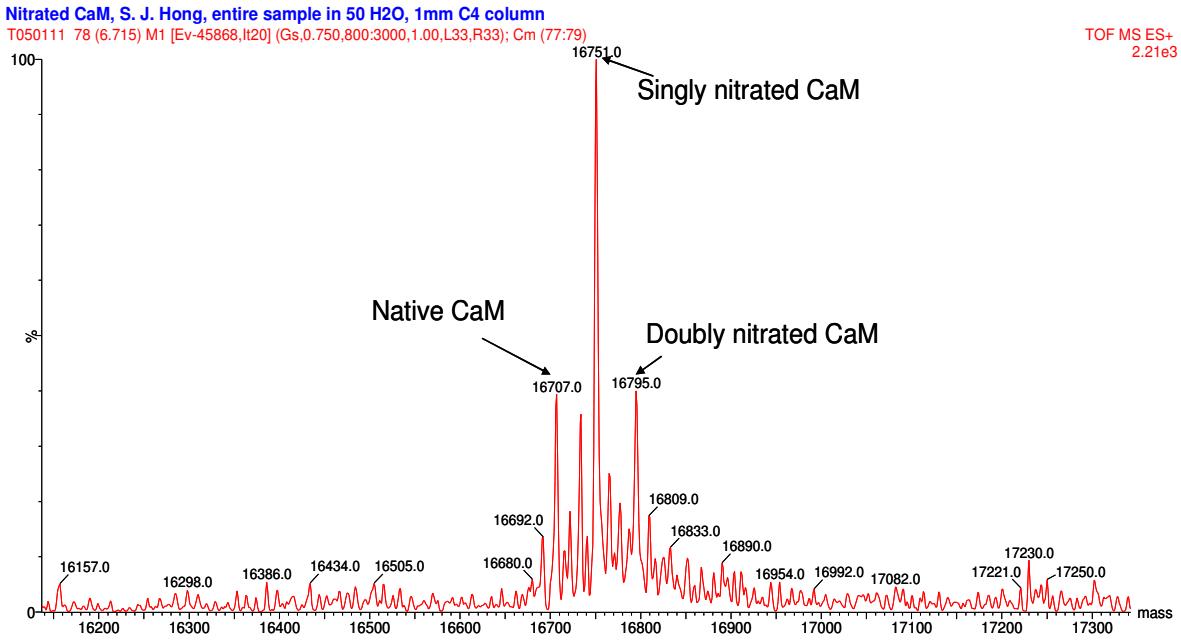

Figure 5.3 Full protein MassLynx transformed MS spectrum for nitrated CaM.

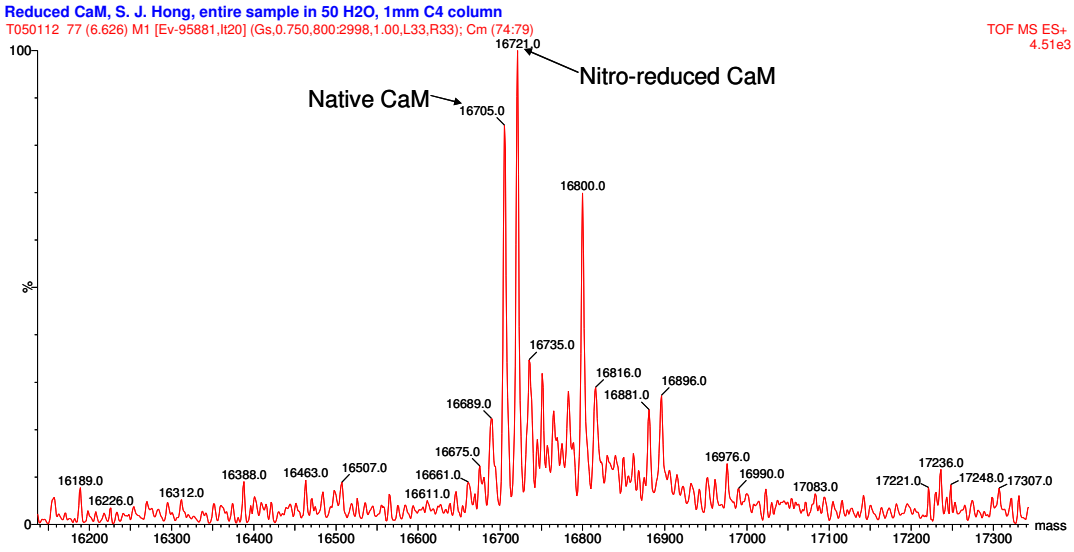

Figure 5.4 Full protein MassLynxs transformed MS spectrum for nitro-reduced CaM.

As with ABS, proteins tagged with APPD can also be fractionated on a gel after the tagging reaction, or after affinity chromatography for further separation and purification. Prior to having the affinity chromatography worked out, we tagged CaM with 2 mM APPD and different iron concentration ranging from 9X to 100X molar excess to 3-NY. We ran these tagged CaM samples on an SDS-PAGE gel (Figure 5.5) and submitted the in-gel digests for mass spectrometry analysis on the FT-ICR-MS. From these in-gel digests, we identified peptides tagged with one and two APPD molecules. Confirmation of the tagging reaction was obtained by MS/MS evidence for the desired products; with one APPD tag, shown in Figure 5.6 and the desired product with two APPD tags,shown in Figure 5.7. Finding these products by MS/MS also confirmed that the tagging reaction with APPD followed the same pattern as the reaction with the ABS tagging reagent discussed in the previous chapter.

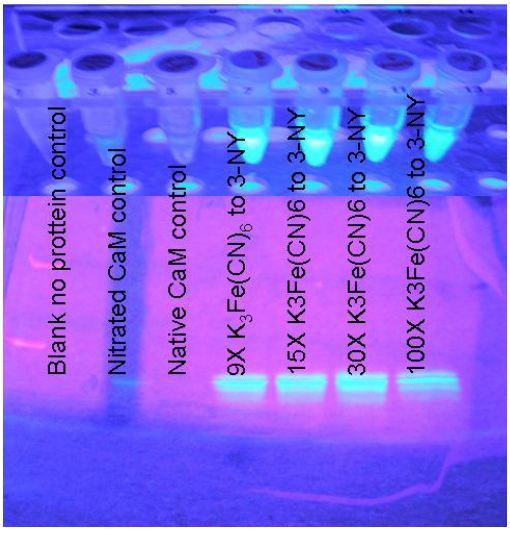

Figure 5.5 SDS-PAGE gel of APPD tagged CaM samples with different iron concentrations.

Fluorescent bands were excised, and subjected to in-gel protein trypsin digestion. Digested proteins were then submitted for FT-ICR MS analysis.

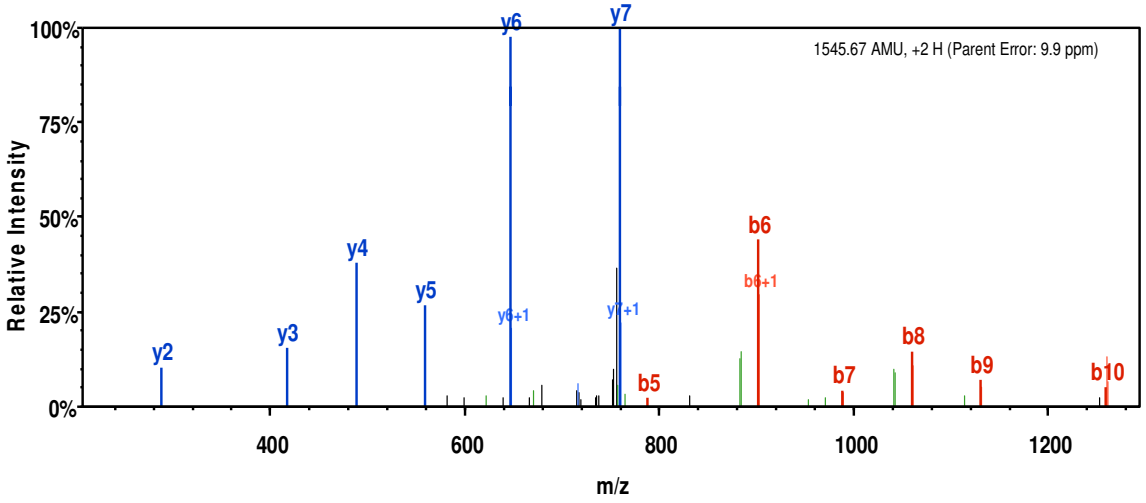

Figure 5.6 MS/MS spectrum from the CaM APPD tagged and in-gel trypsin digested sample with 1 APPD molecule + NH2.

The peptide sequence covered by this spectrum is DGNGY(1APPD/NH2)ISAAELR, where the mass modification in Y+281.1.

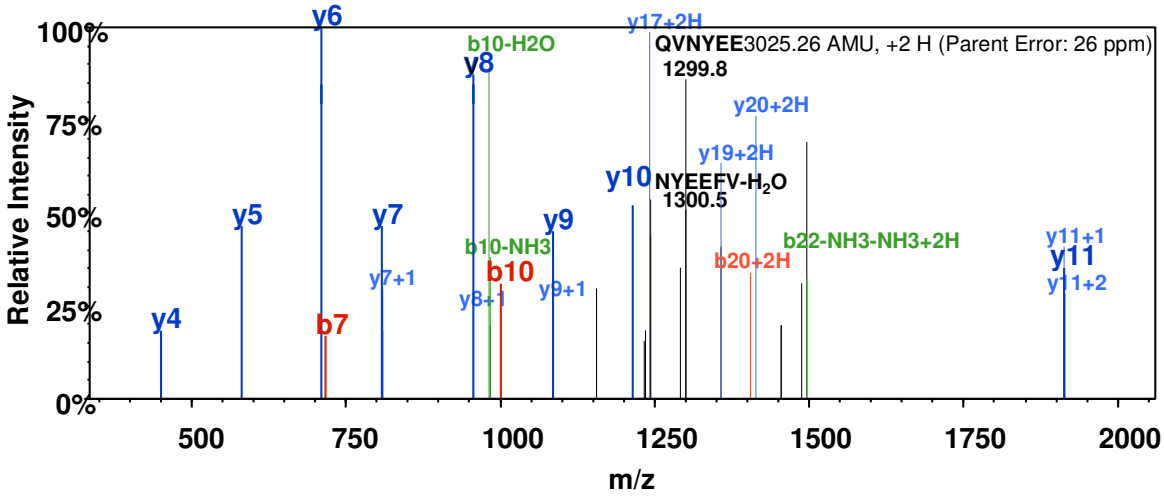

Figure 5.7 MS/MS spectrum from the CaM APPD tagged and in-gel trypsin digested sample with 2 APPD molecules.

The peptide sequence covered by this spectrum is EADIDGDGQVNY(2 APPD)EEFVQMMTAK where the mass modification is Y+536.2.

For the boronate affinity step, several synthetic boronate affinity columns were tested with no successful results of retention of desired products. Finally, we decided to go back to the model peptide FSAY(NO_2)LER and test the affinity chromatography on this simpler system (details on this experiments can be found in Appendix 1). Through this studies, we found the column was bimodal, it had both reversed phase chromatography and affinity chromatography properties. This led us to test several chromatographic conditions and finally, we arrived at the three mobile phase system, where we have three steps in the affinity chromatography, a binding step done in mostly aqueous conditions and pH 7.5, a washing step done at higher organic content and pH7.5, and finally an elution step where we kept the organic content the same as the wash step but decreased the pH to 2.5 to break the affinity bonds as well.

After optimizing conditions for boronate affinity chromatography, CaM samples were processed and derivatized as described in the experimental section. The effect of adding a ten-fold higher excess of tagging reagent than what had been used, from 2 mM to 20 mM was tested. This was done to see if we could increase formation of the desired product and decrease the formation of the cross-linked product and other undesirable products. We observed that fluorescence was higher for tagging reactions with 20 mM APPD, which in turn, exhibited higher affinity retention for the derivatized products during boronate affinity chromatography, compared to tagging reactions with 2 mM APPD (Figure 5.8). The peaks eluted during the washing step and elution step were collected separately for both samples, concentrated by centri-

vap (LABCONCO, Kansas City, MO) and analyzed by Q-TOF full protein mass spectrometry.

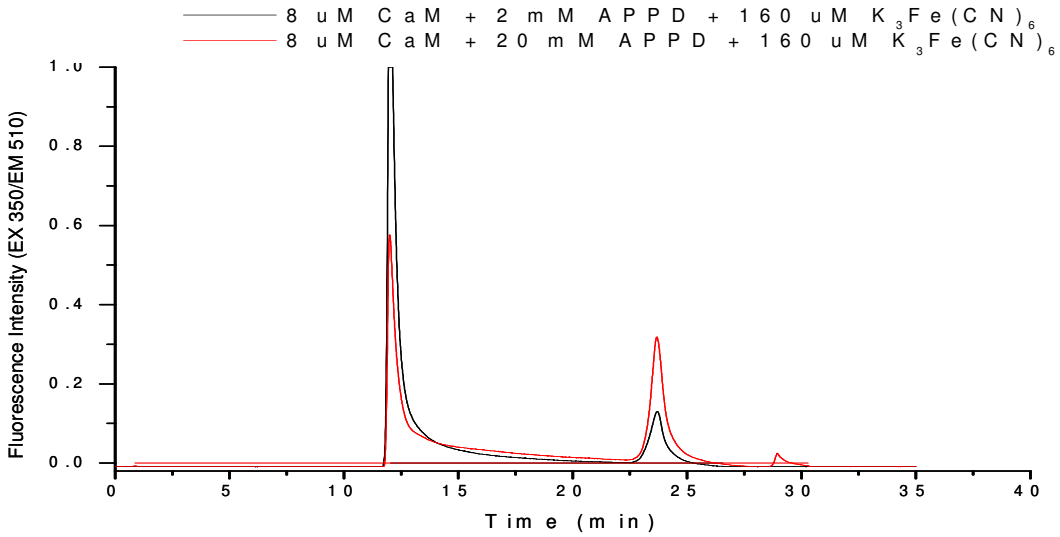

Figure 5.8 APPD derivatized full protein CaM boronate affinity chromatogram with fluorescence detection.

The binding step goes from 0-10 min (pH 7.5), washing step goes from 11-21 min (pH 7.5) and the elution step goes from 22-35 min (pH 2.5). Here we tested two derivatization conditions, 2 mM APPD and 20 mM APPD, keeping iron constant to 30X molar excess to 3-NY.

By mass spectrometry analysis, peak one (washing step) contained the products that bound to the column by reversed phase but no affinity. After careful manual evaluation of the transformed spectra by the software MassLynx, we confirmed that these products included the Lys-Tyr cross-linked product, and the product with only one tag molecule plus an NH_2 group for both reaction conditions of 2 mM APPD (Figure 5.9) and 20 mM APPD (Figure 5.10). Peak two (elution step) on the other hand, contained mainly the product with the two taggging molecules also for both 2 mM APPD (Figure 5.12) and 20 mM APPD (Figure 5.12).

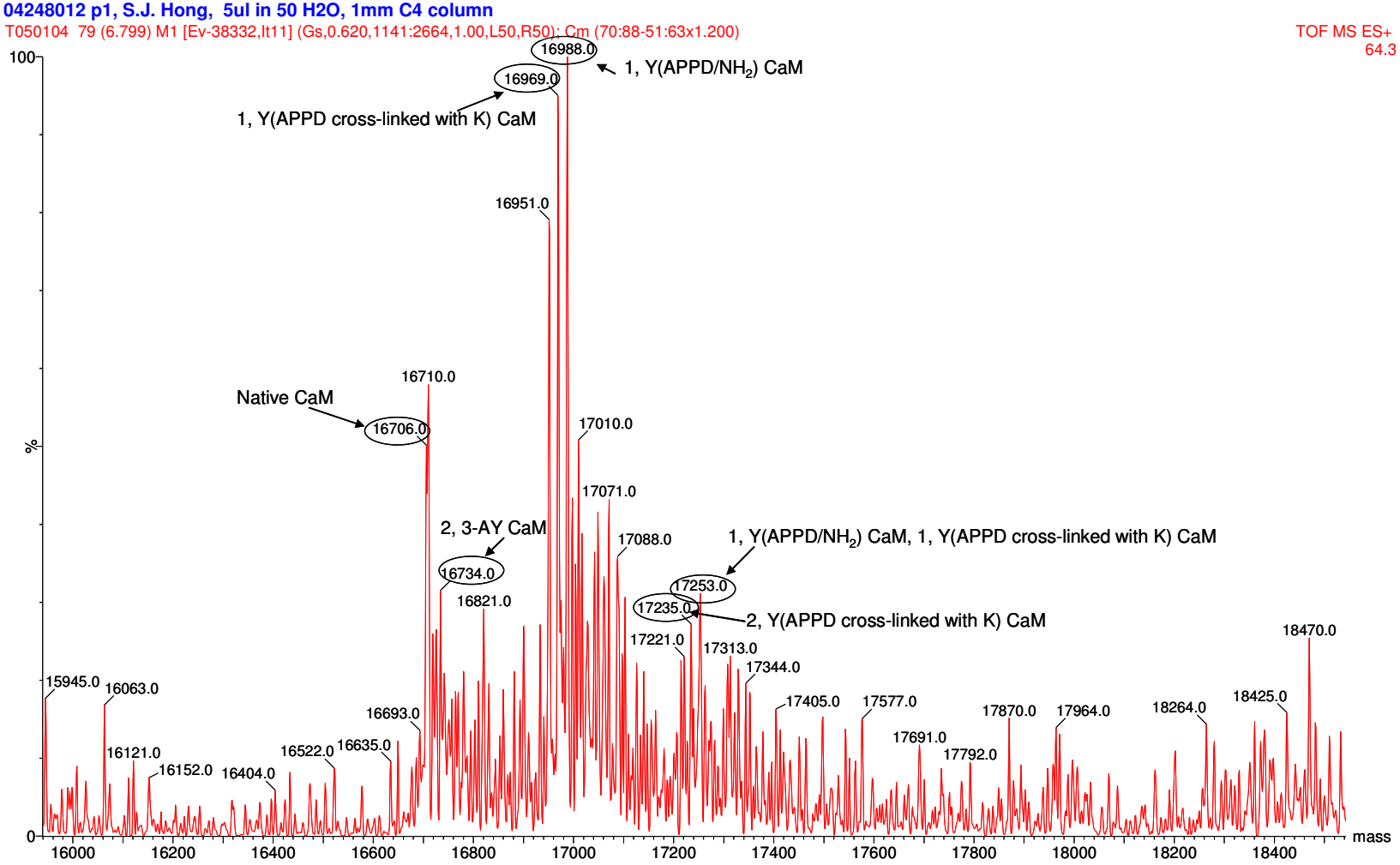

Figure 5.9 Q-TOF MassLynx transformed MS spectrum for Peak 1 of CaM tagged with 2 mM APPD.

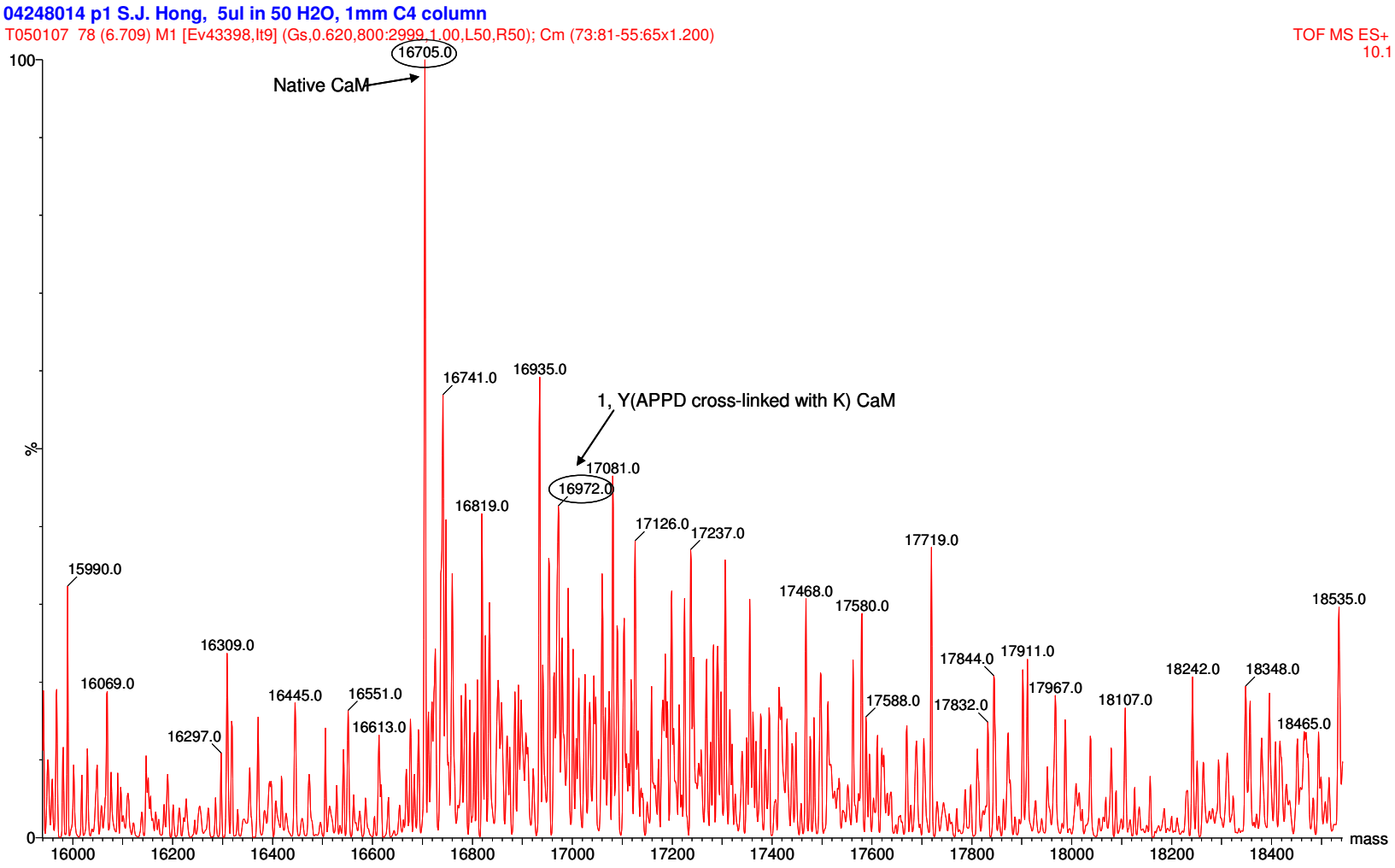

Figure 5.10 Q-TOF MassLynx transformed MS spectrum for Peak 1 of CaM tagged with 20 mM APPD.

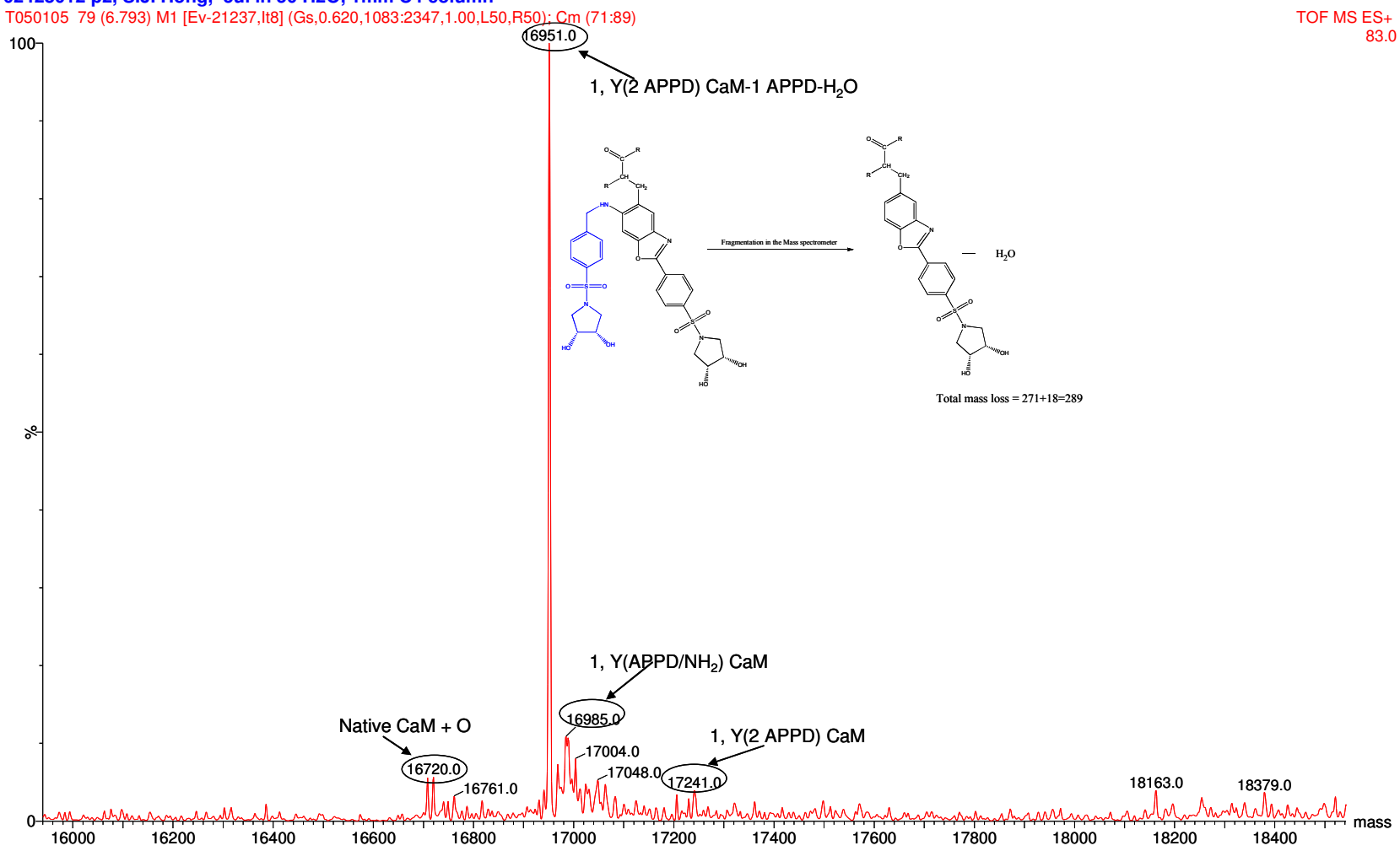

Figure 5.11 Q-TOF MassLynx transformed MS spectrum for Peak 2 of CaM tagged with 2 mM APPD.

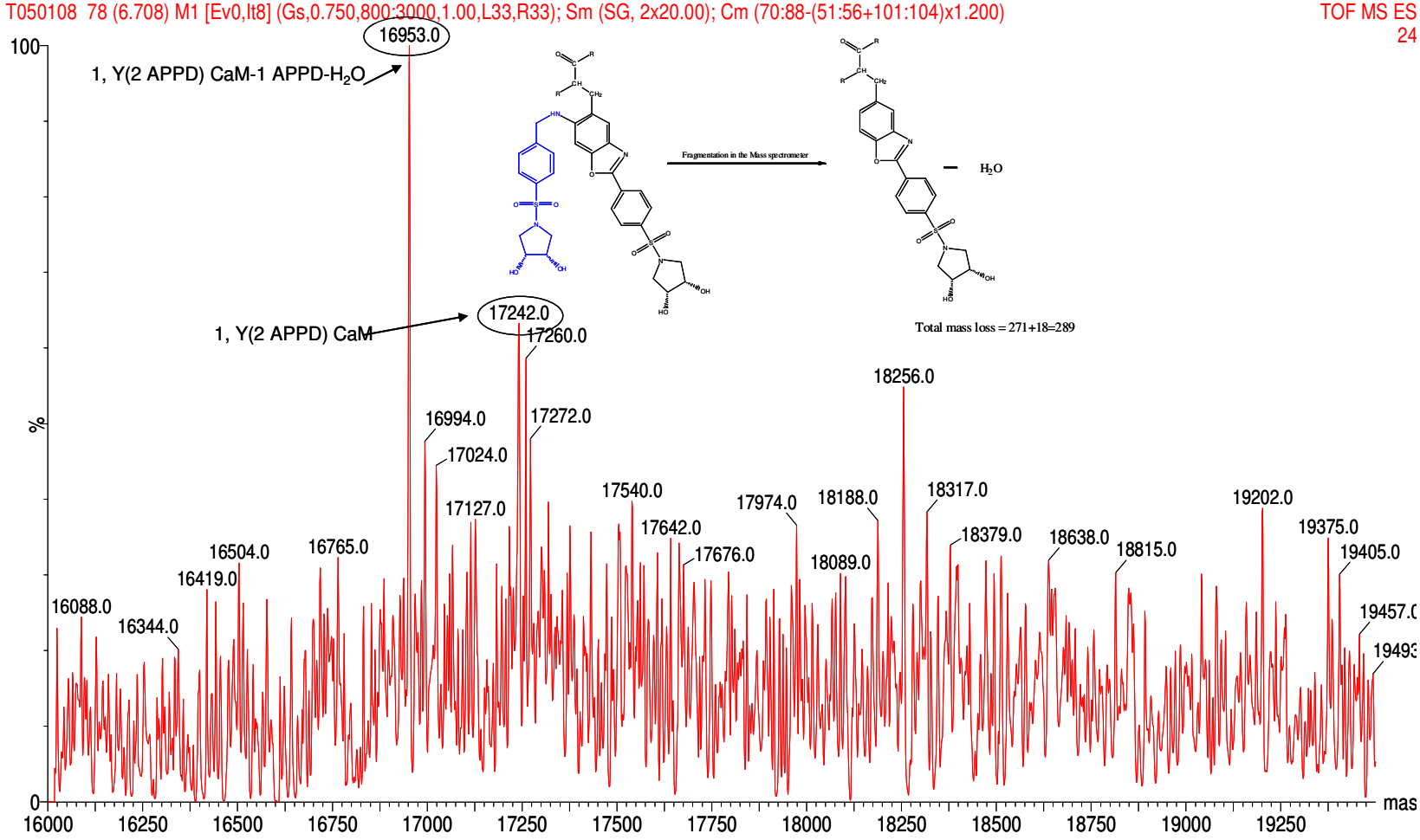

Figure 5.12 Q-TOF MassLynx transformed MS spectrum for Peak 2 of CaM tagged with 20 mM APPD.

It is intuitive to understand why the Lys-Tyr cross-linked product did not have any affinity to the boronate affinity column. For instance, the cis-diol group in the tagged molecule may not have been accessible for affinity due to the cyclic nature in this region. The cross-link may have caused the protein to fold differently on itself, making the cis-diol moiety unavailable for interaction with the column. In addition, only one cis-diol moiety seems to provide some interaction with the column, but not strong enough for complete retention by affinity since this product was mainly identified in sample collected during the washing step by full protein MS. This conclusion was drawn because even without cross-linking, the product with only one tag molecule plus an NH_2 group was also found in the wash peak.

Trypsin-digested CaM was submitted to the same reaction conditions as full protein CaM. Judging from the affinity chromatography chromatogram and fluorescence detection, there were a lot more undesirable products formed because we had elution at all three steps, of binding, washing and eluting, Figure 5.13. The peaks appearing at these three time points were collected and submitted for MS analysis with the FT-ICR-MS. Unfortunately, no useful data was obtained from the mass spectrometry experiments, confirming that reactions done on complex protein digest systems, increases the number of different unknown products formed from the derivatiation reaction, making the identification of 3-NY containing proteins and peptides not possible by this method.

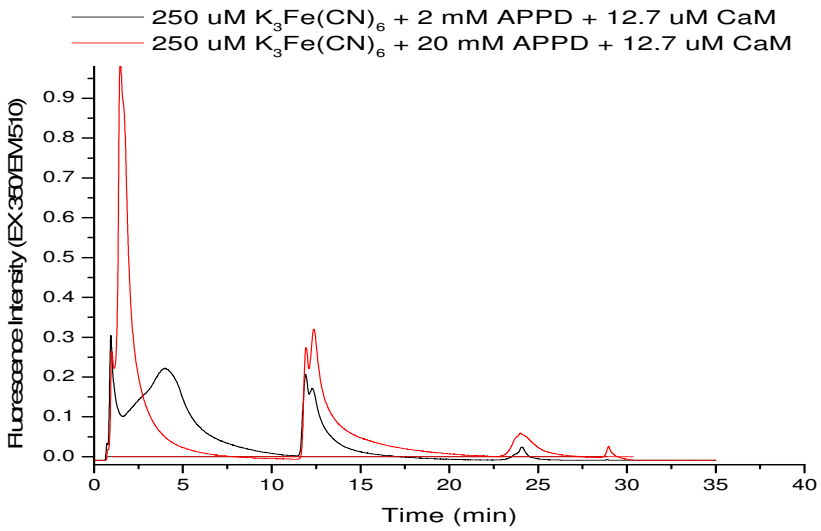

Figure 5.13 Boronate affinity chromatogram of APPD derivatized CaM peptides, with fluorescence detection.

The binding step goes from 0-10 min (pH 7.5), washing step goes from 11-21 min (pH 7.5) and the elution step goes from 22-35 min (pH 2.5). Here we tested two derivatization conditions, 2 mM APPD and 20 mM APPD, keeping iron constant to 30X molar excess to 3-NY.

5.5 Conclusion

Through the experiments carried out for this chapter, we characterized the column as bimodal, having both reversed phase characteristics, as well as affinity characteristics. Derivatization was found to yield higher percentage of desired products when the concentration of tagging reagent was increased. Affinity by the synthetic column was confirmed to be only for the derivatized product containing two APPD molecules. And finally, we also confirmed that fluorescent tagging is very efficient when 3-AY is readily accessible to the tagging reagents, however, in order to

be able to identify derivatized products by mass spectrometry, derivatization needs to be done in simpler systems (full proteins), rather than peptides due to the higher possibilities of primary amines in the latter.

5.5 References

1. Li, X., Pennington, J., Stobaugh, J. F., and Schöneich, C. (2008) *Anal Biochem* **372**, 227-236
2. Souza, J. M., Choi, I., Chen, Q., Weisse, M., Daikhin, E., Yudkoff, M., Obin, M., Ara, J., Horwitz, J., and Ischiropoulos, H. (2000) *Arch Biochem Biophys* **380**, 360-366
3. Bartesaghi, S., Ferrer-Sueta, G., Peluffo, G., Valez, V., Zhang, H., Kalyanaraman, B., and Radi, R. (2007) *Amino Acids* **32**, 501-515
4. Li, X., Sharov V., Dremina E., Thorson M.B., Killmer J., Stobaugh, J.F., Schöneich C. (2008) **(in preparation)**
5. Shen, L., Qiu, S., Chen, Y., Zhang, F., van Breemen, R. B., Nikolic, D., and Bolton, J. L. (1998) *Chem Res Toxicol* **11**, 94-101
6. Johnson, B. A., Shirokawa, J. M., and Aswad, D. W. (1989) *Archives of Biochemistry and Biophysics* **268**, 276-286
7. Sharov, V. S., Dremina, E.S., Pennington, J., Killmer, J., Asmus, C., Thorson, M., Hong, S.J., Li, X., Stobaugh, J.F., and Schöneich, C. (2007) *Methods in Enzymology* **(in press)**
8. Pennington, J. P., Schöneich C., Stobaugh J. (2007) *Chromatographia* **66**, 649-659

9. Sharov, V. S., Dremina, E. S., Li, X., Gokulrangan, G., Stobaugh, J. F., Dobrowsky, R. T., Schöneich, C. . (2008) **(in preparation)**

10. Li, Y., Williams, T. D., Schowen, R. L., and Topp, E. M. (2007) *Anal Biochem* **366**, 18-28

11. Li, Y., Williams, T. D., and Topp, E. M. (2007) *Pharm Res*

12. Richman, P. G., and Klee, C. B. (1978) *Biochemistry* **17**, 928-935

13. Gow, A. J., McClelland, M., Garner, S. E., Malcolm, S., and Ischiropoulos, H. (1998) *Methods Mol Biol* **100**, 291-299

14. Kanski, J., Alterman, M. A., and Schoneich, C. (2003) *Free Radic Biol Med* **35**, 1229-1239

6. Conclusion and Future Directions

In the present study we have presented different proteomics tools applied to the study of protein Tyr nitration, especially the new tagging technique developed by our group and Dr. Stobaugh's group. *In-vitro* studies were performed on creatine kinase, where we observed a major loss of activity due to protein oxidation with peroxynitrite. *In-vivo* studies as a function of aging were performed on rat cardiac muscle proteins, and we observed that there is an increased accumulation of nitrated proteins with aging, and discovered that a few of these proteins are part of the cytoskeleton, which may help understand tissue and organ function deterioration with aging. In order to characterize and demonstrate the characteristics of the new 3-NY specific tagging technique, model protein studies have been performed on calmodulin (CaM), a relatively small and simple model protein that contains only two Tyr residues. The tagging technique has been shown to be very efficient when applied to a full protein and its fluorescent properties have been shown to correlate well with the amount of analyte presence in the samples for both versions of the tag, ABS and APPD.

During the *in-vivo* studies of cardiac protein nitration as a function of aging in Chapter 3, several proteins of interest were identified, among them, cytoskeletal proteins such as myosin, nebulin-related anchoring protein and tropomyosin, and proteins specifically related to disease such as neurofibromin. Isolation of these proteins and studying them at the individual level would be interesting to determine

whether protein nitration is the cause of the hypothesized loss of function and thus muscle deterioration, or an effect from disease or aging.

Then, in chapters 4 and 5, we characterized the tagging technique for both ABS and APPD. The next essential step in this study would be to further characterize the quantitative capabilities of the tagging method by repeating experiments using isotopically labeled tags. This could be accomplished by having a CaM sample nitrated and nitro-reduced. Then, dividing this sample into two equal volumes and tagging them simultaneously, one with a heavy (deuterium) tag, and the other one a light (hydrogen) tag and finally, combining these samples just prior to mass spectrometry analysis. Mass spec analysis would show two different signals with the same intensity for the light and heavy tags. The place for the isotopic labels on ABS and APPD are shown on Figure 1. Both fluorescent tags allow for the incorporation

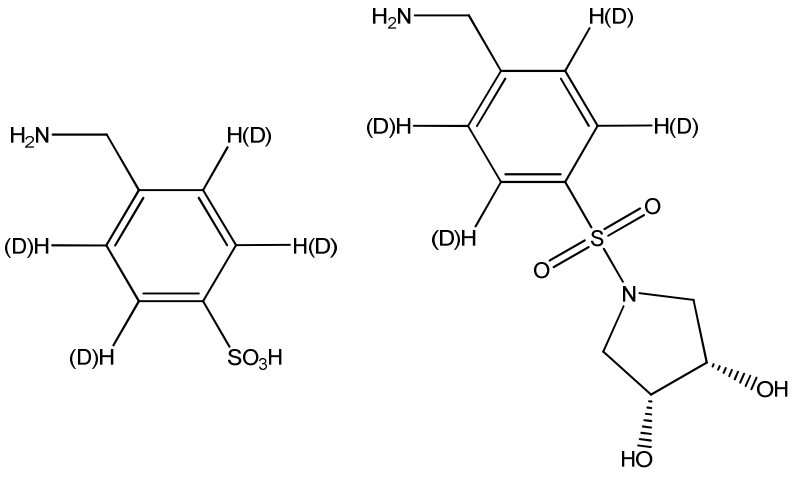

ABS APPD

Figure 6.1 ABS and APPD fluorescent tags with isotopic labels for relative quantitation by mass spectrometry analysis.

four deuteriums (D) per tag molecule leading to a mass difference of 4 in the case of derivatization products with one tag incorporated and a mass difference of 8 in the case of incorporation of two tagging molecules during derivatization, as shown in Chapters 4 and 5 for ABS and APPD respectively.

In the case of APPD, boronate affinity chromatography is a good tool for tagged protein enrichment and this would greatly improve results by helping to overcome the problems that are encountered due to the low abundance of nitrated proteins in complex mixtures such as tissue homogenates when doing *in-vivo* studies. In combination with fluorescence detection, boronate affinity chromatography would be a good source of relative quantitation since the fluorescence intensity in the samples is directly proportional to the amount of analyte present in the sample, and these results could be also confirmed by use of isotopically labeled tagging reagents and mass spectrometry analysis.

Appendix 1: Boronate Affinity column characterization with model peptide FSAY(NO_2)LER

1. List of abbreviations used inside the text

- APPD: (3R,4S)-1-(4-(aminomethyl)phenylsulfonyl)pyrrolidine-3,4-diol
- ROS: Reactive oxygen species
- RNS: Reactive nitrogen species
- MeCN: Acetonitrile
- $K_3Fe(CN)_6$: Potassium Ferricyanide
- 3-NY: Nitrotyrosine
- 3-AY: Aminotyrosine
- ICAT: Isotope-Coded Affinity Tag
- $Na_2S_2O_4$: Sodium dithionite
- FSAY(NO_2)LER: Synthetic model peptide
- K_2HPO_4: Potassium Phosphate

2. Introduction

The boronate affinity chromatography system was synthesized in house by Dr. Xiabao Li and its properties were not well understood. Boronate affinity chromatography data obtained from complex sample mixtures such as cell lysates, full proteins and protein digests was not reproducible. In addition, complete retention with very little elution was observed for a purely aqueous system and very little retention to no retention was observed when high levels of organic solvents (50% MeCN) were added to the mobile phase. As a result, we needed a simpler system to characterize the boronate affinity column as well as the affinity (APPD) labeling conditions to elucidate optimal conditions. Therefore, since extensive work had been done previously on the synthetic peptide FSAY(NO_2)LER for the characterization of the ABS fluorescent label, we picked the same peptide for the characterization of APPD fluorescent affinity labeling and the boronate affinity purification.

3. Experimental

Materials

Potassium ferricyanide ($K_3Fe(CN)_6$), and sodium dithionite ($Na_2S_2O_4$) were purchased from Sigma-Aldrich (St. Louis, MO). Oasis HLB reverse phase solid phase extraction cartriges were purchased from Waters (Milford, MA). (3R,4S)-1-(4-(aminomethyl)phenylsulfonyl)pyrrolidine-3,4-diol (APPD) was synthesized in house by Dr. Xiabao Li. De-ionized distilled water was filtered by a Labconco purification system (Kansas City, MO). Potassium phosphate (K_2HPO_4), HPLC grade Acetonitrile (MeCN), and phosphoric acid were purchased from Fisher Scientific (Pittsburg, PA).

FSAY(NO_2)LER 3-NY reduction to 3-AY

A 1 mg/ml solution of FSAY(NO_2)LER (1 mM) was prepared in 100 mM Phosphate buffer at pH 9. This solution was very yellow because of the presence of large amounts of 3-NY in the sample. Then, from this solution, a 100 µM solution of FSAY(NO_2)LER by taking 100 µl of 1 mM FSAY(NO_2)LER and adding 900 µl of 10 mM $Na_2S_2O_4$ in 50 mM phosphate buffer at pH 4.5. The color immediately disappeared and the solution turned clear, indicating the reduction of 3-NY to 3-AY. The reduced peptides were cleaned with Oasis HLB cartriges by centrifugation following the manufacturer's protocol. The final elution step was in 100% MeOH so the peptides were dried down with a centrivap (Labconco, Kansas City, MO) and resolubilized in 100 mM phosphate buffer at pH 9. At this step, no peptide loss was assumed when proceeding to the next step.

Tagging Reaction

FSAY(NO_2)LER peptide samples

The reduced peptide samples were aliquoted into 3 eppendorf tubes, each containing 500 µl. Two were used for tagging and the third was used as one of the controls.

The samples were set up as follows:

- C1: 100 µM $K_3Fe(CN)_6$ + 500 µl 100 mM K_2HPO_4
- C2: 100 µM $K_3Fe(CN)_6$ + 10 µM FSAY(NO_2)LER in 100 mM K_2HPO_4 (500 µl)
- C3: 100 µM $K_3Fe(CN)_6$ + 2 mM APPD + 100 mM K_2HPO_4
- C4: 100 µM $K_3Fe(CN)_6$ + 2 mM APPD + 10 µM FSAY(NO_2)LER in 100 mM K_2HPO_4 (500 µl)
- C5: 100 µM $K_3Fe(CN)_6$ + 20 mM APPD + 10 µM FSAY(NO_2)LER in 100 mM K_2HPO_4 (500 µl)

After adding all tagging components to the tubes, they were rapidly centrifuged and incubated at room temperature for 2.5 hrs before measuring the fluorescence spectra for the samples.

Fluorescence Characterization

Fluorescence characterization of each tagged sample was done using a fluorescence spectrophotometer (RF 5000U Shimadzu, Japan). Both excitation and emission wavelengths were determined using a 400 µl fluorescence quartz cuvette. Samples were diluted 10 times in 100 mM Phosphate, pH 9 in order to obtain

readings within the instrument's data window. Excitation (EX) for APPD labeled products was found to be 350-360 nm and the emission (EM) was found to be 500-515 nm depending on the nature of the analyte. For peptides, the EM was observed to have a slight red shift compared to whole protein samples.

Boronate Affinity

The boronate affinity material was synthesized in our laboratory by chemical modification of Nucleosil, 5 µm, 500 Å pore size silica gel obtained from Macherey-Nigel as described in (1) by Dr. Xiabao Li. The silica gel was modified with 4-(3 butenylsulfonyl) phenylboronic acid, synthesized as shown in the reaction Schemes 1 and 2 of Li, et. al. (1). In order to functionalize the silica with the synthetic boronic acid, the boronic acid was mixed and sonicated with aezotropically dried silica slurry for 1 hr, heated to 120^{o}C and refluxed for 24 hrs in a moisture free environment. The final boronate affinity functionalized silica was extensively washed with chloroform, deionized water and methanol prior to drying it at 120^{o}C. A slurry of the boronate affinity functionalized silica was made in acetone and the boronate affinity column was packed into a stainless steel column (4.6 i.d x 50 mm) under a pressure of 8000 psi, using an air driven fluid pump (Haskel) (1). The synthetic boronate affinity column was tested in two different HPLC systems. First, it was tested on a Shimadzu HPLC system composed of two pumps (LC-10AS) controlled by the system controller (SCL-10A). Both UV (SPD-10AV) and fluorescence (RF-10AXL) detection were used. In this system, column properties were tested both in purely

aqueous conditions and also in the presence of 50 % MeCN with changing pH for binding and elution phases. The sample loop capacity was 20 µl.

Mobile Phases Aqueous Conditions

A: 50 mM Na_2HPO_4, pH 7.4

B: 0.02% TFA, pH 2.5

Mobile Phases Organic Conditions

A: 50 mM Na_2HPO_4 in 50 % MeCN, pH 7.4

B: 0.02% TFA, in 50% MeCN, pH 2.5

Gradient

The first chromatographic step was done in 100% A for 10 min for binding. Then, the gradient was changed from 100% A to 100% B in one min and kept in 100% B for another 15 min for the affinity elution step. After every run, the column was equilibrated back to 100% A at least for 10 min.

Then, we switched to a Varian (Star 9050) HPLC instrument capable of running a 3 solvent system. The pump was coupled with a Varian UV detector (Star 9012), set at 214 nm and a Shimadzu fluorescence detector (RF-10AXL) set at EX 350 nm and EM 510 nm.

Mobile Phases

A: 10 mM K_2HPO_4 in 10% MeCN, pH 7.4

B: 10 mM K_2HPO_4 in 50% MeCN, pH 7.4

C: 0.02% TFA in 50% MeCN, pH 2.5

Gradient

The first chromatographic step was done in 100% A for 10 min. Then, the gradient was changed from 100% A to 100% B in one min and kept in 100% B for another 10 min to wash all unspecific binding since the column was found to have affinity and reverse phase characteristics. Finally, for the affinity elution step, the mobile phase was changed from 100% B to 100% C in one min and kept at a 100% C for 13 min. After every run, the column was equilibrated back to 100% A at least for 10 min.

4. Results/Discussion

Exitation and Emission properties of the derivatized samples were measured by a fluorescence spectrophotometer. Interestingly, two different EM wavelengths were present when we used 2 mM APPD in the derivatization reaction, at 425 nm and 510 nm. However, when we increased the APPD concentration to 20 mM, only one EM wavelength at 510 nm was present (Figure 1). From previous experiments with APPD in full proteins and protein digests, the target wavelength for desired products was observed to be 510 nm, confirming that higher concentrations of derivatization reagent increases the yields for the desired products.

Then, these samples were injected onto the synthetic boronate affinity column. Affinity conditions were tested both in purely aqueous conditions and 50% MeCN conditions separately. The binding mobile phase was at pH 7.5 and elution mobile phase was at pH 2.5. For aqueous conditions, both mobile phases were made in DD

H_2O and for 50% MeCN, we added 50% MeCN to both binding and elution mobile phases, keeping the ionic strength of the buffers constant.

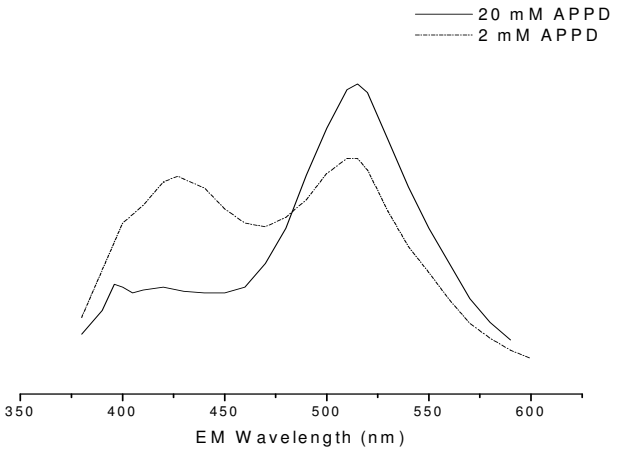

Figure 1 Emission spectra for FSAYLER.

Samples derivatized with 2 mM APPD (---) and 20 mM APPD (___).

From these experiments, we found that there was high retention in aqueous conditions, but almost no elution, even when the pH conditions for elution were met. Then, when we tested the same sample in 50% MeCN conditions, we observed low binding and high percentage of elution in both the binding phase and the elution phase. Figure 2 shows the boronate affinity chromatograms for derivatized FSAYLER in both aqueous and 50% MeCN. Results from these experiments helped us to understand that the column was bimodal, it possessed both reversed phase characteristics as well as affinity properties. Therefore, we decided to move to a 3 mobile phase system where we could take advantage of both properties of the column.

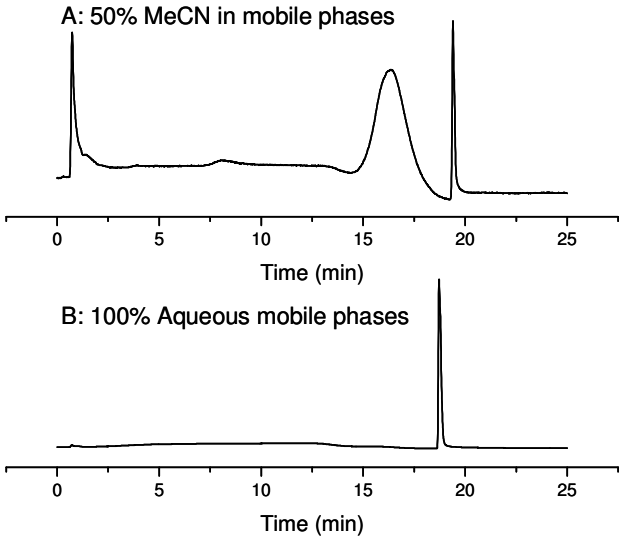

Figure 2 Boronate Affinity chromatograms for derivatized FSAYLER.

(A) 50% MeCN mobile phases and (B) 100% aqueous conditions. For both conditions, the binding aqueous phase is 50 mM phosphate (pH 7.5) and goes from 0 to 10 min. Elution aqueous phase is 0.02% TFA (pH 2.5) and goes from 11 to 25 minutes.

In our 3 mobile phase system, we introduced a binding phase with low MeCN content (10%), pH7.5, and we used the 50% MeCN mobile phase at pH 7.5 as the washing step to wash off all unspecific binding to the column by the reversed phase mechanism. Finally, we kept the elution mobile phase at 50% MeCN and pH 2.5. The reversed phase mechanism helped the compounds stick to the column longer for the binding to occur, and the washing step ensured that all compounds bound to the column only by hydrophobic interactions were washed away. Finally, the desired compounds with affinity to the boronate affinity were eluted by lowering the pH. As a result, this affinity column can be used as an enrichment method for APPD tagged compounds, over several injections if sample volume is high. Figure 3 shows the boronate affinity chromatogram for FSAYLER using this three mobile phase system for both, samples tagged with 2 mM APPD and 20 mM APPD. As predicted from the

fluorescence spectra for both samples where samples derivatized with 2 mM APPD showed the presence of different products with different fluorescent properties, more products were found in the wash step and less in the elution step, when compared to the chromatogram of the samples derivatized with 20 mM APPD.

In conclusion, we achieved a good system for affinity enrichment and we were also able to elucidate that high concentrations of the affinity tag compound APPD are necessary for the formation of our desired products.

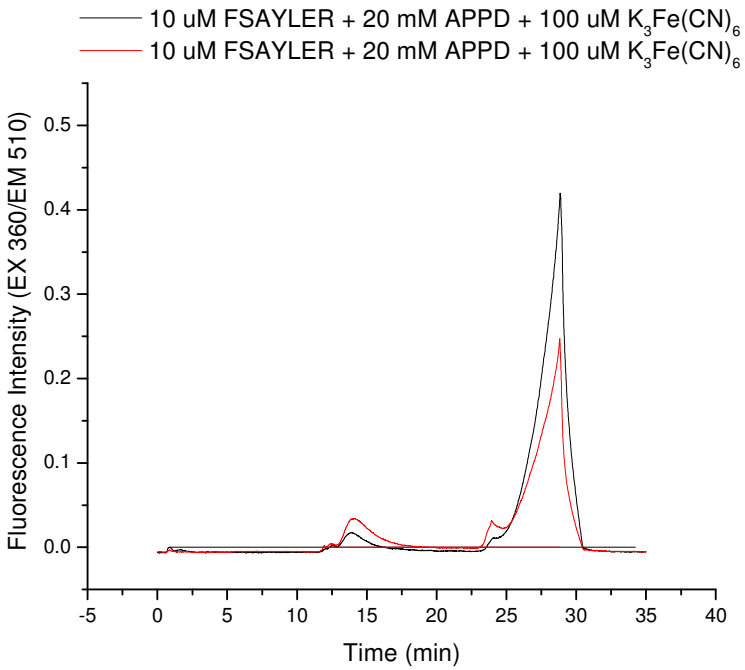

Figure 3 Boronate affinity chromatography with 3 mobile phases.

Binding: 0 to 10 min (10 % MeCN, pH 7.5), washing: 11 to 21 min (50 % MeCN, pH 7.5), and eluting: 22 to 35 min (50 % MeCN, pH 2.5). Here, we also compare affinity for samples tagged with 2 mM APPD (red) and 20 mM APPD (black).